DEVELOPMENT OF END-GROUP FUNCTIONAL TEMPERATURE-RESPONSIVE POLYMERS

A Thesis Submitted to
the Graduate School of Engineering and Sciences of
İzmir Institute of Technology
in Partial Fulfillment of the Requirements for the Degree of

MASTER OF SCIENCE

in Chemical Engineering

by
Ekrem ÖZER

July 2013
İZMİR

We approve the thesis of **Ekrem ÖZER**

Examining Committee Members:

_____
Prof. Dr. Volga BULMUŞ
Department of Chemical Engineering, İzmir Institute of Technology

_____
Assoc. Prof. Dr. Mustafa M. DEMİR
Department of Chemistry, İzmir Institute of Technology

_____
Assist. Prof. Dr. Ayben TOP
Department of Chemical Engineering, İzmir Institute of Technology

10 July 2013

_____
Prof. Dr. Volga BULMUŞ
Supervisor, Department of
Chemical Engineering
İzmir Institute of Technology

_____
Assist. Prof. Dr. Hadi ZAREİE
Co-Supervisor, Department of
Material Science and Engineering
İzmir Institute of Technology

_____
Prof. Dr. Fehime ÖZKAN
Head of the Department of Chemical
Engineering

_____
Prof. Dr. R. Tuğrul SENGER
Dean of the Graduate School of
Engineering and Sciences

ACKNOWLEDGMENT

Firstly, I would like to express my sincere gratitude to my thesis supervisor Prof. Dr. Volga BULMUŞ for giving me the chance to work on this study. Although her timetable never matched with my timetable, she always encouraged me through the study. I also want to thank to my co-supervisor Assist. Prof. Dr. Hadi M. ZAREİE.

I am also grateful to specialist Salih GÜNNAZ and Fırat ZİYANAK for their help and support throughout the NMR experiments.

The financial support of The Scientific Technical Research Council of Turkey (110T759) is thankfully acknowledged.

Grateful thanks go to Tuğba TOKER, not only for being a lab-mate also for being a sister. Also would like to thank my lab-mates, Işıl KURTULUŞ, Esra AYDINLIOĞLU, Damla TAYKOZ, and Vildan GÜVEN.

I would like to thank to Ceren SÜNGÜÇ for her priceless help.

I also want to thank my colleagues, Okan AKIN, Özgün DELİİSMAİL, Seda GÜNEŞ, Mert TUNCER; Emre KILIÇ, Metin UZ, Arda YURTSEVER, Serkan KANGAL and Derya KÖSE for their friendship and support throughout .

At last but not least, I would like to express special thanks to my family. I am grateful for endless support of my father İbrahim ÖZER and sister İrem ÖZER and my mother Serap ÖZER to whom I dedicate this thesis for her never ending love, support and encouragements during my thesis and my life.

ABSTRACT

DEVELOPMENT OF END-GROUP FUNCTIONAL TEMPERATURE-RESPONSIVE POLYMERS

The aim of this thesis was to synthesize temperature-responsive, well-defined, end-group modified (co)polymers of oligoethyleneglycol methyl ether methacrylate (OEGMA$_{300}$) and diethyleneglycol methyl ether methacrylate (MEO$_2$MA) via reversible addition fragmentation chain transfer (RAFT) polymerization, and to investigate in detail the temperature-responsive behaviour of the resultant (co)polymers considering the possible use of these (co)polymers in temperature-controlled biosensing applications.

A series of (co)polymerization kinetic experiments were performed at three different [Total monomer]/[RAFT agent] molar ratios and yielded copolymers of OEGMA$_{300}$ and MEO$_2$MA with controlled molecular weights and low polydispersities (<1.2), indicating RAFT-controlled (co)polymerization mechanism. The reactivity ratios of the comonomers, MEO$_2$MA and OEGMA$_{300}$, determined using Kelen-Tüdŏs method were 0.96 and 0.98, respectively. This indicated that the copolymers were *truly random* and their composition could be controlled by the feed comonomer composition.

A number of (co)polymers having varying molecular weights, compositions and end-group functionalities (i.e. thiocarbonylthio RAFT end-group, pyridyldisulfide (PDS) or phosphonate group) were synthesized to investigate the effects of these parameters on the Lower Critical Solution Temperature (LCST) of the (co)polymers. The end-group functionality, PDS or phosphonate, was chosen considering the possible use of these polymers on gold or alumina surfaces, respectively.

The key factor affecting the LCST was found to be the hydrophilic/hydrophobic balance of the (co)polymers. Increasing the hydrophilic content (OEGMA content) of the (co)polymers increased the LCST values. The effect of end-group on the LCST was more profound for (co)polymers with low molecular weights. Replacement of the thiocarbonylthio end-group with a more hydrophilic group such as PDS or phosphonate resulted in a significant increase in the LCST of the copolymers having a degree of polymerization of less than 30. For the copolymers with higher degree of polymerization, the influence of the end-group chemistry on the LCST became negligible.

ÖZET

UÇ-GRUP FONKSİYONEL SICAKLIĞA DUYARLIĞI POLİMERLERİN GELİŞTİRİLMESİ

Bu tezin amacı; sıcaklık kontrollü biyosensör uygulamalarında potansiyel kullanımları gözönüne alınarak iyi tanımlanmış, uç-grup fonksiyonel, sıcaklığa duyarlı oligoetilenglikol metil eter metakrilat (OEGMA$_{300}$) ve dietilenglikol metil eter metakrilat (MEO$_2$MA) (ko)polimerlerinin tersinir katılma ayrışma zincir transfer (RAFT) polimerizasyonu ile sentezlenmesi, ve oluşan (ko)polimerlerin sıcaklığa-duyarlı davranışlarının ayrıntılı olarak incelenmesidir.

Üç farklı [Toplam monomer]/[RAFT ajanı] mol oranında gerçekleştirilen bir seri kopolimerizasyon kinetiği deneyleri, RAFT-kontrollü (ko)polimerizasyon mekanizmasına işaret eden kontrollü molekül ağırlığı ve dar molekül ağırlığı dağılımına (<1,2) sahip OEGMA$_{300}$ ve MEO$_2$MA kopolimerlerinin senteziyle sonuçlandı. Komonomerlerin, MEO$_2$MA and OEGMA$_{300}$, reaktivite oranları, Kelen-Tüdõs methodu kullanılarak sırasıyla 0,96 (MEO$_2$MA) ve 0,98 (OEGMA$_{300}$) olarak bulundu. Bu sonuç, sentezlenen kopolimerlerin "gerçek rastgele" kopolimerler olduğunu ve kopolimer kompozisyonunun besleme komonomer kompozisyonunu değiştirerek kontrol edilebileceğini gösterdi.

Farklı molekül ağırlıklarında, kompozisyonlarda ve farklı uç-grup fonksiyonelliği (tiyokarboniltiyo RAFT grubu, piridildisülfat veya fosfonat) olan kopolimerler, bu parametrelerin kopolimerlerin Düşük Kritik Çözelti Sıcaklığı (LCST) üzerinde etkilerini incelemek için sentezlendi. Piridil disülfat ve fosfonat uç-grup fonksiyonellikleri bu polimerlerin sırasıyla altın ve aluminyum yüzeylerde uygulamaları göz önünde bulundurularak seçildi.

LCST'yi etkileyen en önemli parametrenin kopolimerlerin hidrofilik/hidrofobik balansı olduğu bulundu. Polimerin hidrofilik içeriğinin (OEGMA) artması LCST değerlerini de arttırdı. Fonksiyonel uç-grubun LCST üzerindeki etkisinin düşük molekül ağırlıklı polimerlerde daha belirgin olduğu bulundu. Tiyokarboniltiyo uç grubun piridildisülfat veya fosfonat gibi daha hidrofilik bir grupla değiştirilmesi polimerizasyon derecesi otuzdan az olan polimerler için LCST de belirgin bir artış ile sonuçlandı. Daha yüksek polimerizasyon derecelerine sahip polimerlerde ise, uç-grup kimyasının LCST üzerindeki etkisinin yok gözardı edilebilecek kadar az olduğu bulundu.

TABLE OF CONTENTS

LIST OF FIGURES

LIST OF TABLES

CHAPTER 1

INTRODUCTION

For the last two decades stimuli-responsive polymers have received significant attention because of their rapid conformational changes in response to an external stimulus. Temperature-responsive polymers are polymers that exhibit a phase separation and change their physical properties as a result of temperature change in the environment. Particularly, polymers exhibiting a lower critical solution temperature (LCST) in aqueous solution are of interest. Since water as a solvent is cheap, safe and biologically relevant, polymers that have thermo-responsive property in water are especially important. Such polymers are promising building blocks of smart responsive materials such as biosensors, matrices for tissue engineering, and drug carriers (Sun et al. 2013).

The lower critical solution temperature (LCST) is the critical temperature below which the components of a mixture are miscible for all compositions. If a polymer exhibits an LCST in water, upon heating above the LCST the hydrogen bonds between polymer and water break, leading to demixing and phase separation. This is an entropy driven process due to the expulsion of water (Gibson et al. 2011). Among various polymers having LCST in water, the most studied polymer is poly(N-isopropylacrylamide) Poly(NIPAAm). (Fujishige et al. 1989, Heskins et al. 1968). However, for last few years a new thermo-responsive polymer family, oligo(ethylene glycol) (meth)acrylates has emerged as an interesting alternative to Poly(NIPAAm) (Lutz 2011).

Poly(ethylene glycol) (PEG) is a non-toxic and non-immunogenic polymer, that consists of repeating ethylene oxide units. Poly(oligo(Ethylene Glycol) Methyl Ether Methacrylate (Poly(OEGMA)) is a comb-type PEG which includes a methacrylate-based polymer backbone and short oligoethyleneglycol chains that are grafted to the methacrylate backbone. The copolymers of OEGMA based monomers combine the advantages of PEG and thermo-responsive polymers in a single macromolecular structure. Excellent bio-repellent property (anti-fouling behaviour) below the LCST

makes OEGMA copolymers a better choice for biosensor applications compared to Poly(NIPAAm) (Lutz 2011).

In commercial polymer production, one of the most widely used techniques is free radical polymerization. Free radical polymerization is a type of chain growth polymerization. Due to challenges in control over the molecular weight and molecular weight distribution, and also difficulties in preparation of end-group functional polymers and varying polymer architectures via conventional free radical polymerization, controlled/living radical polymerization techniques have become popular.

RAFT (reversible addition−fragmentation chain transfer) polymerization, a controlled/living radical polymerization, firstly reported by CSIRO (Commonwealth Scientific and Industrial Research Organization) group in 1998, is one of the most effective and versatile methods for providing living characteristics to radical polymerization. Living character of polymers comes from the fact that radicalic polymer chains formed during polymerization terminate at a negligible level and are able to polymerize with addition of new monomer in the presence of a radical source. The RAFT polymerization can be considered as a conventional free radical polymerization which is carried out with the help of a chain transfer agent (i.e. RAFT agent). (Boyer et al. 2009)

The chain transfer agents used in the RAFT polymerization are organic compounds having a thiocarbonylthio moiety. The rapid equilibrium between the active propagating radicals and the polymeric thiocarbonylthio compounds allows for the production of polymers with controlled molecular weight and narrow molecular weight distribution (low polydispersity) which is the most important advantage of the RAFT polymerization. Another important advantage of RAFT polymerization is, since the final polymer contains non-degraded RAFT end-group, this group can be easily further utilized to chain extend or modify the end-group of the polymers.

The aim of this thesis was to synthesize temperature-responsive, well-defined (co)polymers of oligoethyleneglycol methyl ether methacrylate ($OEGMA_{300}$) and diethyleneglycol methyl ether methacrylate (MEO_2MA) via RAFT polymerization, perform end-group modifications and finally investigate in detail the temperature-responsive behaviour of the resultant (co)polymers considering the possible use of these copolymers in temperature-controlled bio-sensing applications (Zareie et al. 2008). For this aim, firstly kinetic experiments were performed to determine whether the

2

(co)polymerizations were controlled by RAFT mechanism. To investigate the effect of composition, molecular weight and end-group modification on thermo-responsive behaviour of the polymers, a number of copolymers with varying molecular weights, compositions and end-group functionalities were then synthesized. Polymers were characterized by nuclear magnetic resonance spectroscopy (NMR) and gel permeation chromatography (GPC) techniques. Temperature-responsive property of the polymers was characterized using UV-vis spectroscopy. The methods and results are presented in Chapters 3 and 4, respectively.

CHAPTER 2

LITERATURE REVIEW

2.1. Stimuli-Responsive Polymers

Stimuli-responsive, "smart" polymers are macromolecules that undergo fast and reversible changes from hydrophilic to hydrophobic state in response to small changes in their environment. These polymers may be dissolved in solutions, adsorbed or grafted onto solution-solid interfaces, or cross-linked in the form of hydrogels (Figure 2.1) (Hoffman and Stayton 2004). These changes can be observed as precipitation of the smart polymer in solution, changes in wettability of the surface to which the smart polymer is grafted or dramatic shrinking/swelling of the hydrogel. The changes are relatively fast and reversible i.e. the system returns to its initial state when the trigger is removed. (Galaev 2002)
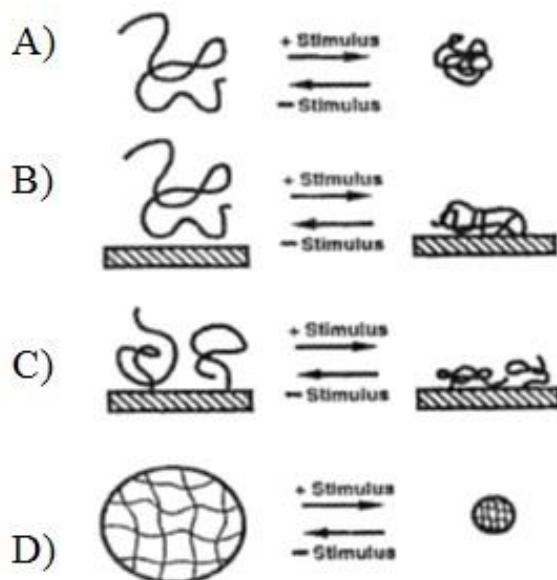
Figure 2.1. Stimuli responsive polymers before and after stimulus A) In solution; B) adsorbed at solid/liquid interface; C) grafted onto a solid; D) hydrogel (Source: Hoffman and Stayton 2004)

The hydrophilic/hydrophobic balance in the structure of the polymer has the key importance in demonstrating the phase transition. Response of polymer may be the

result of different types of stimulus, such as physical stimuli (temperature, ionic strength, electric field), chemical stimuli (pH), biochemical stimuli (metabolite + enzyme) and polymer can respond in different ways, like changing colour, transparency, conductivity or becoming permeable to water.

Applications of stimuli-responsive polymers in drug delivery, tissue engineering, bioseparations, and biosensors have been studied extensively for last two decades (Byeongmoon and Gutowska 2002). Self-assembly of short oligoethyleneglycol (PEG$_{12}$) chains with pyridyldisulfide (pds) end-groups on a gold surface and thermo-responsive behaviour of the surface for biosensor applications were investigated by Zareie and co-workers (Zareie et al. 2008). Okano and coworkers showed thermo-responsive characteristics of poly(*N*-isopropylacrylamide) (Poly(NIPAAm)) on grafted cell culture dishes for tissue engineering (Matsuda et al. 2007). Nolan et al. reported the insulin loaded poly(N-isopropylacrylamide-co-acrylic acid) microgel thin films for the regulation of macromolecule and small molecule release and drug delivery applications (Nolan et al. 2004).

2.1.1. Temperature-Responsive Polymers

Temperature-responsive polymers or thermo-responsive polymers are polymers that exhibit a phase separation and change in their physical properties as a result of temperature change in the environment. The temperature-responsive polymers display a miscibility gap in their temperature-composition diagram. Depending on whether the miscibility gap is found at low or high temperatures, an upper (UCST) or lower (LCST) critical solution temperature, respectively, exists (Figure 2.2) (Hoffman 1995).
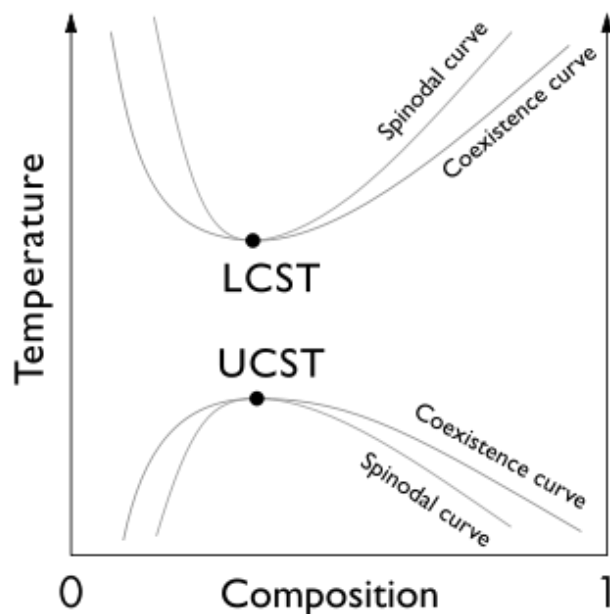
Figure 2.2. A plot of typical polymer binary solution phase behaviour including both an LCST and UCST. (Source: Koningsveld et al. 2001)

Temperature-responsive polymer chains in solution take an expanded coil conformation. At the critical phase-separation temperature, polymer chains collapse to form compact globule. This is followed by the aggregation of globules, subsequently causing turbidity in solution and the formation of visible particles depending on polymer concentration. The phase-separation temperature, at which polymer-poor and polymer-rich phases separate from each other, is dependent on polymer concentration. The phase separation temperature increases when concentration of the polymer increases up to intersection of spinodal and binodal curves, then decreases for UCST and vice versa for LCST (Figure 2.2). In a polymer-solvent binary mixture, the composition of the coexisting phases can be determined by drawing tie-lines; spinodal and binodal curves (Figure 2.2) (Koningsveld et al. 2001). The binodal or coexistence curve implies the condition at which two separated phases may coexist. In other words, it is the boundary between the set of conditions in which it is thermodynamically favourable for the system to be fully mixed and the set of conditions in which it is thermodynamically favourable for it to phase-separate (IUPAC 2013). The spinodal curve is the limit of stability of a solution, stating the boundary of absolute instability of a solution to decomposition into multiple phases (Sandler 2006). Inside this curve, very small fluctuations in composition and density will result in phase separation via spinodal decomposition. Outside of the curve, the polymer solution will be at least

metastable with respect to fluctuations. In general, the spinodal curve lies inside of a binodal curve, which refers to the minimum-energy equilibrium state of the system (Koningsveld et al. 2001).

For a thermodynamically favourable dissolution process of a polymer, the entropy change upon mixing should be positive while the change of Gibbs energy (ΔG) should be negative. From Gibbs-Helmholtz equation, ΔG is determined by the enthalpy of mixing (ΔH) and entropy of mixing (ΔS).

$$\Delta G_{mix} = \Delta H_{mix} - T \cdot \Delta S_{mix} \tag{2.1}$$

In an ideal mixing process where there are no repulsive or attractive interactions between the compounds, there would be no enthalpy change upon mixing. In this case, the change of entropy upon mixing is always positive (the term $-T \cdot \Delta S$ is negative) and ΔG would be negative for all compositions. Thus, the miscibility gaps are due to intermolecular and intramolecular interactions. In polymer solutions three interactions have to be taken into account for dissolution process; polymer-polymer, solvent-solvent and polymer-solvent interactions. Flory and Huggins developed a model for the phenomenological description of polymer phase diagrams also known as Flory-Huggins solution theory (Koningsveld et al. 2001).

The Flory-Huggings equation (Equation 2.2) for the change of Gibbs energy includes a term for the entropy of mixing for polymers and an interaction parameter that describes the sum of all interactions. The first term on the right side of this equation is the entropic contribution to the Gibbs energy and the second term is the enthalpic contribution (Sandler 2006).

$$\frac{\Delta G_{mix}}{RT} = \frac{\emptyset_1}{m_1} \ln\emptyset_1 + \frac{\emptyset_2}{m_2} \ln\emptyset_2 + \chi\emptyset_1\emptyset_2$$

$$\chi = \frac{z\Delta\varepsilon_{12}}{kT} \tag{2.2}$$

where

R = universal gas constant

m = number of occupied lattice sites per molecule (for polymer solutions m_1 is approximately equal to the degree of polymerization and $m_2=1$)

φ = volume fraction of the polymer (1) and the solvent (2), respectively

χ = Flory interaction parameter

ε_{12} = interaction energy between polymer and solvent molecules.

z = number of nearest neighbour atoms of polymer molecule.

k = Boltzman constant

2.1.2. Lower Critical Solution Temperature (LCST)

The lower critical solution temperature (LCST) is the critical temperature below which the components of a mixture are miscible for all compositions and upper critical solution temperature (UCST) is the critical temperature below the mixture is immiscible (IUPAC 2013).

Since the entropy of mixing is low for polymer solutions, miscibility gaps are observed that many polymers show a thermo-responsive property in organic solvents. Polystyrene in cyclohexane, (Schultz et al. 1952, Hashizume et al. 1981) polyethylene in diphenylether (Nakajima et al. 1966, Koningsveld et al. 1968) or polymethylmethacrylate in acetonitrile (Fox 1962) are examples of the polymers that show UCST. LCST is observed for, e.g., polymethylmethacrylate in 2-propanone (Cowie et al. 1976), polypropylene in n-hexane (Cowie et al. 1974), and polystyrene in butylacetate (Pfohl et al. 1995).

Temperature-responsive polymers that have a lower critical solution temperature (LCST) have gained an increasing interest in the last twenty years. On the other hand, polymers that have thermo-responsive property in water are especially important since water as a solvent is cheap, safe and biologically relevant. Among various polymers having LCST in water, the most studied polymer is poly(N-isopropylacrylamide) (Poly(NIPAAm)) (Fujishige et al. 1989, Heskins et al. 1968).

Ding et al. reported that while Poly(NIPAAm-co-HEMA) has similar LCST with NIPAAm homopolymer (32 $^{\circ}$C), the copolymer of NIPAAm with vinyl sulfone have a lower LCST (27.5 $^{\circ}$C). They explained this decrease with increased hydrophobicity of the copolymer due to vinyl sulfone content (Ding et al. 1999).

Barker and co-workers synthesized a series of NIPAAm-based, thermo-responsive copolymers with varying amounts of N,N-dimethylacrylamide (DMAC). The authors altered the hydrophilic/hydrophobic balance through copolymerization by changing copolymer composition. They reported that increasing the DMAC content of NIPAAm/DMAC copolymers raises their LCST to an extent which depends on the amount of the more hydrophilic comonomer (DMAC) in the copolymer structure. Barker and co-workers showed that increasing the hydrophilic/hydrophobic ratio of such thermo-responsive systems serves to raise the LCST (Barker et al. 2003).

Sumerlin et al. reported the synthesis of Poly(NIPAAm)- bovine serum albumin (BSA) conjugates in aqueous media via RAFT polymerization. Conjugation of BSA to a chain transfer agent (CTA) allows the synthesis of block copolymers of polymer and protein since trithiocarbonate group of CTA is capable of extension with a monomer in the presence of a radical source. Sumerlin and co-workers also reported that although Poly(NIPAAm) was conjugated to a protein, it retained thermo-responsive properties (Li et al. 2011).

Both pH- and temperature-responsive copolymers of acrylic acid and NIPAAm were synthesized by Bulmus and co-workers. They also conjugated the copolymer to streptavidin in order to investigate the effect of pH and temperature on the binding and release of biotin. They demonstrated that this copolymer-streptavidin conjugate can provide pH control of biotin binding and triggered release which can be applied to affinity separations, biosensors and drug delivery (Bulmus et al. 2000).

Other than Poly(NIPAAm) which is the most known thermo-responsive polymer in water, further thermoresponsive polymer examples include hydroxypropylcellulose (Kagemoto et al. 1971), poly(vinylcaprolactame) (Maeda et al. 2002) and polyvinyl methyl ether (Schild et al. 1990).

There are also some industrially relevant polymers that show LCST as well as UCST behaviour in aqueous solutions; however the UCST is usually outside the range between 0 and 100 °C, which makes these polymers difficult to be used especially in biotechnology or biomedical applications. Examples of such polymers include polyethylene oxide (Malcolm et al. 1957, Saeki et al. 1976), polyvinylmethylether (Assche et al. 2011) and polyhydroxyethylmethacrylate (Longenecker et al. 2011).

In recent years, a new thermo-responsive polymer family, oligo(ethylene glycol) (meth)acrylates has been found as an interesting alternative to Poly(NIPAAm). These

polymers combine the advantages of poly(ethylene glycol) (PEG) and thermo-responsive polymers in a single macromolecular structure (Lutz 2011).

2.1.3. Oligo(Ethylene Glycol) Methyl Ether Methacrylate (OEGMA) Polymers

Poly(ethylene glycol) (PEG) is a non-toxic and non-immunogenic polymer, that consists of repeating ethylene oxide units. Poly(oligo(Ethylene Glycol) Methyl Ether Methacrylate Poly(OEGMA) is a comb-type PEG which includes a methacrylate-based polymer backbone and short oligoethyleneglycol chains that are grafted to the methacrylate backbone (Figure 2.3).
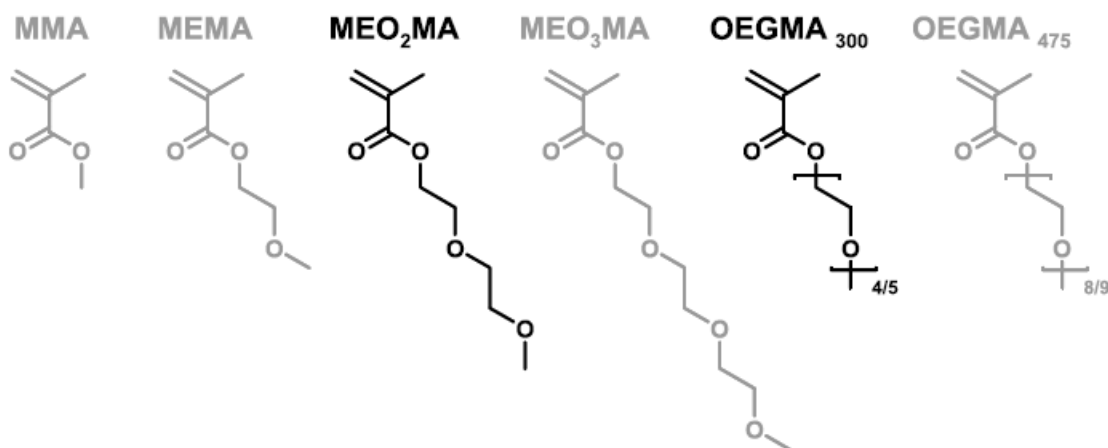
Figure 2.3. Molecular structures of oligo(ethylene glycol) methacrylate (OEGMA) monomers most widely used to make thermo-responsive oligo(ethylene glycol) methyl ether methacrylate polymers (Poly(OEGMA)). (Source: Lutz et al. 2009)

The copolymers of OEGMA based monomers combine the advantages of PEG and thermo-responsive polymers in a single macromolecular structure. OEGMA copolymers also have the following inherent advantages as compared to Poly(NIPAAm);

i)   An excellent bio-repellency below LCST (anti-fouling behaviour)

ii)   Bio-inert properties

Although oligo(ethylene glycol) pendant chains can be connected to various types of polymeric backbones, the polymerization of oligo(ethylene glycol) (meth)acrylates is the most effective strategy for preparing thermo-responsive polymers.

Another point is that these monomers can be easily polymerized by using straightforward controlled radical polymerization techniques such as atom transfer radical polymerization (ATRP) and reversible-addition fragmentation chain transfer (RAFT) polymerization (Lutz 2011).

Lutz and his co-workers synthesized copolymers of MEO_2MA and $OEGMA_{300}$ via ATRP and conventional radical polymerization methods. The authors showed that tuning the LCST between two homopolymers' LCST range with a precision of 0.5 ^{o}C was possible by changing co-monomer ratios in the polymerization feed. They reported the LCST of poly(MEO_2MA) and poly($OEGMA_{300}$) as 28 ^{o}C and 65 ^{o}C respectively (Lutz et al. 2009). This is expected since the hydrophilicty of poly($OEGMA_{300}$) is higher than that of poly(MEO_2MA) .

Effect of polymer concentration on LCST was investigated by Gibson and co-workers using OEGMA (co)polymers (i.e (oligoethyleneglycol) methyl ether methacrylate ($OEGMA_{300}$, $OEGMA_{475}$), diethylene glycol methyl ether methacrylate (MEO_2MA), triethylene glycol methyl ether methacrylate (MEO_3MA)) synthesized via RAFT polymerization. They showed that there is a 6 ^{o}C difference in LCST of a polymer aqueous solution which has a concentration of 0.1 mg/ml and 5 mg/ml. They also show that these OEGMA (co)polymers can exhibit a phase transition at low concentrations which is important in drug delivery applications (Gibson et al. 2011).

Effect of solvent on catalytic chain transfer (co)polymerizations of OEGMA monomers was investigated by Soeriyadi et al. The authors reported that acetonitrile is the best solvent among the solvents examined (i.e water or water/methanol), since it yielded polymers with narrower weight distributions (Soeriyadi et al. 2011).

2.2. Living/Controlled Polymerization

In commercial polymer production, one of the most widely used techniques is free radical polymerization. Free radical polymerization is a type of chain growth polymerization. In a free radical polymerization, propagating species are free radicals formed by an initiator. Free radical polymerization occurs in three steps: initiation, propagation and termination. Firstly, primary radicals are generated. In the second step, monomeric radicals and oligomeric chains propagate by adding monomeric units. In termination step, radicalic polymeric chains terminate since they can self-react by

combination or disproportionation. Due to challenges in control over the molecular weight and molecular weight distribution, and also difficulties in preparation of end-group functional polymers and varying polymer architectures via conventional free radical polymerization, controlled/living radical polymerization techniques become popular.

The living radical polymerization techniques which emerged most recently include nitroxide-mediated polymerization (NMP), atom-transfer radical polymerization (ATRP), reversible addition-fragmentation chain transfer (RAFT) polymerization, and macromolecular design via interchange of xanthates (MADIX) polymerization (Boyer, et al. 2009). RAFT polymerization that was used to prepare (co)polymers in this thesis, has been described below in detailed.

2.2.1. RAFT Polymerization

RAFT (reversible addition−fragmentation chain transfer) polymerization, a reversible deactivation radical polymerization (RDRP), firstly reported by CSIRO (Commonwealth Scientific and Industrial Research Organization) group in 1998, is one of the most effective and versatile methods for providing living characteristics to radical polymerization. Living character of polymers comes from the fact that radicalic polymer chains formed during polymerization terminate at a negligible level and are able to polymerize with addition of new monomer in the presence of a radical source (Boyer et al. 2009).

The RAFT technique is applicable to wide variety of reaction conditions and monomers (Jenkins et al. 2010). It can be performed in bulk, water (Love et al. 2003), emulsion or suspension (Boyer et al. 2009).

The RAFT polymerization can be considered as a conventional free radical polymerization (Figure 2.4) which is carried out with the help of a chain transfer agent (i.e. RAFT agent).
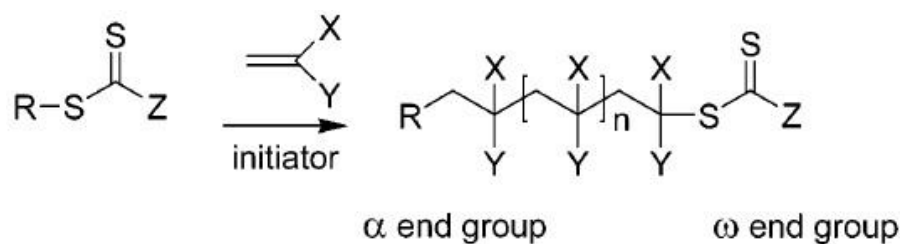
Figure 2.4. Schematic representation of RAFT polymerization
(Source: Chong et al. 2007).

The chain transfer agents used in the RAFT polymerization are organic compounds having a thiocarbonylthio moiety. The general structure of the RAFT agent is shown in Figure 2.5. The mostly used functional Z groups in RAFT agents are dithioesters, trithiocarbonates, and aromatic dithiocarbamates, *N*-alkyl-*N*-aryldithiocarbamates and the O-alkyl xanthates.
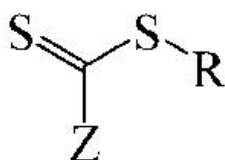
Figure 2.5. General structure of a RAFT agent
(Source: Keddie et al. 2012)

Initiation is the first step of the polymerization, where the starting radicals are created. The most widely known method of initiation is thermal decomposition of a radical initiator, but also different sources of initiation in RAFT polymerizations have been reported, such as photochemical initiation by ultraviolet light (Cowie and Arrighi 2008), γ radiation, pulsed laser irradiation (Odian 2004), and thermal autoinitiation of monomer (Cowie and Arrighi 2008).

In initiation step, the initiator decomposes to form two fragments (I•) which react with a single monomer molecule to yield a propagating polymeric radical of length 1. In propagation step, propagating radical chains of length n, Pn•, add monomer, M, form longer propagating radicals. In RAFT pre-equilibrium step, oligomeric radicals are produced and react with the RAFT agent to form a RAFT adduct radical. The radical intermediate can then fragment back to the original RAFT agent and an oligomeric radical or fragment to yield an oligomeric RAFT agent and a reinitiating R radical (Boyer et al. 2009). This is a reversible step in which the intermediate RAFT adduct

radical is capable of losing either the R group (R•) or the polymeric species (P_n•). The structure of R should be such a good reinitiating group. It should fragment at least as quickly as the initiator or polymer chains from the stabilized radical intermediate. If fragmentation is slow, the intermediate species is consumed in side reactions, or reinitiation is slow or inefficient, and then retardation or inhibition can result (Keddie et al. 2012). In reinitiation, the leaving group radical (R•) reacts with another monomer species, starting another active polymer chain. Following initialization, polymer chains grow by adding monomer, and they rapidly exchange between existing growing radicals (as in the propagation step) and the thiocarbonylthio group capped species. The rapid interchange in the radical intermediate ensures that the concentration of growing radical chains is kept lower than that of the stabilized radical intermediates, therefore limiting termination reactions. In termination step although RAFT is a living polymerization there is still limited termination reactions occur via combination or disproportionation mechanisms (Boyer et al. 2009, Cowie and Arrighi 2008). The generally accepted simplified mechanism of the RAFT polymerization is shown in Figure 2.6.
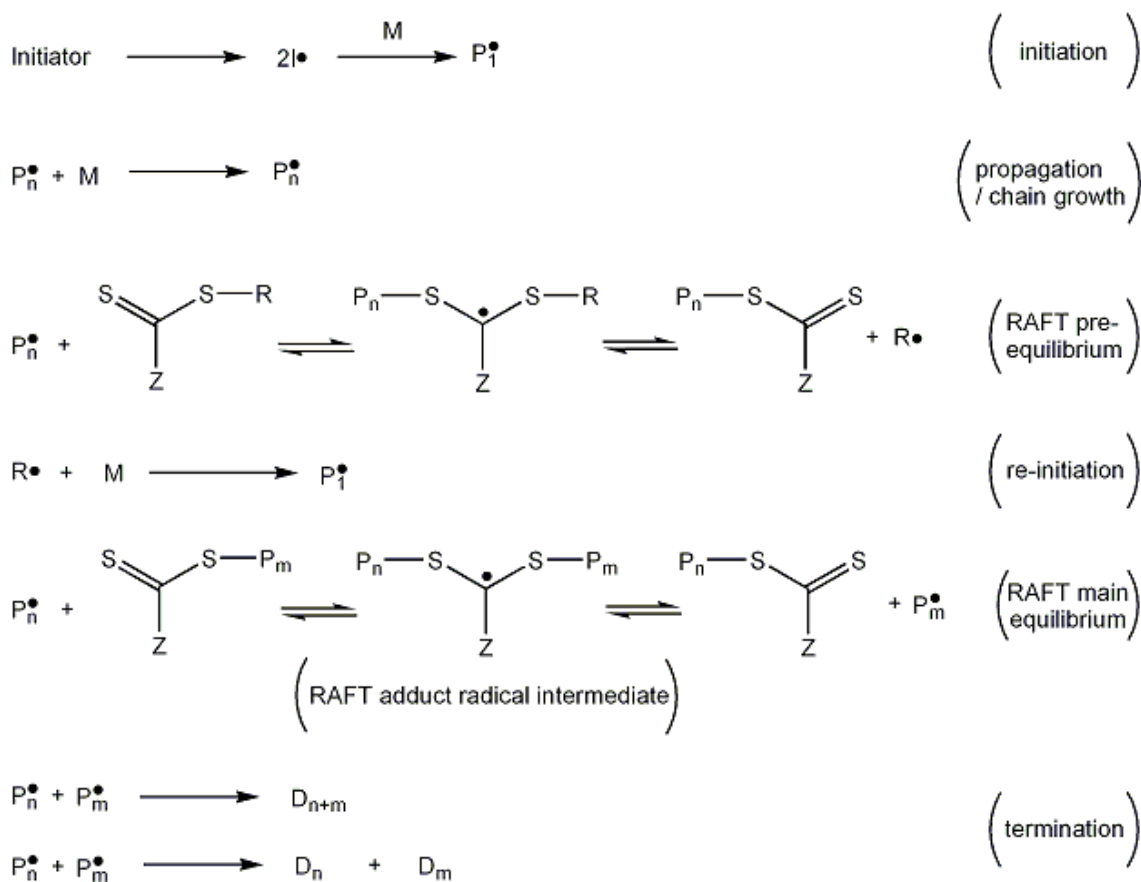
Figure 2.6. Reaction mechanism of RAFT polymerization.
(Source: Cowie and Arrighi 2008)

In RAFT polymerization choosing an appropriate RAFT agent for the monomer(s) to be polymerized and the reaction conditions is the key factor for optimal control. The Z and R groups in RAFT agent structure both play critical roles in determining the result of polymerization. By determining the rate of addition and fragmentation, they control efficiency of chain transfer and the probability of retardation or inhibition (Keddie et al. 2012). The R group is important in the pre-equilibrium stage of the polymerization. The Z group is highly influential in determining the reactivity and consequently effectiveness of the RAFT agent at mediating polymerization.

According to the explained reaction mechanism above, the rapid equilibrium between the active propagating radicals and the polymeric thiocarbonylthio compounds provides equal probability for all chains to grow and allows for the production of polymers with controlled molecular weight and narrow molecular weight distribution (low polydispersity). By considering this fact, a linear relationship between the number average molecular weight and the conversion is assumed, thus the theoretical number average molecular weight can be estimated using Equation 2.3.

$$M_{ntheoretical} = \left[\frac{[M]}{[R]} \text{ x conversion x } MW_{Monomer} \right] + MW_{RAFT} \qquad (2.3)$$

where;

[M] is the monomer concentration

[R] is the RAFT agent concentration

$MW_{monomer}$ is the molecular weight of the monomer

MW_{RAFT} is the molecular weight of the RAFT agent

2.3. End-group Functionalization of RAFT-Synthesized Polymers

The RAFT polymerization technique allows the generation of a wide range of polymers with different functionalities. Polymers with different architectures could be easily synthesized via RAFT polymerization. The colourful RAFT agent (such as yellow, pink and red) is an indication of the final polymer containing non-degraded RAFT end-groups which can be further utilized to chain extend or modify the end-group of the polymers.

As explained above, since RAFT mechanism proceeds by insertion of monomer units into the C-S bond, end-functionalized polymers can be easily produced in one-step by incorporating the functional groups into the RAFT agent (as R or Z-groups) (Chong et al. 2007). There are a number of routes for the synthesis of RAFT agents which allow the incorporation of functional end-groups to polymer chains. The incorporation of functionality into the R or Z group of the RAFT agent results in the direct synthesis of α-end or ω-end-functionalized polymers, respectively (Willcock et al. 2010) with examples including carboxylic acid (Skey et al. 2008), peptide (Hentschel et al. 2008)and lipid-functionalized polymers (Bathfield et al. 2008).

In addition to the direct synthesis of end-group functionalized polymers using functionalized RAFT agents, the ω-end of the RAFT-synthesized polymers, which contains a thiocarbonylthio group allows for post-polymerization modification of the polymers from ω-terminus (Boyer et al. 2009).

To perform post-polymerization modifications on the ω-terminus of the RAFT-synthesized polymers, the first step usually requires the cleavage of thiocarbonylthio group of the polymer. There are number of methods available to cleave thiocarbonylthio groups (Figure 2.7).
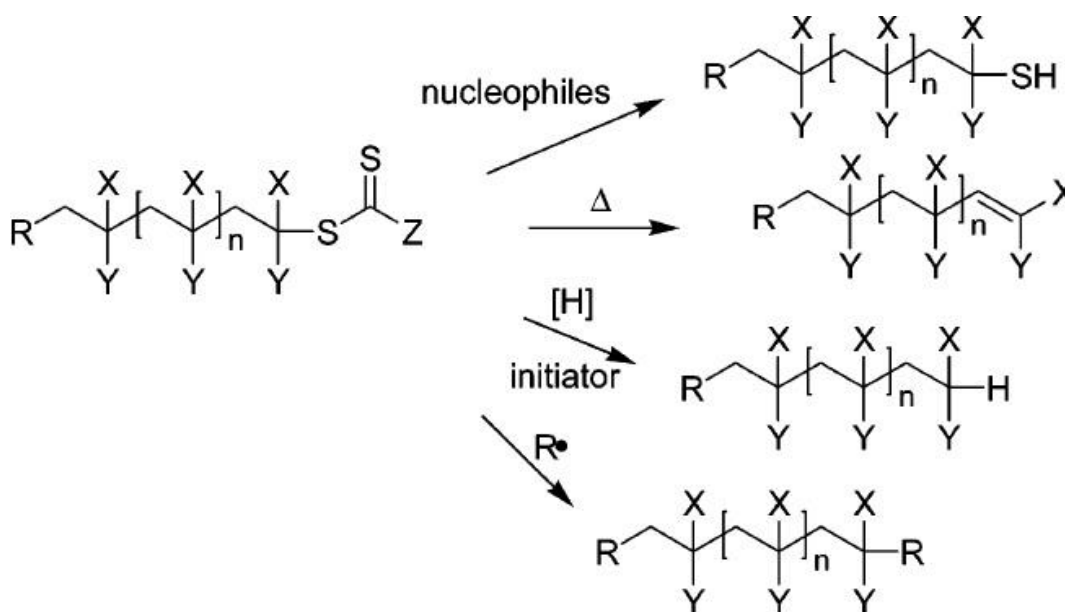
Figure 2.7. Schematic of main methods for cleavage of thiocarbonylthio group in order to perform post-polymerization modification of RAFT-synthesized polymers (Source: Chong et al. 2007)

Reaction of thiocarbonylthio compounds with nucleophiles and ionic reducing agents (e.g. amines (Moad et al. 2005), hydroxide (Kabachii et al. 2006), borohydride (Scales et al. 2006)) is one of the most well-established and widely reported methods for post-polymerization modification of polymer end-groups. The reaction transforms the thiocarbonyl containing group into a thiol which can be utilized in further coupling reactions (Chong et al. 2007).

The kinetics and mechanism of the reaction of thiocarbonythio groups with excess amines were reported in 1990 (Deletre et al. 1990) and the method has since been used to cleave RAFT-end groups from polymers. Today it is one of the most widely used and versatile methods of RAFT end-group conversion, resulting in the formation of a thiol end-group that can be subsequently utilized in a number of reactions (Figure 2.8). Either primary or secondary amines acting as nucleophiles can convert a thiocarbonylthio group to a thiol. The exclusion of oxygen from the reaction is vital as the thiols formed can be readily oxidized to disulfides resulting in dimerization of polymer chains to yield higher molecular weights (Willcock et al. 2010).

Li et al. investigated the efficiency of primary, tertiary amines and phosphines, for the reaction of a range of thiols with dimers and oligomers of some (meth)acrylates. They reported that although primary and tertiary amines required several hours to reach high conversion, they were efficient catalysts for the thiol–ene reaction. On the other hand, the phosphine catalysts, dimethylphenylphosphine (DMPP) and tris-(2-carboxyethyl)phosphine (TCEP), was an efficient catalyst yielding complete conversion in few minutes under optimized conditions. However the concentration of DMPP was found to be very important in reaction. When it was used in higher than catalytic level side reactions occurred. The acidity of TCEP was also found to be important in the same manner due to the side reactions occurred at acidic pH (Li et al. 2010).
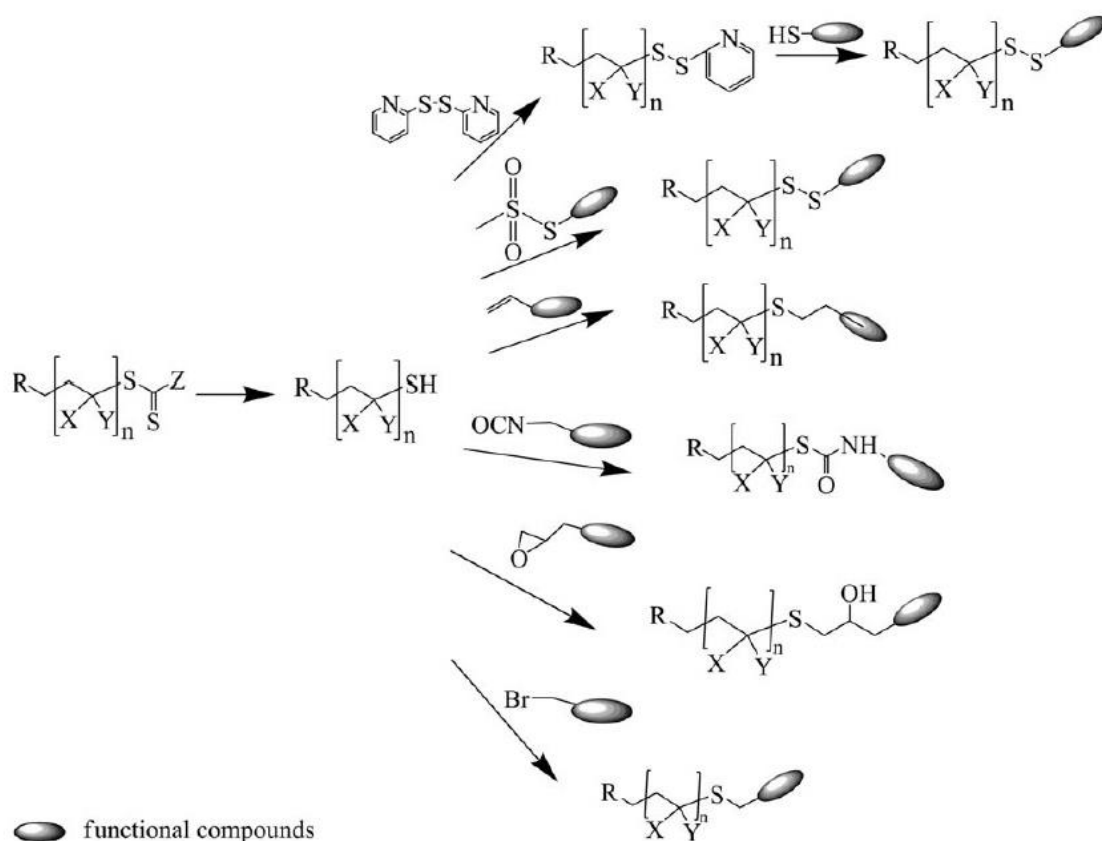
Figure 2.8. Schematic of aminolysis of RAFT end-group and further utilization of thiol
group via pyridyl disulfide, thiol-ene, thiol-iso-cyanate, thiol-epoxy, thiol-
bromo nucleophilic reactions (Source: Boyer et al. 2011).

Boyer et al. reported the investigation of aminolysis of ω-end group of RAFT polymers and simultaneous thiol-ene reactions. In order to overcome the disulfide coupling problem during aminolysis reaction, the authors performed aminolysis reactions in the presence of thiol-reactive compounds, such as pyridyldisulfide-bearing or ene-bearing compounds. This led to simultaneous protection or functionalization of the created thiol groups. They further used this versatile method to yield new architectures (Boyer, Granville, Davis and Bulmus 2009).

Thermal elimination of the RAFT end-group from polymers is a method of end-group removal that can result in sulfur free end-group. Thermolysis provides complete desulfurization of the polymer yielding an unsaturated chain end. It has the advantage of being easy to carry out with no chemical additions. One drawback of this method is that the polymer and any functionality must be stable at the thermolysis conditions, which typically involve temperatures from 120–200 $^{\circ}$C.

Radical induced reduction can also yield a sulfur-free hydrocarbon end group by using hypophosphite salts as the H atom source and has been reported with the advantage that both the excess reagent and by-products are water-soluble and thus can be easily removed from the polymer (Chong et al. 2007). Radical induced reduction has also been used to end-cap the polymer with the required group through the use of functionalised azo-initiators (Heredia et al. 2009).

The end-group of the RAFT synthesized polymers were also modified with free-radical sources via radical cross-coupling. Perrier et al. proved this method for the removal of dithiobenzoate end groups from PMMA using 2,2'-azo(bis)isobutyronitrile (AIBN) as the initiating species. They showed the complete removal of the RAFT end-group along with the recovery of the RAFT agent with this method (Perrier et al. 2005).

There are also a number of examples of the use of the thiocarbonyl as a dienophile with both small molecule dienes (Inglis et al. 2008) and dienes at polymer chain ends (Sinnwell et al. 2008) in reversible hetero-Diels–Alder reactions. Such reactions have been used to synthesise diblock copolymers as well as more complex macromolecular structures such as star polymers (Willcock et al. 2010).

CHAPTER 3

EXPERIMENTAL STUDY

3.1. Materials

Diethyleneglycol methyl ether methacrylate (MEO$_2$MA) (number-average molecular weight M_n= 188 g/mol) (95%) and oligo(ethylene glycol) methyl ether methacrylate (OEGMA) (number-average molecular weight M_n= 300 g/mol) (%95) were purchased from Sigma-Aldrich and deinhibited by passing through a basic aluminium oxide column before use. 2,2 –Azobisisobutyronitrile (AIBN) was purchased from Wako Chemicals and recrystallized in methanol twice before use. 4-Cyano-4-(thiobenzoylthio)pentanoic acid (CDTB, 97%) and, 2,2′-dithiodipyridine (DTDP), diethyl bromopropylphosphonate (DEBrPP, 97%), triethylamine (TEA,>99%), hexylamine (HEA, 99%), and potassium carbonate (K$_2$CO$_3$) were purchased from Aldrich and used as received. Diethylether (Sigma, >99.7%), acetonitrile (Sigma-Aldrich, >99.9%), dichloromethane (Sigma-Aldrich, >99.8%), dimethylformamide (Sigma-Aldrich, >99.9%), chloroform-d (Sigma-Aldrich, >99.8%), N,N-dimethylacetamide (DMAc, Sigma-Aldrich, HPLC grade >99.9%, Alfa Easer HPLC grade > 99.5%) were used as received and deionized water was obtained using a Millipore MILIQ system with a resistivity of 18.2 mΩ/cm.

3.2. Methods

3.2.1. Synthesis of Polymers

Homo- and co-polymers of diethyleneglycol methyl ether methacrylate (MEO$_2$MA) and oligo(ethylene glycol) methyl ether methacrylate (OEGMA) were synthesized via RAFT polymerization.

Polymerizations were carried out at 65 ºC using AIBN as a radical initiator (I), CDTB as a chain transfer agent (CTA) and acetonitrile as a solvent. Figure 3.1 shows

schematically the polymerization reaction. Samples were synthesized at varying [Total Monomer]/[CTA]/[I] and feed comonomer molar ratios. The total monomer concentration was kept constant to be 1 M for all polymerizations. Table 3.1 shows the [Total Monomer]/[CTA]/[I] and comonomer ratios in the feed and reaction conditions used in copolymerization experiments. Briefly, all reagents at specified ratios were dissolved in acetonitrile and the solution was placed in a reaction vial. Vial sealed with septum was placed in an ice-bath and purged with nitrogen for 30 minutes. The vial was then placed in an oil-bath at 65 ℃. Polymerization was allowed to take place for a predetermined time and then stopped by placing the vial in an ice-bath. The solvent was removed under vacuum. Aliquot from the sample was taken for monomer conversion analysis by ^{1}H NMR.
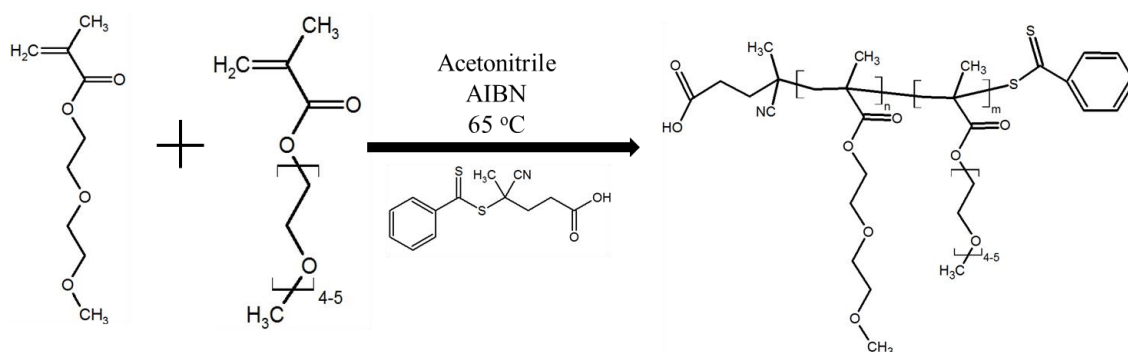
Figure 3.1. Copolymerization of MEO$_2$MA and OEGMA via RAFT polymerization

In order to purify (co)polymers, 3 different purification strategies were applied. The first strategy was used for the polymers that have equal or higher than %50 OEGMA content. In the first strategy polymerization mixture after the removal of the polymerization solvent was precipitated in diethylether. The samples were centrifuged at 15000 rpm for 1 min. The supernatant was removed and fresh diethylether was added to precipitate and the sample was redispersed in diethylether followed by centrifugation. The same procedure was repeated 10 times. The final product was collected after drying under vacuum. In order to determine purity and final copolymer composition ^{1}H NMR analysis was performed.

The second purification strategy was used for the polymers that produced contained 75% MeO$_2$MA and 25% OEGMA, thus was not enough polar to precipitate in diethylether. In the second strategy, water / ether extraction was applied to purify samples. After the removal of polymerization solvent, polymer sample was dissolved in

water and then extracted against diethylether using a water:ether (v:v) ratio of 1:3. The extraction was repeated 10 times. The water phase was collected. The final product was obtained after freeze-drying.

For the polymers that have 100% MEO$_2$MA, since polymers are not polar enough to use first two strategies the third strategy, i.e. thermal precipitation method was then used. In this method, after removal of the polymerization solvent, the polymerization mixture was dissolved in water at 4 ºC. The solution was then heated to 80 ºC, followed by centrifugation at 40 ºC and 15000 rpm for 1 minute. The supernatant was removed. The precipitate was dissolved again in water at 4 ºC to repeat the purification procedure. This process was repeated ten times. The final product was obtained after freeze-drying.

After purification all polymers were characterized with ^{1}H-NMR to satisfy the polymers purity and for calculation of degree of polymerization, and final monomer composition and also characterized with GPC for molecular weight and polydispersity index determination.

Table 3.1. Feed monomer composition and reaction conditions of the samples

POLYMERIZATIONS PERFORMED TO INVESTIGATE POLYMERIZATION KINETICS				
Polymer Code [a]	[Total Monomer]/[b] [CDTB]/[AIBN]	Feed Composition MEO$_2$MA%	OEGMA%	Polymerization Time
RCM-1	[20]/[1]/[0.25]	75	25	1hr
RCM-2	[20]/[1]/[0.25]	75	25	3hr
RCM-3	[20]/[1]/[0.25]	75	25	4hr
RCM-4	[20]/[1]/[0.25]	75	25	5hr
RCM-5	[20]/[1]/[0.25]	75	25	6hr
RCM-6	[50]/[1]/[0.25]	75	25	1hr
RCM-7	[50]/[1]/[0.25]	75	25	2hr
RCM-8	[50]/[1]/[0.25]	75	25	4hr
RCM-9	[50]/[1]/[0.25]	75	25	5hr
RCM-10	[50]/[1]/[0.25]	75	25	6hr
RCM-11	[100]/[1]/[0.25]	75	25	1hr
RCM-12	[100]/[1]/[0.25]	75	25	2hr
RCM-13	[100]/[1]/[0.25]	75	25	3hr
RCM-14	[100]/[1]/[0.25]	75	25	4hr
RCM-15	[100]/[1]/[0.25]	75	25	5hr

(cont.)

Table 3.1. (cont.)

POLYMERIZATIONS PERFORMED TO INVESTIGATE REACTIVITY RATIO OF COMONOMERS				
RR-1	[500]/[1]/[0.25]	90	10	20min
RR-2	[500]/[1]/[0.25]	80	20	20min
RR-3	[500]/[1]/[0.25]	70	30	20min
RR-4	[500]/[1]/[0.25]	60	40	20min
RR-5	[500]/[1]/[0.25]	50	50	20min
RR-6	[500]/[1]/[0.25]	40	60	20min
RR-7	[500]/[1]/[0.25]	30	70	20min
RR-8	[500]/[1]/[0.25]	20	80	20min
RR-9	[500]/[1]/[0.25]	10	90	20min

POLYMERIZATIONS PERFORMED TO SYNTHESIZE POLYMERS FOR INVESTIGATION OF TEMPERATURE-RESPONSIVE BEHAVIOR				
PT-1	[20]/[1]/[0.25]	100	0	3hr
PT-2	[50]/[1]/[0.25]	100	0	2hr 45min
PT-3	[100]/[1]/[0.25]	100	0	3hr 15min
PT-4	[200]/[1]/[0.25]	100	0	3hr 45min
PT-5	[20]/[1]/[0.25]	75	25	3hr
PT-6	[20]/[1]/[0.25]	75	25	3hr
PT-7	[50]/[1]/[0.25]	75	25	3hr 30min
PT-8	[200]/[1]/[0.25]	75	25	3hr 30min
PT-9	[20]/[1]/[0.25]	50	50	2h 30min
PT-10	[20]/[1]/[0.25]	50	50	2hr 40min
PT-11	[50]/[1]/[0.25]	50	50	3hr 30min
PT-12	[200]/[1]/[0.25]	50	50	3h 45min
PT-13	[20]/[1]/[0.25]	25	75	2h 15min
PT-14	[40]/[1]/[0.25]	25	75	2h 15min
PT-15	[50]/[1]/[0.25]	25	75	3hr 30min
PT-16	[200]/[1]/[0.25]	25	75	3hr
PT-17	[20]/[1]/[0.25]	0	100	2hr
PT-18	[50]/[1]/[0.25]	0	100	2hr 40min
PT-19	[30]/[1]/[0.25]	0	100	5hr
PT-20	[50]/[1]/[0.25]	0	100	5hr

[a] All samples were synthesized at 65°C.
[b] In all reactions total monomer concentration was 1M.

3.2.2. End-group Modification

3.2.2.1. End-group Modification of Polymers with DiThioDiPyridine (DTDP)

Modification of polymers with dithiodipyridine (DTDP) to yield pyridyldisulfide (pds) ended polymers was performed via one-pot aminolysis reaction following the procedures reported previously (Boyer, Liu, Bulmus and Davis 2009). In pds modification reactions, all reagents were dissolved and reacted in one-pot. Figure 3.2 shows schematically the modification of polymers' end group by pds group.
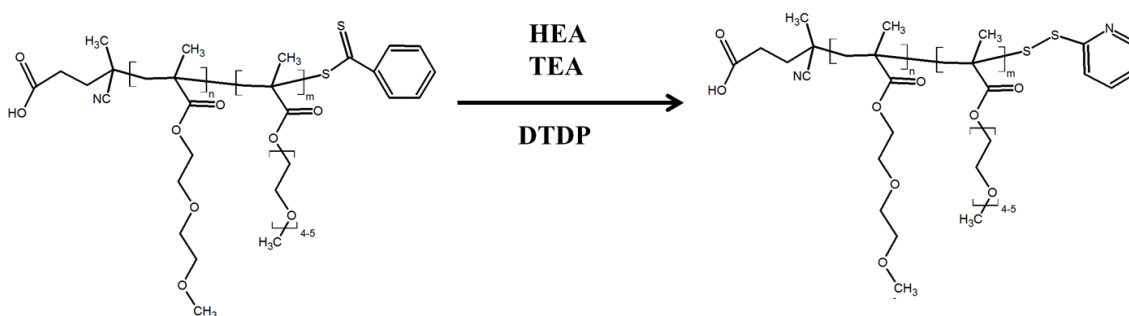
Figure 3.2. Reaction scheme for pds-terminated polymer synthesis via one-pot aminolysis reaction

Briefly, [Polymer]/[DTDP]/[HEA]/[TEA] were dissolved in acetonitrile at a molar ratio of 1/10/10/10. Polymer concentration was set to 4 mM. After purging the solution with N_2 for 30 min, the reaction mixture was allowed to react for 3 hours. After the reaction, reaction mixture was purified via ether precipitation or water/ ether extraction to yield pds-terminated polymer.

After purification all polymers were characterized with ^{1}H-NMR to satisfy the polymers purity and to examine the efficiency of modification reaction. Polymers also characterized with GPC for molecular weight and polydispersity index determination.

3.2.2.2. End-group Modification of Polymers with DiEthylBromoPropylPhosphonate (DEBrPP)

In order to modify polymers with phosphonate end-group, modification was performed in two steps: The first step was to aminolyze the polymer to thiol-terminated polymer. The thiol-terminated polymer was purified and then reacted with DEBrPP in the presence of a base, potassium carbonate (K_2CO_3) to yield phosphonate-terminated polymer via Michael addition reaction (Figure 3.3).
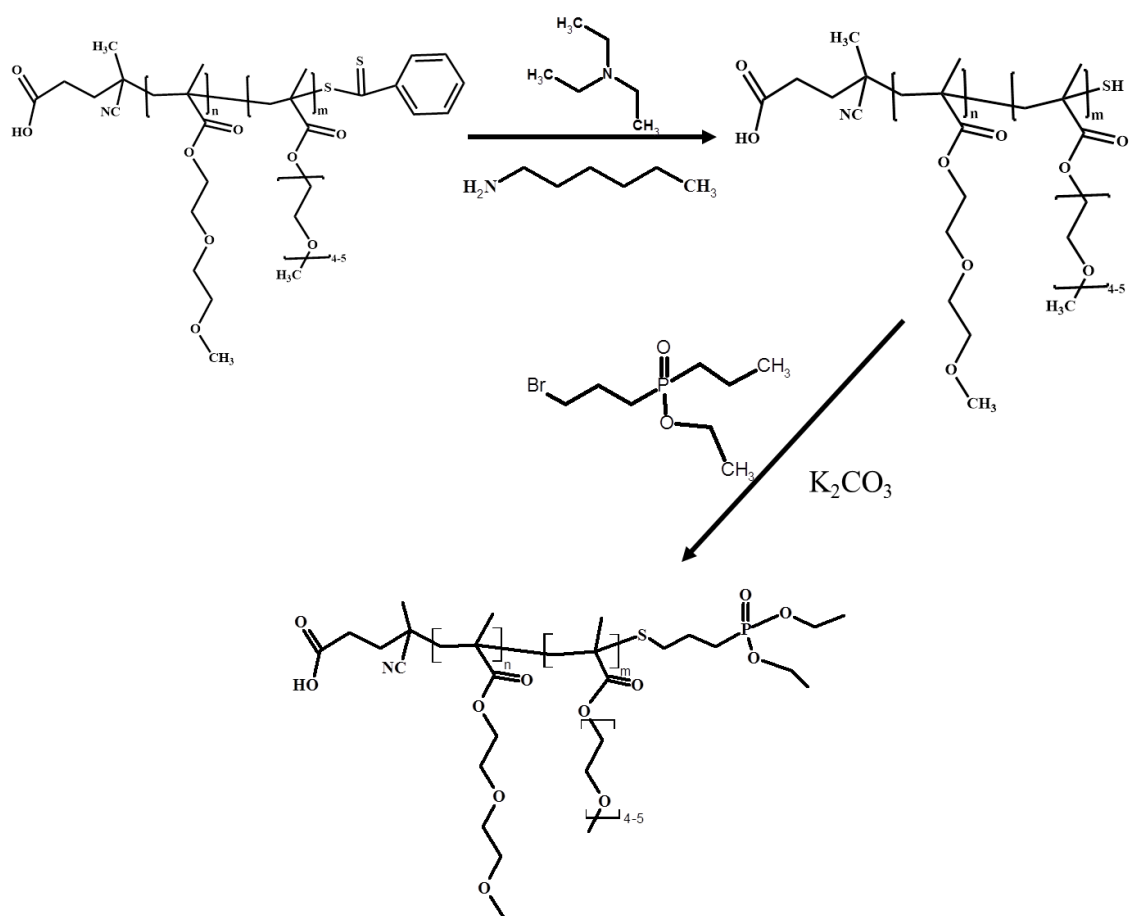
Figure 3.3. Reaction scheme for phosphonate-terminated polymer synthesis via a two-step strategy, Michael addition reaction performed subsequent to aminolysis.

Briefly, poly(MEO$_2$MA) homopolymer or (poly(MEO$_2$MA-*co*-OEGMA) copolymer (4 mM) was first aminolyzed in acetonitrile at room temperature using a [Polymer]/[HEA]/[TEA] molar ratio of 1/10/10 for 3 hours under N_2. After purification via ether precipitation, the thiol-terminated polymer was dried in vacuum. The following phosphonation reactions conditions were modified from Sanfrutos et al.

(Sanfrutos et al. 2011). Briefly, purified, thiol-terminated polymer was dissolved in acetonitrile (60 mM) and reacted with DEBrPP in the presence of K_2CO_3 at room temperature for 24 hours. The reaction was performed at a [Polymer]/[DEBrPP]/[K_2CO_3] molar ratio of 1/1.2/1.8. After the reaction, the reaction mixture was purified via ether precipitation to yield phosphonate-terminated polymer.

After purification polymers were characterized with ^{1}H-NMR to satisfy the polymers purity and with ^{31}P to examine the modification reaction successful or not. Polymers also characterized with GPC for molecular weight and polydispersity index determination.

3.3. Instruments

3.3.1. Nuclear Magnetic Resonance (NMR) Spectroscopy

All ^{1}H and ^{31}P NMR spectra were taken using a Varian VNMRJ 400 spectrometer at Izmir Institute of Technology or Varian Mercury Plus 400 Actively Shielded NMR spectrometer at Ebiltem NMR Laboratory, Ege University, Izmir by using CDCl$_3$ as solvent. The purity, chemical composition, molecular weight and end-group modifications of all polymers produced were determined by NMR spectroscopy.

3.3.2. Gel Permeation Chromatography (GPC)

Gel permeation chromatography (GPC) analyses were performed using *N,N*-dimethylacetamide (DMAc containing 0.05% w/v LiBr) as mobile phase. Analyses were performed using a Shimadzu modular system consisting of an DGU-20A degasser, LC-20AD pump, SIL-20HT auto-injector, CTO-10AS VP column oven, PSS-UDC-810 connection unit and a Polymer Standarts Service 10μm particle-size guard column (50 × 8.0mm) followed by two analytical PSS (Gram) columns (30 and 100 Å) at 25 ºC (flow rate = 1ml/min) and an RID-10A refractive-index detector. The calibration was performed with poly(methyl methacrylate) standards having molecular weights ranging from 410 to 46000 g/mol and narrow polydispersity.

3.3.3. UV-Visible (UV-Vis) Spectrophotometer

For determination of Lower Critical Solution Temperature (LCST), either Thermo-Scientific Evolution 201 or Perkin-Elmer Lambda-45 double beam spectrophotometers with a detection range from 190 to 1100 nm and a photometric detection range of 3.5 absorbance units was used. The instruments were equipped with a thermostatted heating cell unit and a heating bath. LCST of polymers were determined at 500 nm wavelength using polymer solutions in water prepared at 1 mg/ml concentration. The heating rate was constant for all measurements (2 ^{O}C/min). The temperature, at which 10% of maximum absorbance was observed, was defined as LCST.

CHAPTER 4

RESULTS and DISCUSSIONS

4.1. Synthesis of Oligoethyleneglycol Methyl Ether Methacrylate (OEGMA) and Diethyleneglycol Methyl Ether Methacrylate (MEO₂MA) (Co)polymers via RAFT Polymerization

Oligoethyleneglycol methyl ether methacrylate (OEGMA) and diethyleneglycol methyl ether methacrylate (MEO$_2$MA) were copolymerized in the presence of 4-Cyano-4- (thiobenzoylthio)pentanoic acid (CDTB) as a RAFT agent and AIBN as a radical initiator. A series of polymerization kinetic experiments were first performed to determine the conditions at which the (co)polymerizations were controlled by RAFT mechanism. In these experiments, comonomers at a [MEO$_2$MA]/[OEGMA] ratio of 75/25 were polymerized at three different monomer/RAFT agent molar ratios ([M]/[R]) (100/1, 50/1 and 20/1) for varying polymerization times (from 1 to 6 h). Monomer conversion, molecular weight and molecular weight distribution (polydispersity index, (PDI)) were investigated by NMR and GPC, respectively to investigate whether the polymerizations were RAFT-controlled.

The polymerization conditions and the conversion values determined from NMR analysis of the crude polymerization mixture are listed in Table 4.1. The conversion values were calculated according to Equation 4.1. In this equation, the integral of the signal between 4.0 and 4.4 ppm belongs to 2 protons of methylene group of oligoethylene glycol side chains (a in Figure 4.1) of both the monomers and polymer. On the other hand, the integral of the signal between 5.6 ppm and 6.2 ppm belongs to cis- and trans- protons of vinyl protons monomer (b in Figure 4.1). The conversion values increased gradually with polymerization time, as expected.

$$\text{Conversion \%} = \frac{\int_{4.0\text{ppm}}^{4.4\text{ppm}} - \int_{5.6\text{ppm}} - \int_{6.1\text{ppm}}}{\int_{4.0\text{ppm}}^{4.4\text{ppm}}} \times 100 = \frac{a\text{-}b}{a} \qquad (4.1)$$
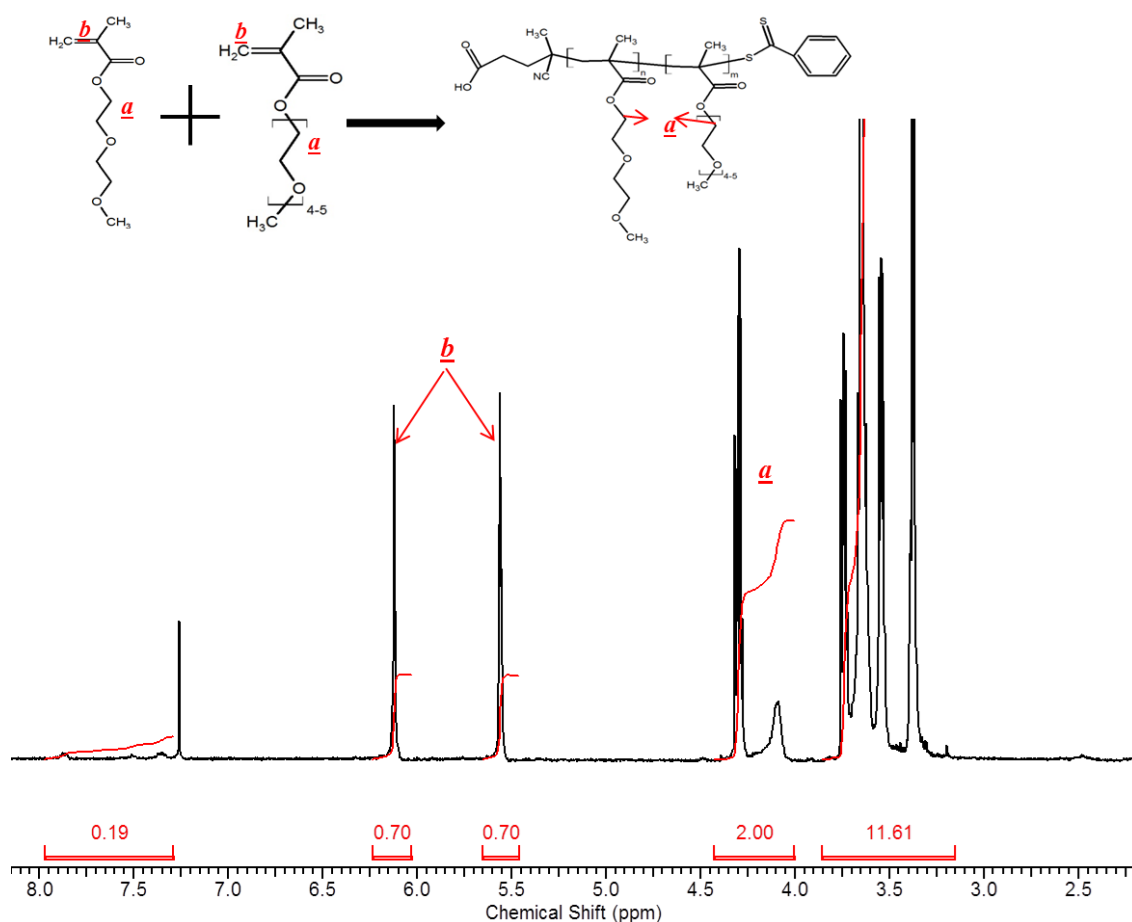
Figure 4.1. ^{1}H-NMR spectrum of polymerization crude mixture obtained at a [Monomer]/[CDTB]/[AIBN] molar ratio of 20/1/0.25, a feed comonomer [MEO$_2$MA]/[OEGMA] ratio of 75/25 and polymerization time= 3 hours.)

According to the conversion values, the first-order monomer conversion plot (i.e. logarithmic plot of the ratio of the initial monomer concentration (Mo) to the monomer concentration left after a determined polymerization time) was drawn against polymerization time (ln (Mo/M) vs. time) in Figure 4.2. The linear increase in ln(Mo/M) with respect to time is an expected result for a living/controlled polymerization such as RAFT polymerization. This linear increase shows that the polymerization is in a stationary state and occurs under constant propagating radical concentration.

The number average molecular weight (Mn) and molecular weight distribution (i.e. polydispersity index, PDI) of polymers were also characterized using gel permeation chromatography (GPC). Table 4.1 shows both the theoretical and experimental Mn's of the purified polymers. Theoretical molecular weights were calculated according to Equation 2.3.

Since in propagation step polymer chains are growing equally molecular weight distribution of final polymer product is narrow. This behaviour was shown in Figure 4.3
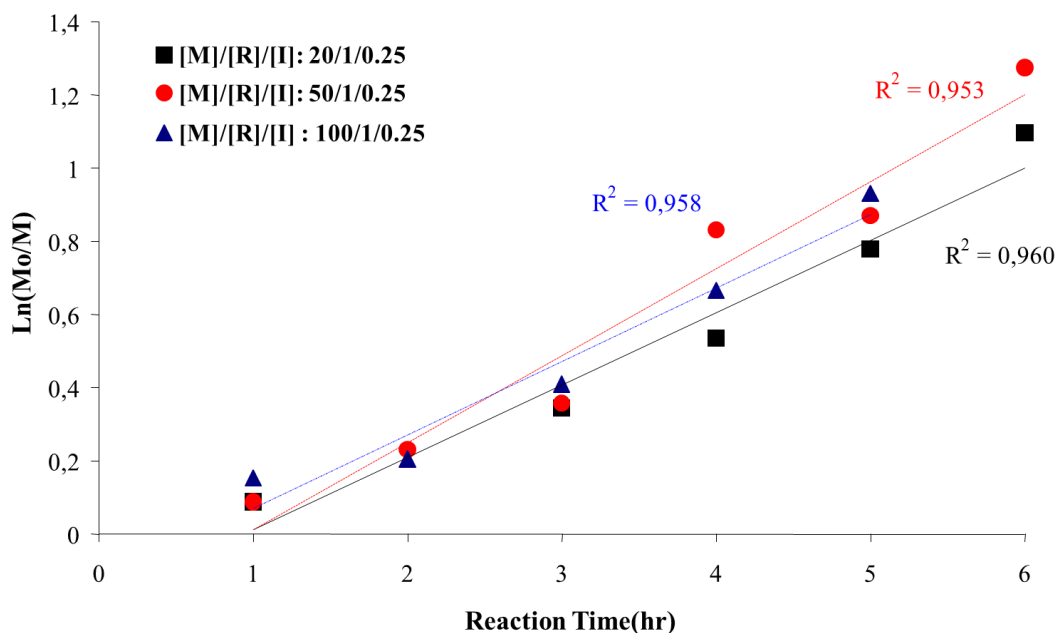

Figure 4.2. Ln(Mo/M) versus polymerization time graph

Table 4.1. Polymerization conditions and the properties of the polymers obtained from the polymerization kinetic experiments.

Polymer Code	[Monomer]/ [a] [CDTB]/[AIBN]	Polymerization Time (h)	Conversion (mol %)[b]	$Mn_{(GPC)}$[c]	$Mn_{(Theo)}$[d]	PDI[c]
RCM-1	20/1/0.25	1	8.5	1000	650	1.13
RCM-2	20/1/0.25	3	30.0	1800	1500	1.18
RCM-3	20/1/0.25	4	41.5	2100	2100	1.18
RCM-4	20/1/0.25	5	54.0	2600	2600	1.17
RCM-5	20/1/0.25	6	66.5	3100	3150	1.17
RCM-6	50/1/0.25	1	8.5	3100	1200	1.85
RCM-7	50/1/0.25	2	20.5	3900	2500	1.10
RCM-8	50/1/0.25	4	56.5	6800	6400	1.18
RCM-9	50/1/0.25	5	58.0	6600	6550	1.11
RCM-10	50/1/0.25	6	72.0	7300	8050	1.16
RCM-11	100/1/0.25	1	14.0	3900	3300	1.09
RCM-12	100/1/0.25	2	18.5	4200	4300	1.13
RCM-13	100/1/0.25	3	33.5	6100	7500	1.17
RCM-14	100/1/0.25	4	48.5	8300	10750	1.16
RCM-15	100/1/0.25	5	60.5	9100	13350	1.14

[a] The molar ratio of total monomer, RAFT agent (CDTB) and initiator (AIBN). [b] The monomer conversion was determined by ^{1}H-NMR according to Equation 4.1. [c] (Mn_{GPC}) and polydispersity index (PDI) determined by gel permeation chromatography [d] Calculated according to Equation 2.3
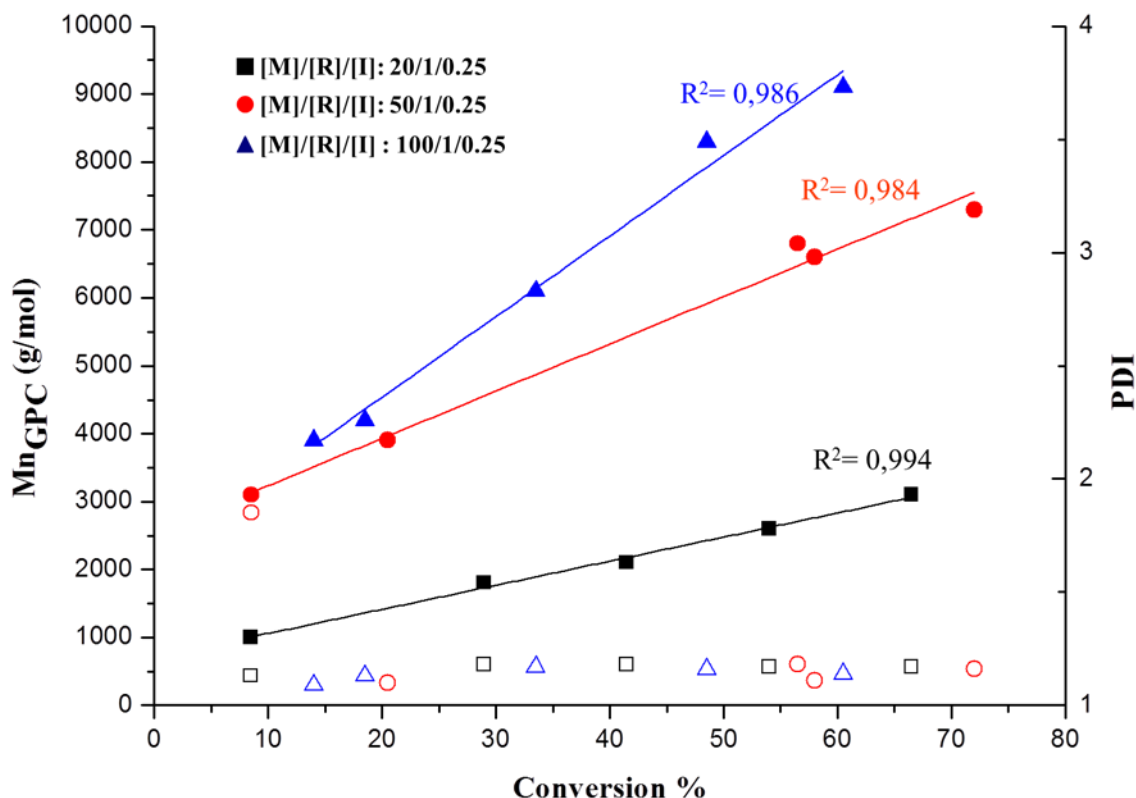
Figure 4.3. Number Average Molecular Weight (Mn_{GPC}) (filled data points) and Polydispersity Index(PDI) (empty data points) of copolymers obtained at a [MEO_2MA]/[$OEGMA_{300}$] feed ratio of 75/25 and varying [Total monomer]/[RAFT]/ [Initiator] ([M]/[R]/[I]) ratios with respect to monomer conversion (%).

The linear increase in molecular weight (Figure 4.3) with respect to monomer conversion and low PDI values (<1.2) proves the RAFT-controlled mechanism of MeO_2MA and OEGMA copolymerizations (Boyer et al. 2009). The increase in Mn with the increase in [M]/[R] ratio, and the good agreement between the theoretical and experimental molecular weights are also direct evidences of RAFT-controlled copolymerization mechanism (Boyer 2011). Since all polymeric chains in propagation step grows equally, in final polymer product all chains are at similar length. As a result of this, low PDI values are obtained. RAFT agent controls the rate of addition and fragmentation, the rapid equilibrium between the active propagating radicals and the polymeric thiocarbonylthio compounds provides equal probability for all chains to grow and allows for the production of polymers with controlled molecular weight. This leads to a linear relationship between molecular weight and conversion.

4.2. Determination of Reactivity Ratios of MEO$_2$MA and OEGMA$_{300}$

In order to determine the type of copolymers to be synthesized from the comonomer pair used, i.e. MEO$_2$MA and OEGMA$_{300}$, a series of copolymerization experiments were performed by changing the comonomer molar ratios in the polymerization feed. Copolymerizations were deliberately stopped at low conversions (<10%) to be able to determine the reactivity ratios of comonomers without having an effect due to the feed comonomer composition drifts. The resultant copolymer compositions were determined using ^{1}H-NMR spectra of the purified copolymer samples (Figure 4.4, top spectrum). The resultant copolymer composition was calculated using Equations 4.2 and 4.3.Table 4.2 shows the polymerization conditions and the properties of the final polymer products obtained in reactivity ratio determination experiments.
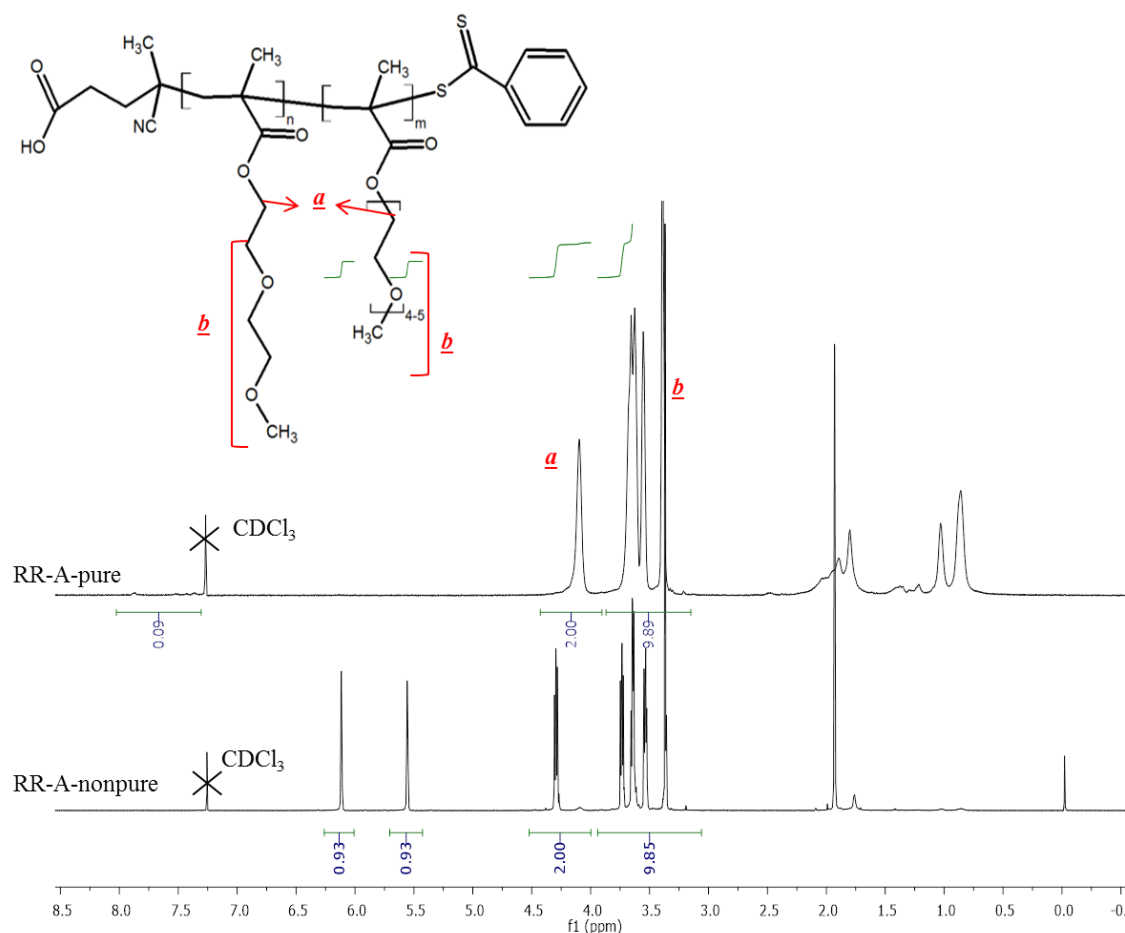

Figure 4.4. ^{1}H-NMR spectra of a copolymer sample before and after purification. The copolymer was obtained using a [MEO$_2$MA]/[OEGMA$_{300}$] feed ratio of 91/9 and a [M]/[R]/[I]) ratio of 500/1/0.25 (RR-A in Table 4.2).

In Figure 4.4, a is the signal of 2 protons of methylene group (CH$_2$-**CH$_2$**-O-C(=O)) next to the ester group present in both comonomers and b is the signal of the remaining 9 protons in the oligoethyleneglycol side chain of MEO$_2$MA and 19 protons in that of OEGMA. Copolymer compositions calculated using these signals and Equations 4.2 and 4.3, are plotted versus feed composition (Figure 4.5).

$$2M+2O = \int_{4.0ppm}^{4.4ppm} = a \text{ (in Figure 4.4 top)} \quad (4.2)$$

$$9M+19O = \int_{3.1ppm}^{3.9ppm} = b \text{ (in Figure 4.4 top)} \quad (4.3)$$

where,

M and O: molar fractions of MEO$_2$MA and OEGMA in copolymer, respectively

a and b: Integral value of 2 protons of methylene group adjacent to the ester group and integral value of remaining oligoethyleneglycol side chain protons, respectively.

Simultaneous solution of Equations 4.2 and 4.3 directly gives the composition of copolymer.

Table 4.2. Polymerization conditions used for determination of reactivity ratios of comonomers and the properties of the resultant polymers

Sample Code	Feed Composition [a]		[Total Monomer]/ [CDTB]/[AIBN]	Polymerization Time	Conversion % [a]	Copolymer Composition[b]	
	MEO$_2$MA%	OEGMA%				MEO$_2$MA%	OEGMA%
RR-A	91	9	[500]/[1]/[0.25]	20min	7.0	91	9
RR-B	84	16	[500]/[1]/[0.25]	20min	9.0	84	16
RR-C	74	26	[500]/[1]/[0.25]	20min	8.5	73	27
RR-D	61	39	[500]/[1]/[0.25]	20min	6.0	63	37
RR-E	53	47	[500]/[1]/[0.25]	20min	8.0	53	47
RR-F	44	56	[500]/[1]/[0.25]	20min	8.0	45	56
RR-G	37	63	[500]/[1]/[0.25]	20min	6.5	36	64
RR-H	27	73	[500]/[1]/[0.25]	20min	8.0	28	72
RR-I	17	83	[500]/[1]/[0.25]	20min	3.0	17	83

[a] Calculated by using Equation 4.1 from ^{1}H-NMR spectrum of non-purified sample
[b] Calculated by using Equation 4.2 and 4.3 from ^{1}H-NMR spectrum of purified sample
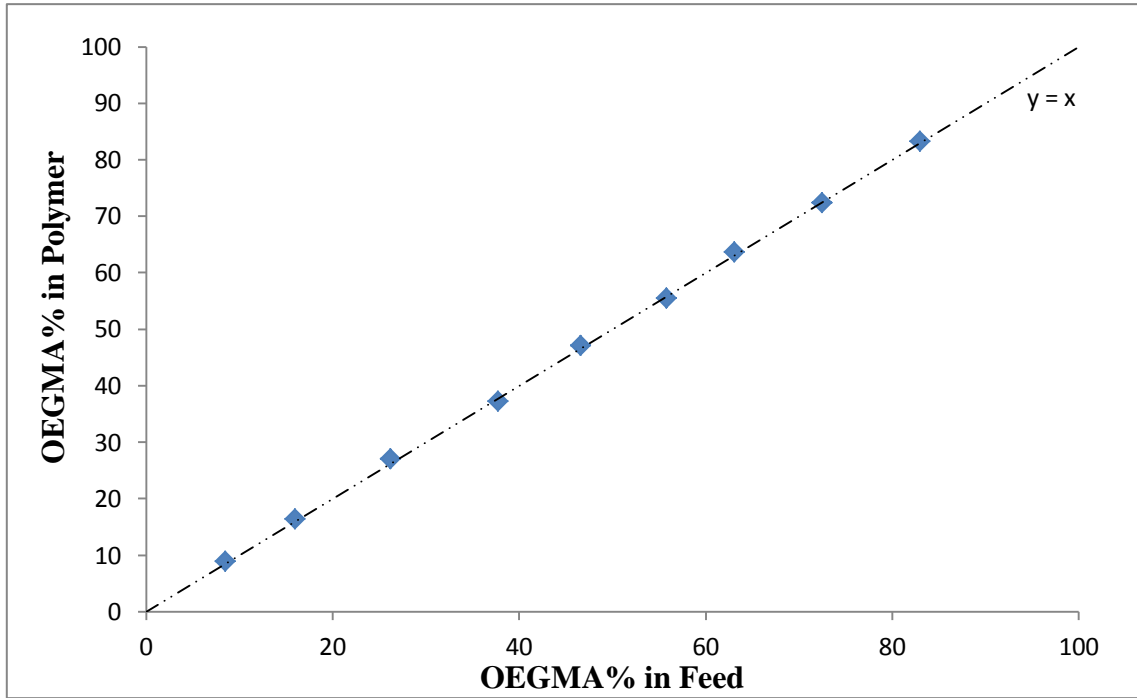
Figure 4.5. Copolymer OEGMA content versus OEGMA content in the feed (mol%)

The diagonal trendline (dashed line) in the graph represents the perfect statistical copolymerization. In a statistical copolymerization (ideal random copolymerization) the feed composition of the comonomers determines exactly the copolymer composition. As it can be seen from the graph, the data obtained experimentally fits very well with the diagonal line representing the statistical copolymerization, suggesting that the copolymers of OEGMA and MEO_2MA are statistical. To verify this, reactivity ratios, defined as the relative preferences of the radical species for the monomers, were calculated using Kelen-Tüdŏs method (Equation 4.4) (Painter 2008).

$$\eta = r_1 \xi - \frac{r_2}{\alpha}(1-\xi) \tag{4.4}$$

where;

$$\eta = \frac{x(y-1)/y}{\alpha + x^2/y} \qquad \xi = \frac{x^2/y}{\alpha + x^2/y} \qquad \alpha = \sqrt{(x^2/y)_{low} * (x^2/y)_{high}}$$

and $\qquad x = [M_1]/[M_2] \qquad y = d[M_1]/d[M_2]$

r_1 and r_2 : reactivity ratio of monomer 1 and monomer 2, respectively.

34

d[M1] and d[M2]: instantaneous concentrations of monomer 1 and monomer 2 respectively

[M1] and [M2]: feed concentrations of monomer 1 and monomer 2 respectively

With the values calculated based on Equation 4.4 in which monomers 1 and 2 were MEO$_2$MA and OEGMA, respectively, Kelen-Tüdŏs Plot was constructed (Figure 4.6).
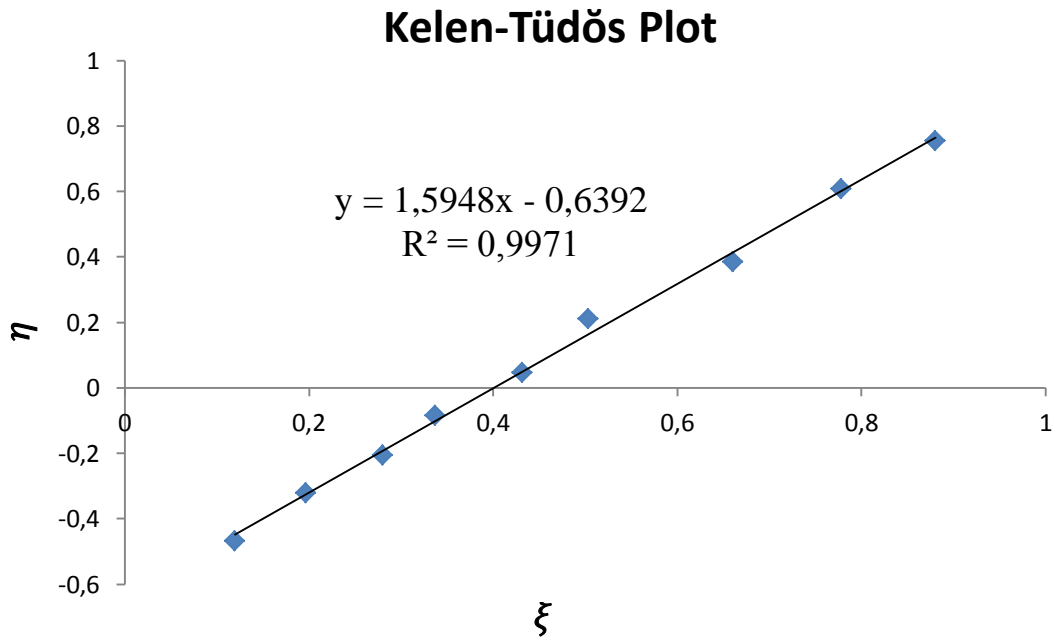

Figure 4.6. Kelen-Tüdŏs Plot of MEO$_2$MA and OEGMA copolymerization

According to Figure 4.6 the reactivity ratios are calculated at $\xi=1$ and $\xi=0$. When $\xi=1$ Equation 4.4 becomes $\eta = r_1$ and when $\xi=0$ $\eta = -r_2/\alpha$. From the plot, r_1 (monomer 1= MEO$_2$MA) was found to be 0.96 and r_2 (monomer 2= OEGMA) was found to be 0.98. This condition provides a special case where $r_1 = r_2 = 1$, which shows that both MEO$_2$MA and OEGMA comonomers add with equal probability to the growing chains, regardless of the nature of the radical species in the terminal position. The resulting copolymer is *truly random* and its composition is exactly the same as the "feed composition" (Painter 2008).

4.3. Characterization of Temperature-Responsive Behaviour

From the results above, it was shown that the copolymerization of OEGMA and MEO$_2$MA is well controlled by RAFT mechanism. Thus the molecular weight and end-group of the copolymers can be controlled and well-defined copolymers can be synthesized. Furthermore, the copolymer composition can be easily controlled by the polymerization feed composition. Based on these findings, a large number of copolymers with varying molecular weights, compositions and end-group functionalities were synthesized to investigate the effect of these properties on the temperature-responsive behaviour of the copolymers. The synthesis of the copolymers is described below, followed by the characterization of temperature-responsive behaviour.

4.3.1. Synthesis of Polymers

In order to investigate the effect of copolymer composition and molecular weight on lower critical solution temperature (LCST) of the polymers, polymers were synthesized at 5 different feed compositions targeting 4 different degrees of polymerization ($\overline{DP} \approx 10$, $\overline{DP} \approx 20$, $\overline{DP} \approx 30$, $\overline{DP} \approx 50$) at each feed composition. Properties of the synthesized polymers are shown in Table 4.3.

Table 4.3. Properties of polymers synthesized to have varying molecular weights, compositions and end-group functionalities.

Sample Code	Mn_{NMR} [b]	$\overline{DP}$ [a]	Mn_{GPC} [d]	PDI [d]	Composition [c] MEO$_2$MA	Composition [c] OEGMA
PT-1	2.3K	11	2.4K	1.15	100%	0%
PT-2	3.6K	18	3.2K	1.14	100%	0%
PT-3	5.8K	29	4.4K	1.22	100%	0%
PT-4	9.7K	53	8.6K	1.18	100%	0%
PT-5	2.4K	10	2.0K	1.20	77%	23%
PT-6	4.3K	19	3.2K	1.08	74%	26%
PT-7	6.1K	27	4.7K	1.08	75%	25%
PT-8	11.7K	53	9.6K	1.21	75%	25%
PT-9	3.4K	12	2.9K	1.08	51%	49%
PT-10	4.9K	19	3.4K	1.14	50%	50%
PT-11	7.5K	29	4.9K	1.18	51%	49%
PT-12	13.7K	55	10.3K	1.29	51%	49%
PT-13	3.2K	11	2.6K	1.09	25%	75%
PT-14	4.9K	17	3.0K	1.15	25%	75%
PT-15	8.2K	29	5.2K	1.23	25%	75%
PT-16	13.0K	47	9.0K	1.21	26%	74%
PT-17	3.3K	10	2.2K	1.20	0%	100%
PT-18	5.6K	18	3.5K	1.15	0%	100%
PT-19	8.7K	28	6.0K	1.17	0%	100%
PT-20	16.8K	55	9.9K	1.22	0%	100%

[a-b] Calculated by using Equation 4.5 and 4.6 respectively from ^{1}H-NMR spectrum of purified sample [c] Calculated by using Equation 4.2 and 4.3 from ^{1}H-NMR spectrum of purified sample [d](Mn_{GPC}) and (PDI) determined by gel permeation chromatography.

The number average molecular weight (Mn_{GPC}) and PDI of the samples were determined using GPC. The Mn (Mn_{NMR}), degree of polymerization ($\overline{DP}$) and copolymer compositions were determined via ^{1}H-NMR spectroscopy. Copolymer compositions were calculated using Equations 4.2 and 4.3. Degree of polymerization of copolymers ($\overline{DP}$) and Mn_{NMR} of polymers were calculated according to Equations 4.5 and 4.6 respectively, using the integration of the characteristic signals belonging to RAFT agent (r signal at 7.4, 7.5 and 7.9 ppm, Figure 4.7) and oligoethylene glycol side chains (a signal at 4.1 ppm, Figure 4.7) in ^{1}H-NMR spectrum. For calculation of Mn_{NMR} and $\overline{DP}$, it was assumed that there were negligible termination reactions in polymerizations. Hence each polymeric chain was assumed to possess a RAFT end-

group. Equation 4.5 can therefore be used to find the number of monomeric units per RAFT group or in other words the degree of polymerization $(\overline{DP})$. Degree of polymerization can be related to the molecular weight using Equation 4.6.
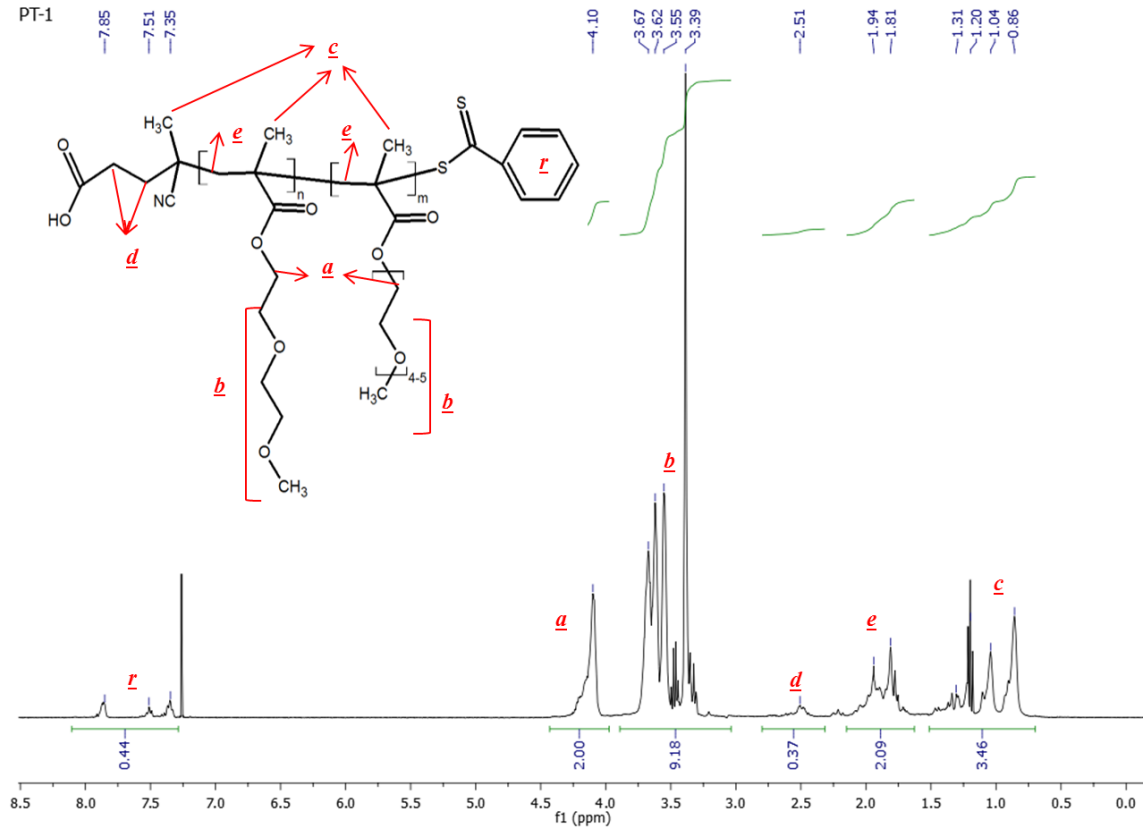

Figure 4.7. ^{1}H-NMR spectrum of purified Poly(MEO$_2$MA) was obtained using a [M]/[R]/[I]) ratio of 20/1/0.25 (PT-1 in Table 4.3).

$$\text{Degree of Polymerization } (\overline{DP}) = \frac{\int_{4.1\text{ppm}}^{\text{PEG}} /2}{\int_{7.3\text{-}7.9\text{ppm}}^{\text{RAFT}} /5} = \frac{a/2}{r/5} \tag{4.5}$$

$$\text{Mn}_{\text{NMR}} = \left\{ \begin{array}{c} (\overline{DP}) * (MW_{\text{monomer-1}}) * y_1] + \\ [\ (\overline{DP}) * (MW_{\text{monomer-2}}) * y_2] + [MW_{\text{CDTB}}] \end{array} \right\} \tag{4.6}$$

where,

y_1 and y_2: molar fraction of the monomer 1 and monomer 2 in the polymer respectively

Mw$_{\text{monomer-1}}$ and Mw$_{\text{monomer-2}}$ and MW$_{\text{CDTB}}$: Molecular weights of monomer 1, monomer 2 and RAFT agent respectively.

38

4.3.2. End-Group Modification with Pyridyl DiSulfide (PDS)

In order to investigate the effect of end-group chemistry on the temperature-responsive behaviour, the ω-end group of the polymers synthesized via RAFT polymerization was modified with pyridyl disulfide (PDS) group. PDS group was shown before to have affinity to gold surfaces (Zareie et al. 2008). Considering the possible use of the polymers with gold surfaces polymers were modified with PDS group. After purification, the PDS-modified polymers were characterized via ^{1}H-NMR spectroscopy. Additionally, GPC was used to see if there was any change in molecular weight of polymers after modification reaction. Replacement of the RAFT end group of polymers with PDS group is shown in Figure 4.8. It is clearly seen in NMR spectra that the benzylic protons of the RAFT end-group at 7.4, 7.5 and 7.9 ppm disappear after modification while PDS group protons at 7.1- 7.6 -8.4 ppm appear. Figure 4.9 shows the GPC chromatogram of the polymer before and after modification with PDS. There was not a significant change in molecular weight, indicating the absence of disulphide coupling between two thiol-terminated polymer chains, which were intermediate molecules formed after aminolysis reaction of the polymer RAFT end-groups. According to GPC chromatograms, Mn_{GPC} of polymer before modification was 2400 and after modification 2700. PDI before and after modification was 1.15 and 1.17, respectively.

The properties of all polymers before and after PDS modification are listed in Table 4.4.
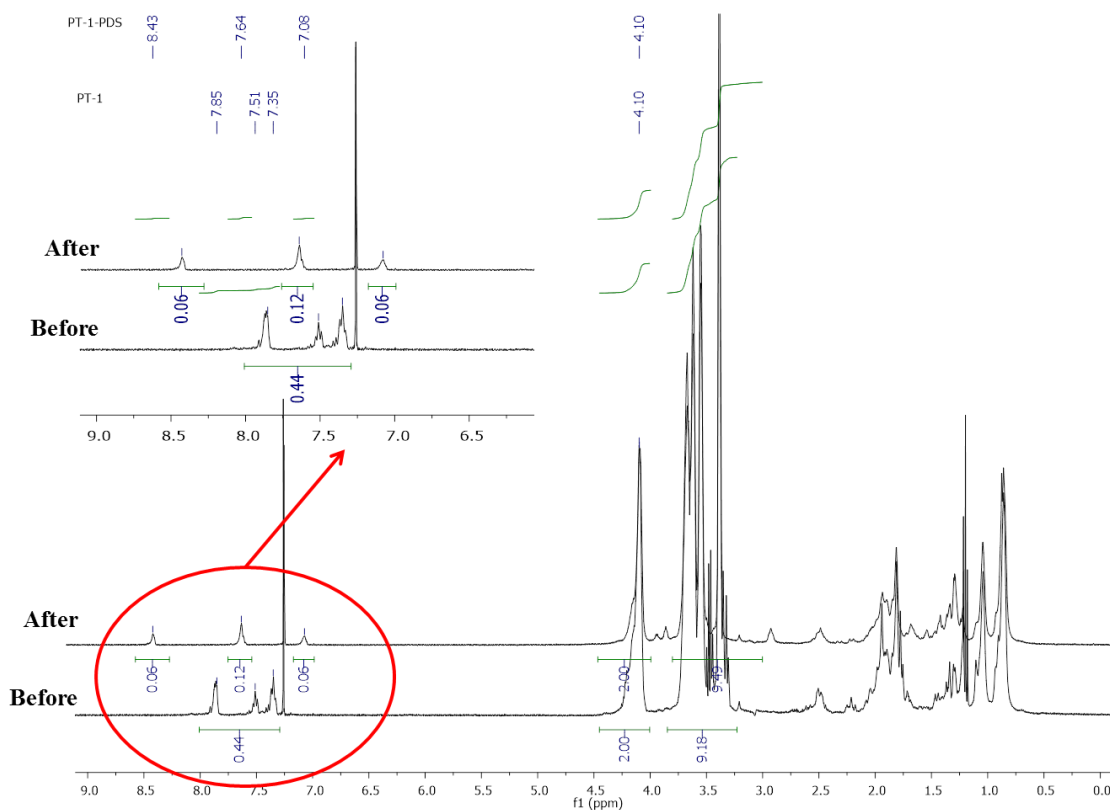
Figure 4.8. ^{1}H-NMR spectra of Poly(MEO$_2$MA) having Mn of 2,4K, PDI of 1.15, $\overline{DP}$ of 11 (PT-1 coded polymer in Table 4.3) before and after PDS modification.
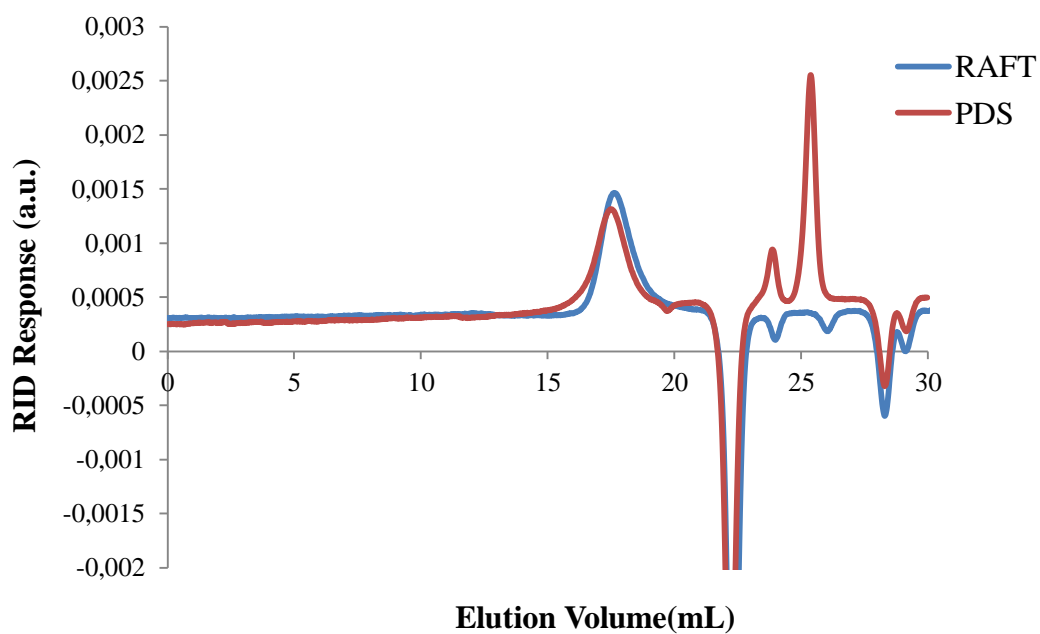

Figure 4.9. GPC chromatogram of PT-1 coded polymer before and after PDS modification

Table 4.4. Properties of polymers before and after PDS modification

Sample	Mn$_{NMR}$	$\overline{DP}$	Mn$_{GPC}$	PDI	Mn$_{GPC}$	PDI
	BEFORE MODIFICATION				AFTER MODIFICATION	
PT-1	2.3K	11	2.4K	1.15	2.8K	1.17
PT-2	3.6K	18	3.2K	1.14	3.4K	1.15
PT-3	5.8K	29	4.4K	1.22	5.4K	1.14
PT-4	9.7K	53	8.6K	1.18	8.8K	1.20
PT-5	2.4K	10	2.0K	1.20	2.0K	1.17
PT-6	4.3K	19	3.2K	1.08	3.4K	1,17
PT-7	6.1K	27	4.7K	1.08	5.0K	1.22
PT-8	11.7K	53	9.6K	1.21	10.0K	1.25
PT-9	3.4K	12	2.9K	1.08	3.2K	1.16
PT-10	4.9K	19	3.4K	1.14	3.6K	1.19
PT-11	7.5K	29	4.9K	1.18	5.5K	1.26
PT-12	13.7K	55	10.3K	1.29	11.3K	1.33
PT-17	3.3K	10	2.2K	1.20	2.8K	1.23
PT-18	5.6K	18	3.5K	1.15	3,.9K	1.20
PT-19	8.7K	28	6.0K	1.17	6.1K	1.27
PT-20	16.8K	55	9.9K	1.22	10.0K	1.27

4.3.3. End-Group Modification with Phosphonate

The RAFT-end group of polymers was also replaced with a phosphonate group. In order to perform this reaction diethyl bromopropyl phosphonate (DEBrPP) was used. Phosphonate group was shown before to have affinity to Al_2O_3 surfaces. Considering the possible use of the polymers with Al_2O_3 surfaces polymers were modified with phosphonate group. The end-group modification was characterized by ^{31}P-NMR spectroscopy. Polymers were also characterized using GPC to investigate whether there was any change in molecular weight and PDI.

Figure 4.10 shows the ^{1}H-NMR spectra of Poly(MEO$_2$MA) having Mn of 2,4 K, PDI of 1.15, $\overline{DP}$ of 11 (PT-1 coded polymer in Table 4.5) before and after phosphonate modification. The RAFT end-group was efficiently removed as indicated by the disappearance of its characteristic signals at 7.3-7.9 ppm after modification. Figure 4.11 shows the ^{31}P-NMR spectra of phosphonate modified polymer and non-reacted DEBrPP. DEBrPP has an identical signal at 30.4 ppm. Upon thio-bromo reaction between the aminolyzed polymer and DEBrPP, a shift in ^{31}P-NMR spectrum to 31.0 ppm is observed. This shows the successful modification of the RAFT end-group of the polymer with phosphonate group.
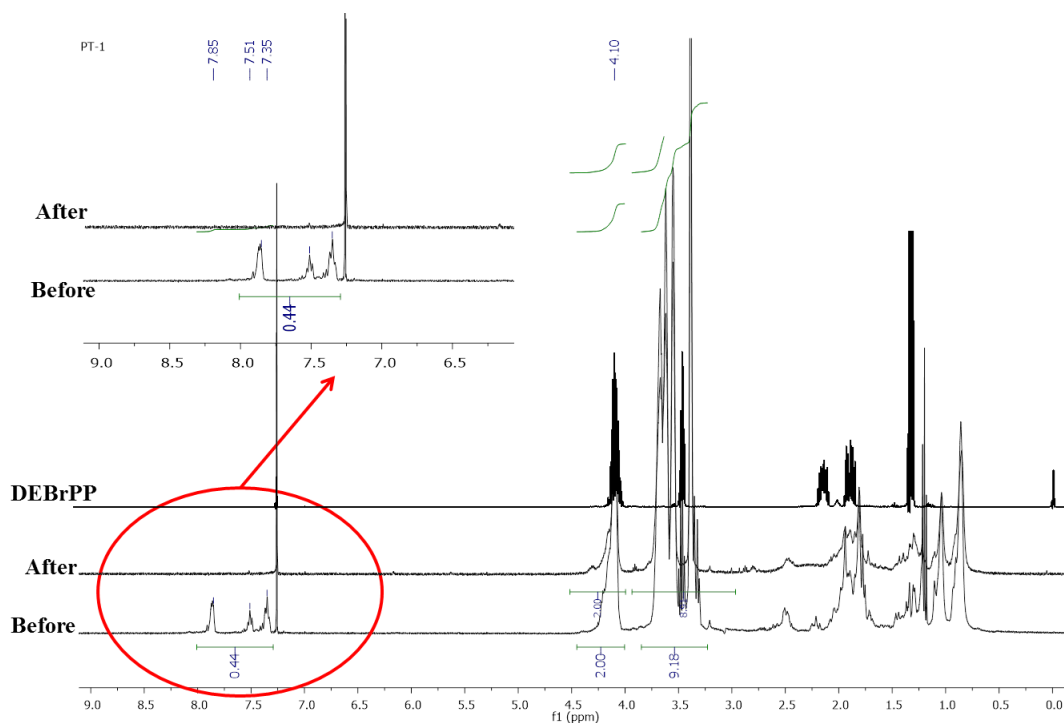
Figure 4.10. ^{1}H-NMR spectra of poly(MEO$_2$MA) having Mn of 2,4K, PDI of 1.15, $\overline{DP}$ of 11 (PT-1 coded polymer in Table 4.5) polymer before and after phosphonate modification and non-reacted DEBrPP
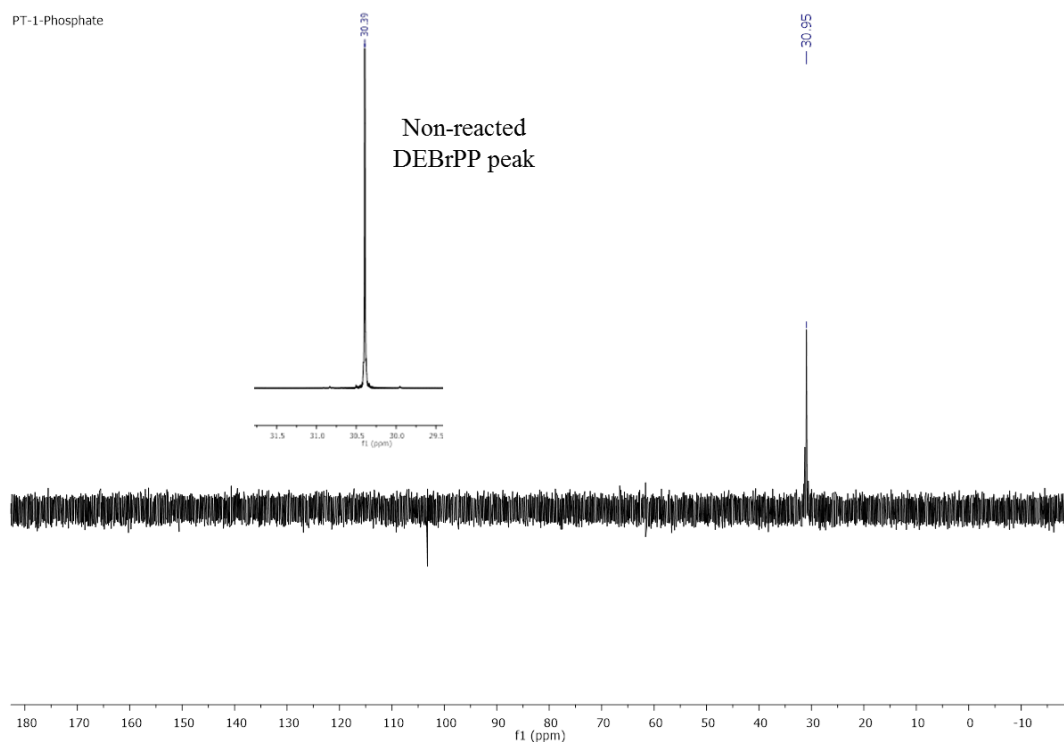

Figure 4.11. ^{31}P-NMR spectrum of poly(MEO$_2$MA) having Mn of 2,4 K, PDI of 1.15, $\overline{DP}$ of 11 (PT-1 coded polymer in Table 4.5) polymer after phosphonate modification and non-reacted DEBrPP spectrum.

According to Figure 4.12, elution time of the polymer after phosphonate modification shifts insignificantly to shorter elution times. According to these chromatograms, Mn_{GPC} of polymer before and after modification was 2400 and 2900, respectively. Also PDI before and after modification were 1.15 and 1.19, respectively. This means that while modification reaction occurs, polymer chains undergo disulphide coupling reactions insignificantly.
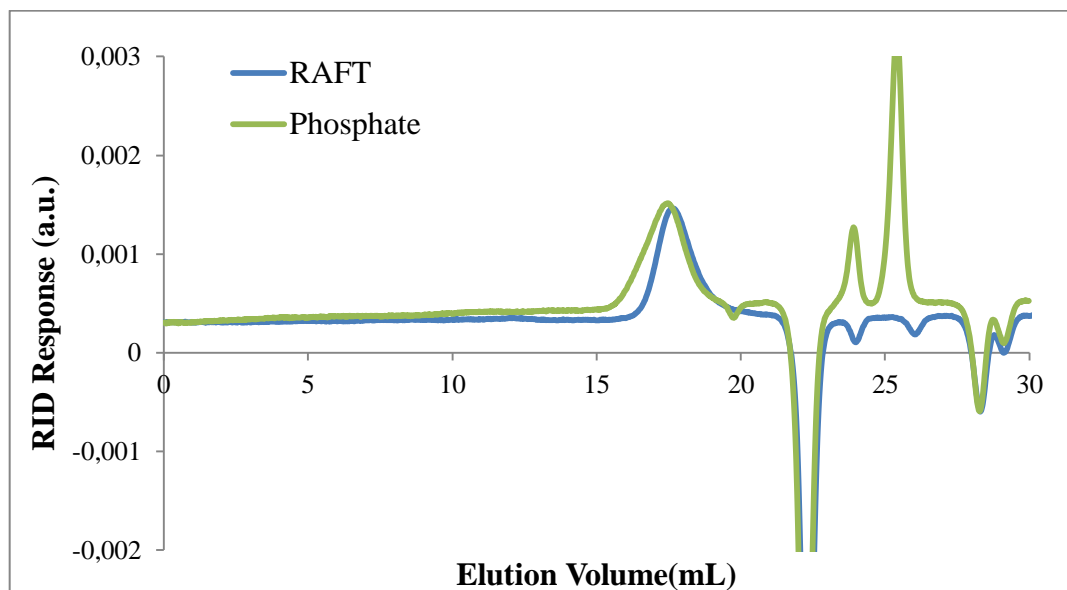

Figure 4.12. GPC chromatogram of PT-1 coded polymer before and after modification

Table 4.5. Properties of polymers before and after phosphonate modification

Sample	BEFORE MODIFICATION				AFTER MODIFICATION	
	Mn_{NMR}	$\overline{DP}$	Mn_{GPC}	PDI	Mn_{GPC}	PDI
PT-1	2.3K	11	2.4K	1.15	2.9K	1.19
PT-2	3.6K	18	3.2K	1.14	3.7K	1.20
PT-3	5.8K	29	4.4K	1.22	5.9K	1.23
PT-4	9.7K	53	8.6K	1.18	10.4K	1.25
PT-5	2.4K	10	2.0K	1.20	2.5K	1.23
PT-6	4.3K	19	3.2K	1.08	3.5K	1.24
PT-7	6.1K	27	4.7K	1.08	4.9K	1.28
PT-8	11.7K	53	9.6K	1.21	10.5K	1.33
PT-9	3.4K	12	2.9K	1.08	3.5K	1.23
PT-10	4.9K	19	3.4K	1.14	4.5K	1.27
PT-11	7.5K	29	4.9K	1.18	5.5K	1.29
PT-12	13.7K	55	10.3K	1.29	12.6K	1.34

4.4. Lower Critical Solution Temperature (LCST) Determination

Lower critical solution temperature (LCST) measurements were performed using a UV-vis spectrophotometer. Polymer concentrations were constant at 1 mg/ml. 10% of maximum absorbance at 500 nm was defined as LCST of polymer. Measurement for each sample was repeated for 3 times, and the average LCST values were calculated. Figure 4.13 is an example of the absorbance versus temperature graphs of polymers (For the absorbance vs. temperature graph of other polymers see Appendix A). Polymer chains in solution below the critical solution temperature are in expanded coil conformation. When temperature reaches lower critical solution temperature (LCST), polymer chains collapse and form compact globules. This phase change causes an increase in the turbidity of solution. Increase in temperature up to LCST of polymer does not result in turbidity and after LCST absorbance increases sharply. This was clearly seen in Figure 4.13. Effect of copolymer composition, molecular weight (degree of polymerization) and end-group modification on the LCST of polymers were investigated. Table 4.6 lists the LCST of RAFT, PDS and phosphonate terminated polymers with varying compositions and molecular weights.
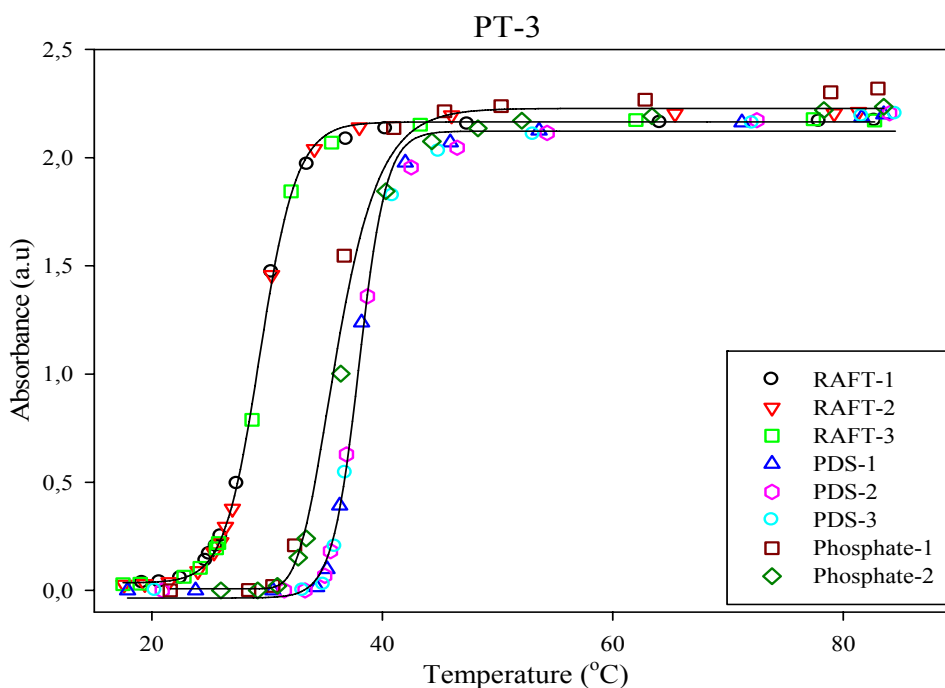

Figure 4.13. Absorbance versus temperature graphs of poly(MEO$_2$MA) having Mn of 5.8 K, PDI of 1.22, $\overline{\text{DP}}$ of 29 (PT-3 coded polymer in Table 4.6) polymer with RAFT, PDS or phosphonate end-groups. Three different measurements of each sample are shown in the figure.

Table 4.6. Lower critical solution temperature (LCST) of RAFT, PDS and phosphonate terminated polymers having varying compositions, number average molecular weights (Mn) and degree of polymerizations ($\overline{DP}$).

| Sample Code | Mn_{NMR} | $\overline{DP}$ | Mn_{GPC} | PDI | Copolymer Composition(mol%) | | LCST (ºC) | | |
					MEO_2MA	OEGMA	RAFT	PDS	Phosphate
PT-1	2.3K	11	2.4K	1.15	100%	0%	<14.0	34.9±0.6	35.5±0.5
PT-2	3.6K	18	3.2K	1.14	100%	0%	22.4±0.2	38.1±0.6	35.6±0.8
PT-3	5.8K	29	4.4K	1.22	100%	0%	25.8±0.2	35.8±0.2	32.8±0.4
PT-4	9.7K	53	8.6K	1.18	100%	0%	30.9±0.9	31.6±0.3	31.1±0.7
PT-5	2.4K	10	2.0K	1.20	77%	23%	19.3±0.8	58.8±0.7	53.0±1.4
PT-6	4.3K	19	3.2K	1.08	74%	26%	42.8±0.8	51.5±0.5	49.1±0.4
PT-7	6.1K	27	4.7K	1.08	75%	25%	47.5±0.5	51.4±0.3	51.5±0.1
PT-8	11.7K	53	9.6K	1.21	75%	25%	46.3±0.2	47.5±0.5	47.2±0.1
PT-9	3.4K	12	2.9K	1.08	51%	49%	51.1±1.0	60.3±0.7	61.4±0.9
PT-10	4.9K	19	3.4K	1.14	50%	50%	54.7±0.6	65.3±0.6	62.2±0.2
PT-11	7.5K	29	4.9K	1.18	51%	49%	57.2±0.2	59.6±0.8	61.5±0.5
PT-12	13.7K	55	10.3K	1.29	51%	49%	56.7±0.6	56.9±0.7	57.7±0.5
PT-13	3.2K	11	2.6K	1.09	25%	75%	57.0±0.7	N.D.	N.D.
PT-14	4.9K	17	3.0K	1.15	25%	75%	64.7±0.3	N.D.	N.D.
PT-15	8.2K	29	5.2K	1.23	25%	75%	66.4±0.2	N.D.	N.D.
PT-16	13.0K	47	9.0K	1.21	26%	74%	68.3±0.3	N.D.	N.D.
PT-17	3.3K	10	2.2K	1.20	0%	100%	66.5±0.5	76.0±1.6	N.D.
PT-18	5.6K	18	3.5K	1.15	0%	100%	72.8±0.6	81.0±0.9	N.D.
PT-19	8.7K	28	6.0K	1.17	0%	100%	73.7±0.3	75.0±0.4	N.D.
PT-20	16.8K	55	9.9K	1.22	0%	100%	73.3±1.1	74.6±0.2	N.D.

*N.D. not determined

4.4.1. Effect of Copolymer Composition and Molecular Weight on LCST

In order to investigate the effect of monomer composition on LCST, polymers at 5 different compositions were synthesized. LCST values of these polymers are shown in Figure .4.14. According to Figure .4.14 approximately at the same degree of polymerization, when the OEGMA content of the copolymers increases, the LCST increases. Since OEGMA has more hydrophilic units (longer oligoethylene glycol chain) than MEO_2MA, hydrophilic-hydrophobic balance of the copolymer shifts to hydrophilic side when OEGMA content of the copolymer increases. Increase in hydrophilicity increases the LCST of the polymer. This gives the opportunity for tuning the LCST of oligoethylene glycol methacrylate copolymers by changing the comonomer ratios in the copolymer. As Lutz and his team reported, (Lutz et al. 2009) the LCST of P(OEGMA-*co*- MEO_2MA) can be precisely tuned in the range of the LCST of two homopolymers. They reported the LCST of poly(MEO_2MA) (Mn= 21 K) and poly(OEGMA) (Mn= 30 K) as 28 and 65 ^{o}C, respectively. However, we found the LCST of poly(MEO_2MA) (Mn= 10 K) and poly(OEGMA) (Mn=17 K) polymers as 31 ^{o}C and 73 ^{o}C. Difference in the LCST of polymers is the because of different polymer concentrations in measurement; they performed experiments with 3mg/ml polymer concentration while in this study experiments were performed with 1mg/ml polymer concentration. In our study, it was possible to synthesize copolymers that have a LCST between the LCST of two respective homopolymers by only changing the comonomer ratio in the copolymer.

On the other hand, at the same copolymer composition, an increase in the degree of polymerization (or molecular weight) results in an increase in the LCST up to a certain level, that depending again on the hydrophilic/hydrophobic balance of the copolymer. For example, the LCST of poly(MEO_2MA) (0% OEGMA) increases gradually from 14 ^{o}C to 31 ^{o}C, while degree of polymerization ($\overline{DP}$) increases from 10 to 50, however the LCST of poly(OEGMA) (100% OEGMA) increases only from 67 ^{o}C 73 ^{o}C when $\overline{DP}$ of polymer increases from 10 to 20 and then further increase in $\overline{DP}$ does not affect the LCST of poly(OEGMA). It was hypothesized that this effect was due to the decreasing effect of the hydrophobic RAFT-end group, rather than the direct effect

of $\overline{DP}$, on the LCST of the copolymers with increasing $\overline{DP}$. Since there is a thiocarbonylthio end-group of the polymer which is relatively hydrophobic compared to the polymer structure itself, it increases the hydrophobicity of the whole structure which overall decreases the LCST of the polymer by simply making the polymer less water soluble. When the $\overline{DP}$ of the polymer increases, hydrophobic effect of this RAFT end-group becomes negligible. This hypothesis was further investigated in later sections, as explained below.
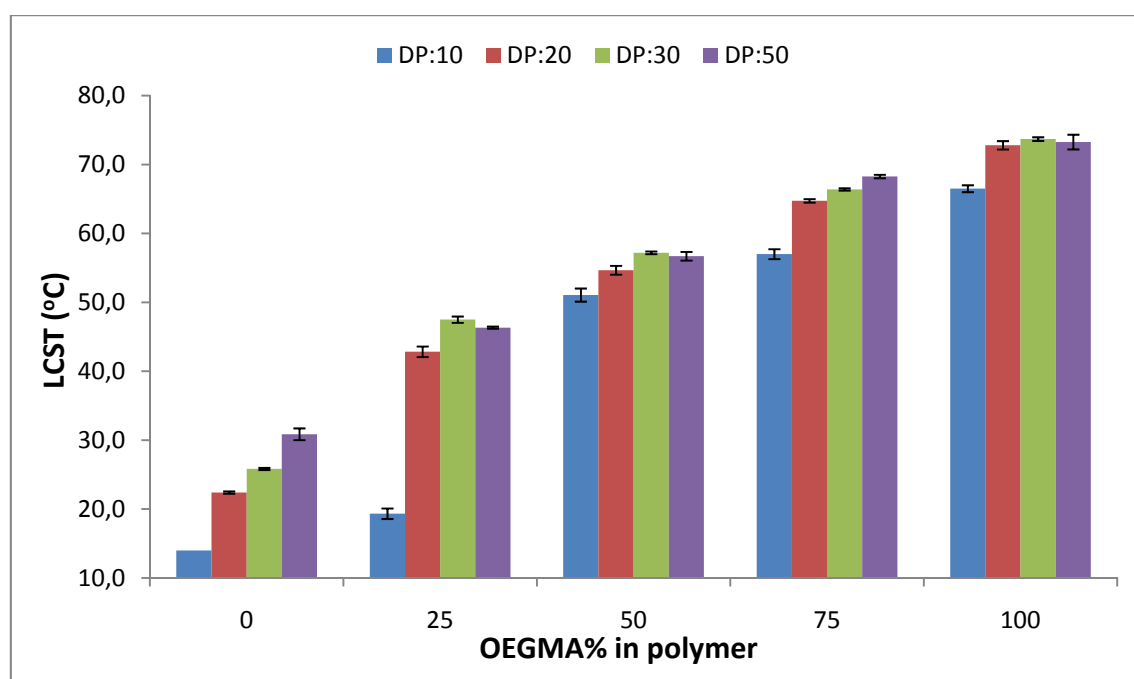
Figure .4.14. Effect of both monomer composition and degree of polymerization on LCST of polymers with RAFT end-group

4.4.2. Effect of End-group Modification and Molecular Weight on LCST

Effect of end-group modification (with RAFT, PDS or phosphonate group) on LCST of polymers was investigated at 4 different copolymer compositions (Poly(MeO$_2$MA), Poly(MeO$_2$MA$_{0.75}$-co-OEGMA$_{0.25}$) and Poly(MeO$_2$MA$_{0.50}$-co-OEGMA$_{0.50}$)) and Poly(OEGMA). One exception was that the effect of phosphonate modification of Poly(OEGMA) was not investigated as the LCST value of this most hydrophilic polymer was already above 75 ºC which was at the limit of heating system

used in the experiments. In Figure 4.15 the effect end-group modification and molecular weight (degree of polymerization) on the LCST of Poly(MEO$_2$MA) (0%OEGMA) is shown. According to the figure, replacement of the hydrophobic RAFT end-group with a relatively more hydrophilic PDS or phosphonate group, changes the hydrophilic/hydrophobic balance of the polymer. Since a relatively more hydrophilic group (PDS or phosphonate) was added to the polymer structure, the LCST of the lowest molecular weight polymer increased by about 20 $^{\circ}$C. However, the increase in LCST with the addition of hydrophilic end-group appeared to depend on molecular weight of poly(MEO$_2$MA) polymer, as the polymer with a $\overline{DP}$ of 50 a change in the LCST change was not observed. When molecular weight (hence the $\overline{DP}$) of the polymer is relatively small, the effect of end-group modification on LCST becomes more significant. When molecular weight of the polymer gets higher, the effect of the hydrophilicity or hydrophobicity of the end-group becomes negligible. This results in a less profound in LCST of the polymer. In summary; when polymers' molecular weight is low, end-groups' hydrophilicity or hydrophobicity is more effective on the total hydrophilic/hydrophobic balance of the polymer.
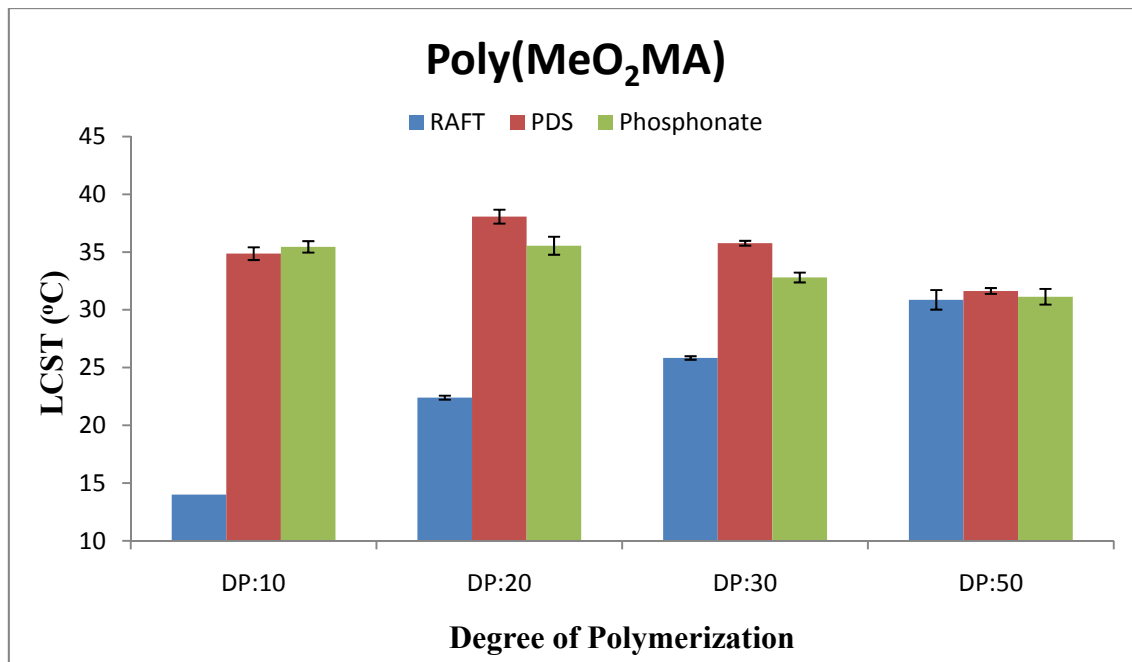
Figure 4.15. Effect of end-group modification and degree of polymerization on LCST of Poly(MeO$_2$MA).

In Figure 4.16 and Figure 4.17, LCST of Poly(MeO$_2$MA$_{0.75}$-co-OEGMA$_{0.25}$) and Poly(MeO$_2$MA$_{0.50}$-co-OEGMA$_{0.50}$) having varying $\overline{DP}$s is shown, respectively. Similar

findings observed with Poly(MEO$_2$MA) were also seen for the LCST values of Poly(MeO$_2$MA$_{0.75}$-*co*-OEGMA$_{0.25}$) and Poly(MeO$_2$MA$_{0.50}$-*co*-OEGMA$_{0.50}$). Removal of the hydrophobic RAFT end-group clearly increases the LCST and with increasing degree of polymerization the effect of the end-group modification becomes negligible.

Polymers with PDS and phosphonate end-group appeared to be much less affected by the change in their $\overline{DP}$ values. This was attributed to the relatively more hydrophilic character of these groups which was not very different than the hydrophilicity of the (co)polymer structure itself.
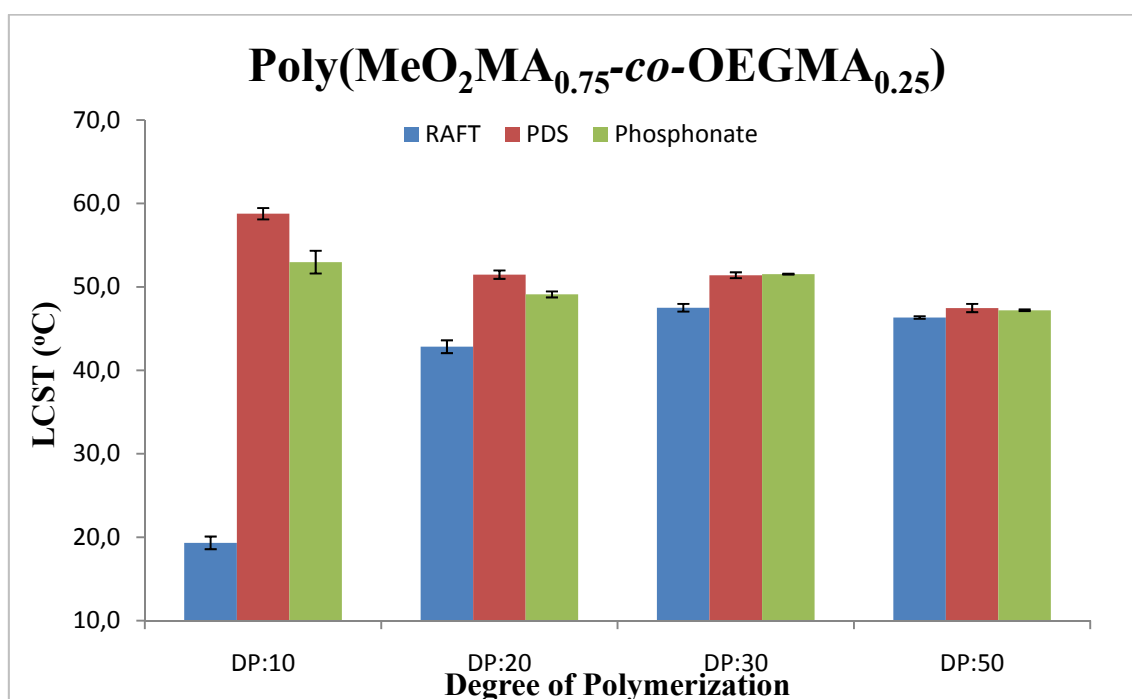
Figure 4.16. Effect of end-group modification and degree of polymerization on LCST of Poly(MeO$_2$MA$_{0.75}$-*co*-OEGMA$_{0.25}$).
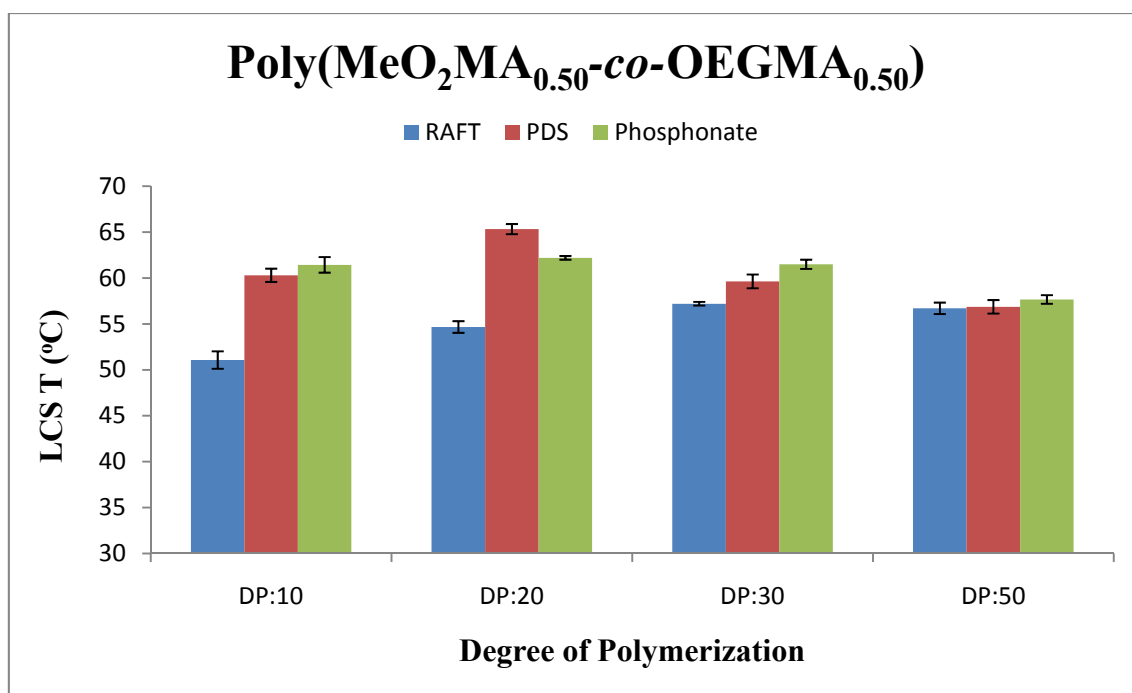
Figure 4.17. Effect of end-group modification and degree of polymerization on LCST of Poly(MeO$_2$MA$_{0.50}$-*co*-OEGMA$_{0.50}$).

Figure 4.18 shows the effect of PDS modification on LCST of Poly(OEGMA).. Similar trends obtained with previous polymers were also observed with the LCST behaviour of Poly(OEGMA). The effect of end-group modification of Poly(OEGMA) was much less profound even at a $\overline{DP}$ of 10. At a $\overline{DP}$ of 10 and 20, PDS modification increased the LCST of Poly(OEGMA) by approximately 10 ^{o}C while the same modification increased the LCST of Poly(MeO$_2$MA) by 20 ^{o}C. While at 30 $\overline{DP}$, the effect of PDS modification on the LCST of Poly(MeO$_2$MA) was 10 ^{o}C, its effect on the LCST of Poly(OEGMA) became negligible. In a similar fashion, the effect of the end-group modification on the LCST of Poly(MeO$_2$MA) became negligible at a $\overline{DP}$ of 50. This is the result of the chemical nature of the monomers, since OEGMA monomer has a longer oligoethylene glycol chain which is highly hydrophilic. When the hydrophilic/hydrophobic balance of poly(MeO$_2$MA) and poly(OEGMA) was compared, Poly(MeO$_2$MA) has 2 hydrophilic ethyleneglycol units per each hydrophobic methacrylate backbone unit whereas poly(OEGMA) has 4.5 hydrophilic ethyleneglycol units per each hydrophobic methacrylate backbone unit. This results in the less profound effect of less end-group modification on the LCST of the most hydrophilic polymer, Poly(OEGMA) even at low $\overline{DP}$ values.
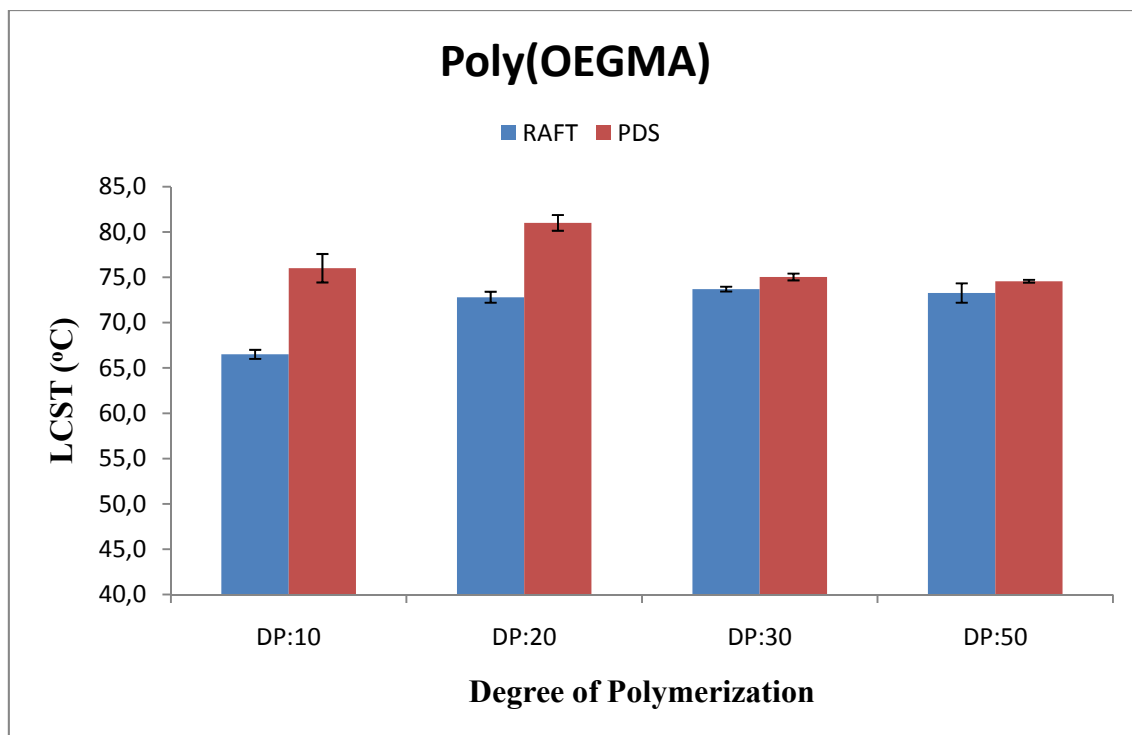
Figure 4.18. Effect of PDS end-group modification and degree of polymerization on LCST of Poly(OEGMA).

CHAPTER 5

CONCLUSION

The aim of this thesis was to synthesize temperature-responsive, well-defined (co)polymers of oligoethyleneglycol methyl ether methacrylate (OEGMA$_{300}$) and diethyleneglycol methyl ether methacrylate (MEO$_2$MA) via RAFT polymerization, perform end-group modifications and finally investigate in detail the temperature-responsive behaviour of the resultant (co)polymers considering the possible use of these copolymers in temperature-controlled biosensing applications (Zareie et al. 2008).

A series of polymerization kinetic experiments were performed to determine whether the (co)polymerizations were controlled by RAFT mechanism. In these experiments, comonomers at a [MEO$_2$MA]/[OEGMA] mole ratio of 75/25 were polymerized at three different total monomer/RAFT agent mole ratios ([M]/[R]) (100/1, 50/1 and 20/1) for varying polymerization times (from 1 to 6 h). Polymers were characterized by nuclear magnetic resonance spectroscopy (NMR) and gel permeation chromatography (GPC) techniques. A combination of the results obtained from GPC measurements and NMR spectroscopy proved the RAFT-controlled synthesis of the copolymers under the conditions applied. Well-defined copolymers of OEGMA$_{300}$ and MEO$_2$MA with controlled molecular weights and low polydispersities (<1.2) were successfully synthesized.

To determine the reactivity ratios of (MEO$_2$MA) and (OEGMA$_{300}$) a series of copolymerization experiments were performed by changing the comonomer molar ratios in the polymerization feed at a [Monomer]/[RAFT agent] ([M]/[R]) mole ratio of 500/1. Copolymerizations were deliberately stopped at low conversions (<10%) to be able to determine the reactivity ratios of comonomers without having an effect due to the feed comonomer composition drifts. The reactivity ratios of MEO$_2$MA (1) and OEGMA$_{300}$ (2) were calculated using Kelen-Tüdõs method and found to be r$_1$= 0.96 and r$_2$= 0.98, respectively. This condition provides a special case where r$_1$ = r$_2$ = 1, resulting in the synthesis of *truly random* copolymers with copolymer compositions exactly the same as the "feed composition".

In order to investigate the effect of composition, molecular weight and end-group modification on thermo-responsive behaviour of the (co)polymers, a large

number of copolymers with varying molecular weights, compositions and end-group functionalities were synthesized. Polymers were synthesized at 5 different feed compositions (MEO$_2$MA/OEGMA ratio of 100/0, 75/25, 50/50, 25/75, 0/100) targeting 4 different degrees of polymerization ($\overline{DP}\approx10$, $\overline{DP}\approx20$, $\overline{DP}\approx30$, $\overline{DP}\approx50$) at each feed composition. Polymers that were synthesized via RAFT polymerization were then modified with pyridyl disulphide (PDS) or phosphonate group. End-group modifications were verified via NMR spectroscopy. According to GPC measurements polymers' molecular weight did not change after the modification reactions.

Lower critical solution temperature (LCST) characterizations of the polymers were performed using a UV-vis spectrophotometer at 500 nm. The copolymer content was found to have a significant influence on the LCST of copolymers. Hydrophilic/hydrophobic balance of (co)polymers was the key factor affecting the LCST values. On the other hand, the end-group hydrophilicity appeared to have a direct effect on the LCST depending on the degree of polymerization of the (co)polymers. In relatively high molecular weight polymers the influence of the end-group was negligible on the total hydrophilic/hydrophobic balance of the (co)polymers, hence the effect on their LCST becomes negligible. The LCST of poly(MEO$_2$MA) with a degree of polymerization of 10, increased by 20 ^{o}C after both PDS and phosphonate end-group modification while the LCST of poly(MEO$_2$MA) with a degree of polymerization of 50 did not increase after modifications. The LCST of RAFT group-terminated homopolymers of MEO$_2$MA increased from 14°C to 31 ^{o}C and that of OEGMA homopolymers from 67 ^{o}C to 73 ^{o}C when the degree of polymerization increased from 10 to 50. The LCST of the RAFT-synthesized copolymers were precisely tuneable in this range simply by changing the copolymer composition.

Future investigations on the topic may include the following suggestions:

- RAFT polymerization kinetics can be further investigated at different comonomer compositions to show that the polymerization is RAFT-controlled at all compositions.

- LCST of (co)polymers can be measured at varying polymer concentrations to investigate the effect of polymer/solvent ratio on LCST.

- The potential of the end-group functional, temperature-responsive, well-defined (co)polymers developed in this thesis as building blocks for temperature-controlled biosensor applications can be investigated.

REFERENCES

Assche, G. V.; Van Mele, B.; Li, T.; Nies, E., Adjacent UCST phase behavior in aqueous solutions of Poly(vinyl methyl ether): Detection of a narrow low temperature UCST in the lower concentration range, Macromolecules, **2011**, *44*, 993-998.

Barker, I. C.; Cowie, J. M. G.; Huckerby, T. N.; Shaw, D. A.; Soutar, I.; Swanson, L., Studies of the "Smart" thermoresponsive behavior of copolymers of *N*-isopropylacrylamide and *N,N*-dimethylacrylamide in dilute aqueous solution, Macromolecules, **2003**, 36, 7765-7770

Bathfield, M.; Daviot, D.; D'Agosto, F.; Spitz, R.; Ladaviere,C.; Charreyre M. T.; Delair, T., Macromolecules, **2008**, *41*, 8346–8353.

Boyer, C.; Bulmus, V.; Davis, T. P.; Ladmiral, V.; Liu, J. Q.; Perrier, S., Bioapplications of RAFT Polymerization. *Chem Rev* **2009,** *109* (11), 5402-5436.

Boyer, C.; Liu, J.; Bulmus, V.; Davis, T. P., RAFT polymer end-group modification and chain coupling/conjugation via disulfide bonds, Aust. J. Chem., **2009**, *62*, 830-847

Boyer, C.; Granville, A.; Davis, T. P.; Bulmus, V., Modification of RAFT-Polymers via Thiol-Ene Reactions: A General Route to Functional Polymers and New Architectures. *J Polym Sci Pol Chem* **2009,** *47* (15), 3773-3794.

Boyer, C.; Stenzel, M. H.; Davis, T. P., Building Nanostructures Using RAFT Polymerization. *J Polym Sci Pol Chem* **2011,** *49* (3), 551-595.

Bulmus, V.; Ding, Z. L.; Long, C. J.; Stayton, P. S.; Hoffman, A. S., Site-specific polymer-streptavidin bioconjugate for pH-controlled binding and triggered release of biotin. *Bioconjugate Chem* **2000,** *11* (1), 78-83.

Byeongmoon, J.; Gutowska, A., Lessons from nature: stimuli-responsive polymers and their biomedical applications, Trends in Biotechnology, 2002, *20* (7), 305-311.

Chong, Y. K.; Moad, G.; Rizzardo, E.; Thang, S. H., Thiocarbonylthio end group removal from RAFT-synthesized polymers by radical-induced reduction. *Macromolecules* **2007,** *40* (13), 4446-4455.

Cowie, J. M. G.; McEwen, I. J., Lower critical solution temperatures of polypropylene solutions, Journal of Polymer Science: Polymer Physics Edition, **1974**, *12*, 441-443.

Cowie, J. M. G.; McEwen, I J., Influence of microstructure on the upper and lower critical solution temperatures of poly(methylmethacrylate) solutions, Journal of the Chemical Society, Faraday Transactions 1: Physical Chemistry in Condensed Phases, **1976**, *72*, 526-533.

Cowie, J. M. G.; Arrighi, V., Polymers: Chemistry and Physics of Modern Materials, 3rd ed., **2008**, Scotland: CRC Press.

Deletre M.; Levesque, G., Macromolecules, **1990**, *23*, 4733–4741.

Ding, Z.; Long, C. J.; Hayashi, Y.; Bulmus, V.; Hoffman, A. S.; Stayton P. S., Temperature control of biotin binding and release with a streptavidin-poly(*N*-isopropylacrylamide) site-specific conjugate, Bioconjugate Chem., **1999**, *10*, 395-400

Fox, T. G., Properties of dilute polymer solutions III: Intrinsic viscosity/temperature relationships for conventional polymethylmethacrylate, Polymer, **1962**, *3*, 111-128.

Fujishige, S.; Kubota, K.; Ando, I. , Phase transition of aqueous solutions of poly(*N*-isopropylacrylamide) and poly(N-isopropylmethacrylamide), *Journal of Physical Chemistry*, **1989**, *93*, 3311–3313.

Galaev, I. Y.; Mattiasson B., Smart polymers for bioseparation and bioprocessing, Taylor & Francis, **2002**

Gibson, M. I.; Bebis, K.; Jones, M. W.; Haddleton, D. M., Thermoresponsive behaviour of poly[(oligo(ethyleneglycol methacrylate)]s and their protein conjugates: importance of concentration and solvent system. *Polym Chem-Uk* **2011,** *2* (4), 975-982.

Hashizume, J.; Teramoto, A.; Fujita, H., Phase equilibrium study of the ternary system composed of two monodisperse polystyrenes and cyclohexane, Journal of Polymer Science, Polymer Physics Edition, **1981**, *19*, 1405-1422.

Hentschel, J.; Bleek, K.; Ernst, O.; Lutz J. F.; Borner, H. G., Macromolecules, **2008**, *41*, 1073–1075.

Heredia, K. L.; Grover, G. N.; Tao L.; Maynard, H. D., Macromolecules, **2009**, *42*, 2360–2367.

Heskins, M.; Guillet, J. E., Solution properties of poly(*N*-isopropylacrylamide), *Journal of Macromolecular Science: Part A - Chemistry*, **1968**, *2*, 1441-1455

Hoffman, A. S., Intelligent Polymers in Medicine and Biotechnology. *Artif Organs* **1995,** *19* (5), 458-467.

Hoffman, A. S.; Stayton, P. S., Bioconjugates of smart polymers and proteins: Synthesis and applications. *Macromol Symp* **2004,** *207*, 139-151.

Inglis, A. J.; Sinnwell, S.; Davis, T. P.; Barner-Kowollik C.; Stenzel, M. H., Macromolecules, **2008**, *41*, 4120–4126.

IUPAC Compendium of Chemical Terminology, binodal curve definition http://old.iupac.org/goldbook/BT07273.pdf accessed May 2013

IUPAC Compendium of Chemical Terminology, Lower critical solution temperature definition http://old.iupac.org/goldbook/LT07279.pdf accessed May 2013

Jenkins, A. D.; Jones, R. G.; Moad, G., Terminology for reversible-deactivation radical polymerization previously called "controlled" radical or "living" radical polymerization (IUPAC Recommendations 2010). *Pure Appl Chem* **2010,** *82* (2), 483-491.

Kabachii, Y. A.; Kochev, S. Y. Polym. Sci., Ser. A **2006**, *48*, 717-722.

Kagemoto, A.; Baba, Y., Kobunshi Kagaku, **1971**, *28*, 784.

Keddie, D. J.; Moad, G.; Rizzardo, E.; Thang, S. H., RAFT Agent Design and Synthesis. *Macromolecules* **2012,** *45* (13), 5321-5342.

Koningsveld, R.; Staverman, A. J., Liquid-liquid phase separation in multicomponent polymer solutions. II. The critical state, Journal Polymer Science, Polymer Physics Editions, **1968**, *6*, 325-347.

Koningsveld, R.; Stockmayer, W.; Nies, H. E., Polymer phase diagrams, Oxford University Press, Oxford, 2001

Li, G. Z.; Randev, R. K.; Soeriyadi, A. H.; Rees, G.; Boyer, C.; Tong, Z.; Davis, T. P.; Becer, C. R.; Haddleton, D. M., Investigation into thiol-(meth)acrylate Michael addition reactions using amine and phosphine catalysts. *Polym Chem-Uk* **2010,** *1* (8), 1196-1204.

Li, M.; Li, H. M.; De, P.; Sumerlin, B. S., Thermoresponsive Block Copolymer-Protein Conjugates Prepared by Grafting-from via RAFT Polymerization. *Macromol Rapid Comm* **2011,** *32* (4), 354-359.

Longenecker, R.; Mu, T.; Hanna, M.; Burke, N. A. D.; Stöver, H. D. H., Thermally responsive 2-Hydroxyethyl methacrylate polymers: Soluble-insoluble and soluble-insoluble-soluble transitions, Macromolecules, **2011**, *44*, 8962-8971.

Lowe, A. B.; Sumerlin, B. S.; Donovan, M. S.; Thomas, D. B.; Hennaux, P.; McCormick, C., L. ACS Symp Ser **2003**, *854*, 586–602.

Lutz, J. F.; Hoth, A.; Schade, K., Design of Oligo(ethylene glycol)-Based Thermoresponsive Polymers: an Optimization Study. *Des Monomers Polym* **2009,** *12* (4), 343-353.

Lutz, J. F., Thermo-Switchable Materials Prepared Using the OEGMA-Platform. *Adv Mater* **2011,** *23* (19), 2237-2243.

Maeda, Y.; Nakamura, T.; Ikeda, I., Hydration and phase behavior of Poly(*N*-vinylcaprolactam) and poly(N-vinylpyrrolidone) in water, Macromolecules, **2002**, *35*,217-222.

Malcolm, G. N.; Rowlinson, J. S., The thermodynamic properties of aqueous solutions of polyethylene glycol, polypropylene glycol and dioxane, Transactions of the Faraday Society, **1957**, *53*, 921-931.

Matsuda, N.; Shimizu, T.; Yamato, M.; Okano, T., Tissue engineering based on cell sheet technology. *Adv Mater* **2007,** *19* (20), 3089-3099.

Moad, G.; Chong, Y. K.; Rizzardo, E.; Postma, A.; Thang, S. H. Polymer **2005**, *46*, 8458-8468.

Nakajima, A.; Hamada, F.; Hayashi, S., Unperturbed chain dimensions of polyethylene in theta solvents, Journal of Polymer Science, Part C: Polymer Symposium, **1966**, *15*, 285-294.

Nolan, C. M.; Serpe, M. J.; Lyon, L. A., Thermally modulated insulin release from microgel thin films. *Biomacromolecules* **2004,** *5* (5), 1940-1946.

Odian, G., Principles of Polymerization, 4th ed., **2004** New York: Wiley-Interscience.

Painter P. C.; Coleman M. M., Essentials of polymer science and engineering, DEStech Publications Inc, 2008

Perrier, S.; Takolpuckdee, P.; Mars, C. A., Reversible addition-fragmentation chain transfer polymerization: End group modification for functionalized polymers and chain transfer agent recovery. *Macromolecules* **2005,** *38* (6), 2033-2036.

Pfohl, O.; Hino, T.; Prausnitz, J. M., Solubilities of styrene-based polymers and copolymers in common solvents, Polymer, **1995**, *36*, 2065-2073

Saeki, S.; Kuwahara, N.; Nakata, M.; Kaneko, M., Upper and lower critical solution temperatures in poly (ethylene glycol) solutions, Polymer, **1976**, *17*, 685-689

Sandler, S. I., Chemical, biochemical and engineering thermodynamics, John Wiley & Sons Inc., **2006**

Sanfrutos, J. M.; Fernandez, A. M.; Mateo, F. H.; Gonzalez, M. D. G.; Gonzalez, R. S.; Gonzalez F. S., Alkyl sulfonyl derivatized PAMAM-G2 dendrimers as nonviral gene delivery vectors with imroved transfection efficiencies, Org. Biomol. Chem., *2011*, *9*, 851-864.

Scales, C. W.; Convertine, A. J.; McCormick, C. L. Biomacromolecules **2006**, *7*, 1389-1392.

Schild, H. G.; Tirrell, D. A., Microcalorimetric detection of lower critical solution temperatures in aqueous polymer solutions, Journal of Physical Chemistry, **1990**, *94*,4352-4356.

Schultz, A. R.; Flory, P. J.; Phase Equilibria in Polymer-Solvent Systems, Journal of the American Chemical Society, **1952**, *74*, 4760–4767.

Sinnwell, S.; Inglis, A. J.; Davis, T. P.; Stenzel M. H.; Barner- Kowollik, C., Chem. Commun., **2008**, 2052–2054.

Skey, J.; O'Reilly, R. K., Chem. Commun., **2008**, 4183–4185.

Soeriyadi, A. H.; Li, G. Z.; Slavin, S.; Jones, M. W.; Amos, C. M.; Becer, C. R.; Whittaker, M. R.; Haddleton, D. M.; Boyer, C.; Davis, T. P., Synthesis and modification of thermoresponsive poly(oligo(ethylene glycol) methacrylate) via catalytic chain transfer polymerization and thiol-ene Michael addition. *Polym Chem-Uk* **2011,** *2* (4), 815-822.

Sun, S. T.; Wu, P. Y., On the Thermally Reversible Dynamic Hydration Behavior of Oligo(ethylene glycol) Methacrylate-Based Polymers in Water. *Macromolecules* **2013,** *46* (1), 236-246.

Willcock, H.; O'Reilly, R. K., End group removal and modification of RAFT polymers. *Polym Chem-Uk* **2010,** *1* (2), 149-157.

Zareie, H. M.; Boyer, C.; Bulmus, V.; Nateghi, E.; Davis, T. P., Temperature-responsive self-assembled monolayers of oligo(ethylene glycol): Control of biomolecular recognition. *Acs Nano* **2008,** *2* (4), 757-765.

DETERMINATION OF LOWER CRITICAL SOLUTION TEMPERATURE
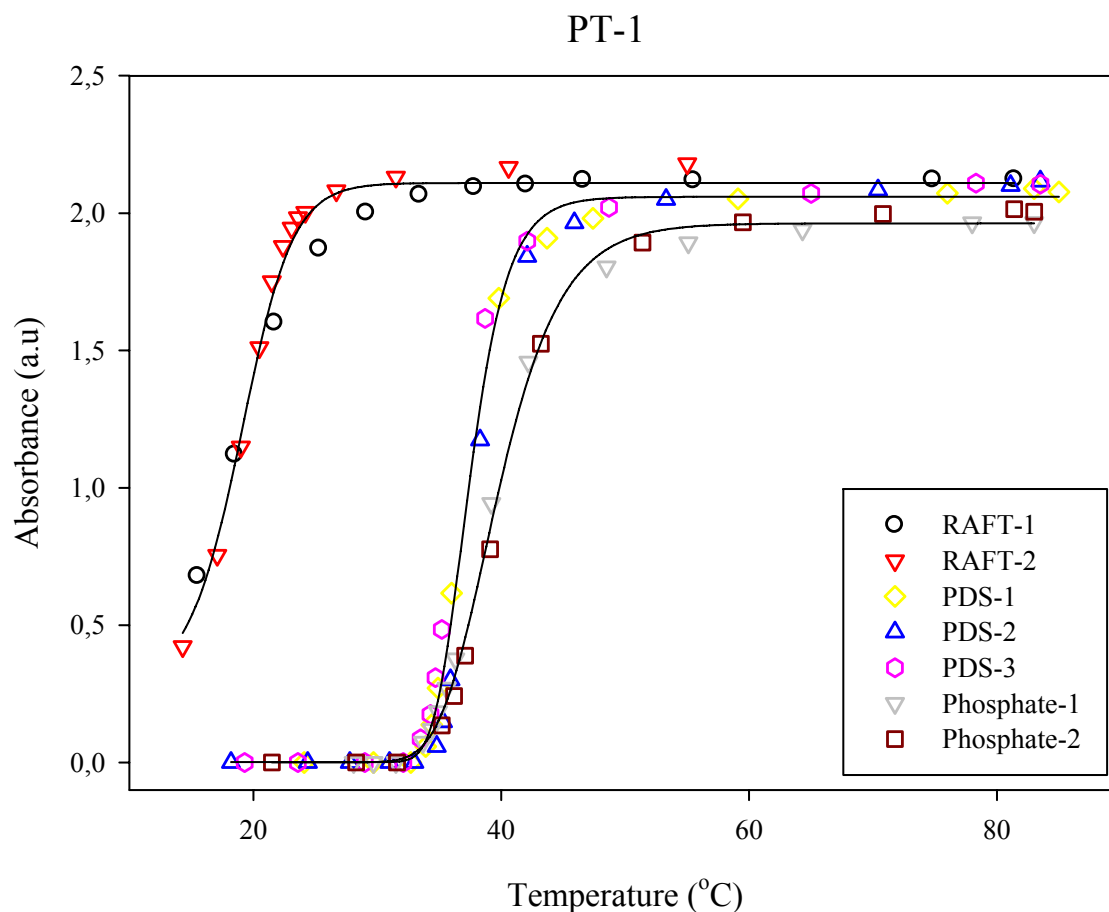
Figure A.1. Absorbance versus temperature graphs of poly(MEO$_2$MA) having Mn of 2.3 K, PDI of 1.15, $\overline{DP}$ of 11 (PT-1 coded polymer in Table 4.6) polymer with RAFT, PDS or phosphonate end-groups. Three different measurements of each sample are shown in the figure.
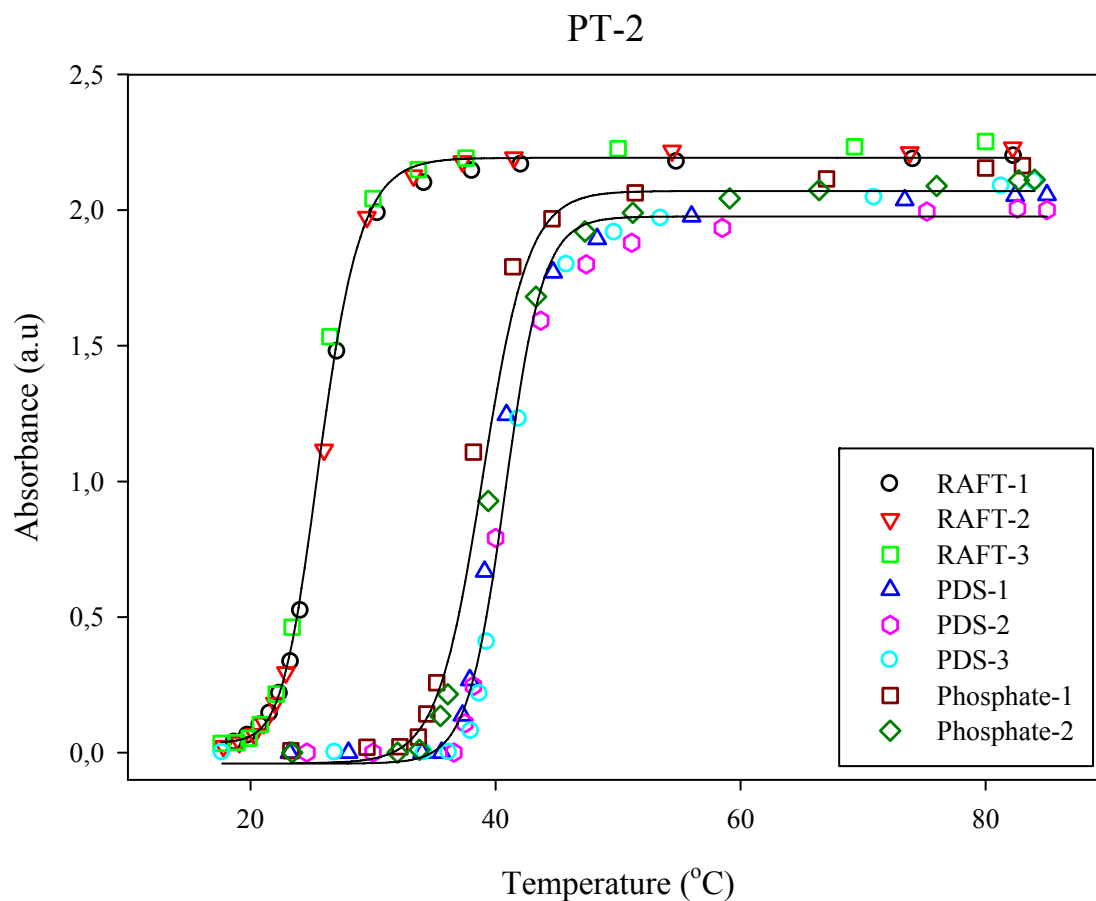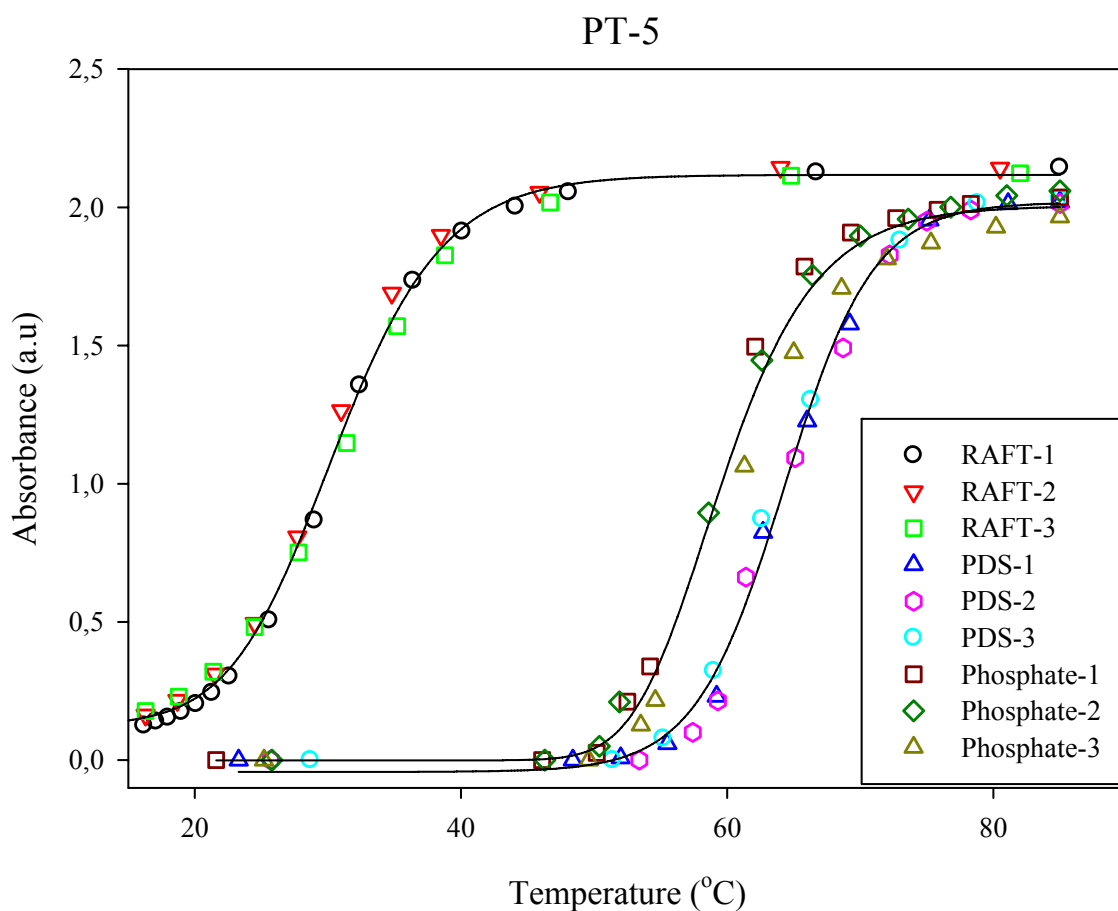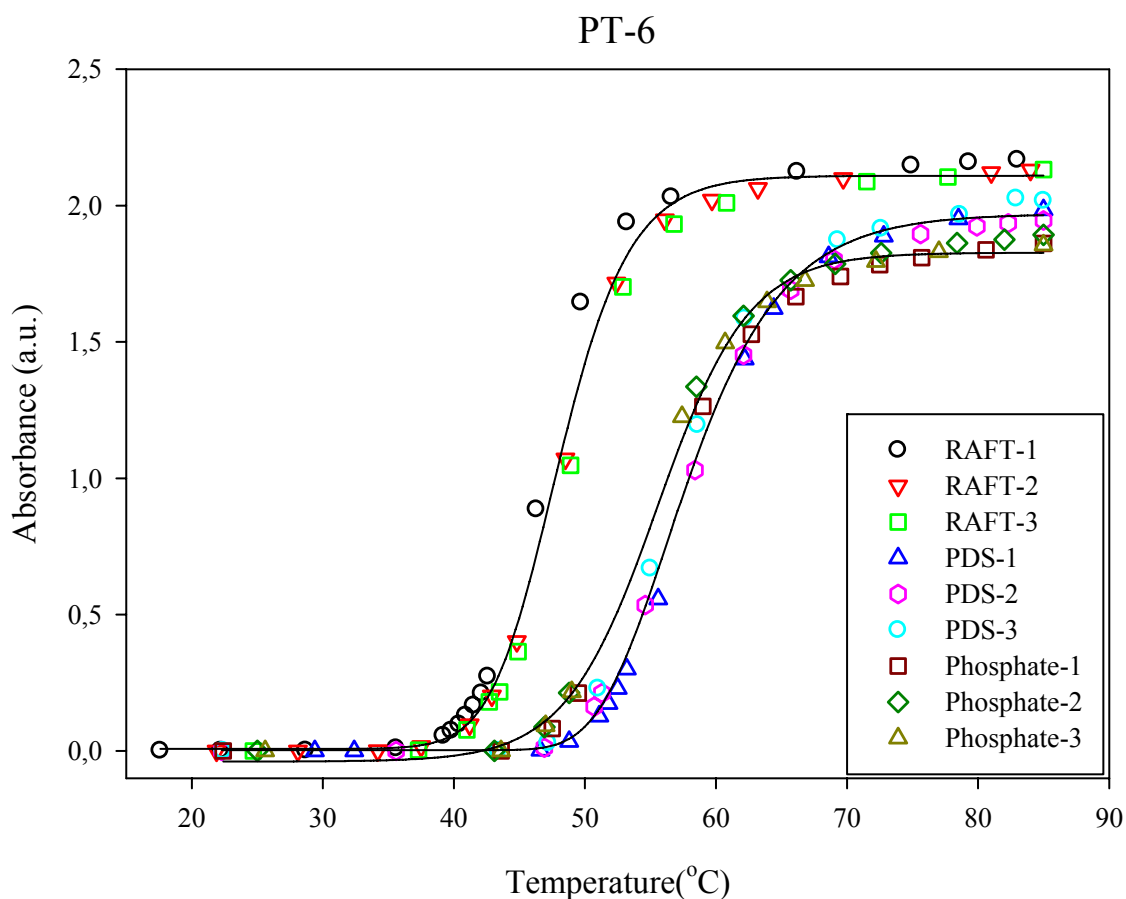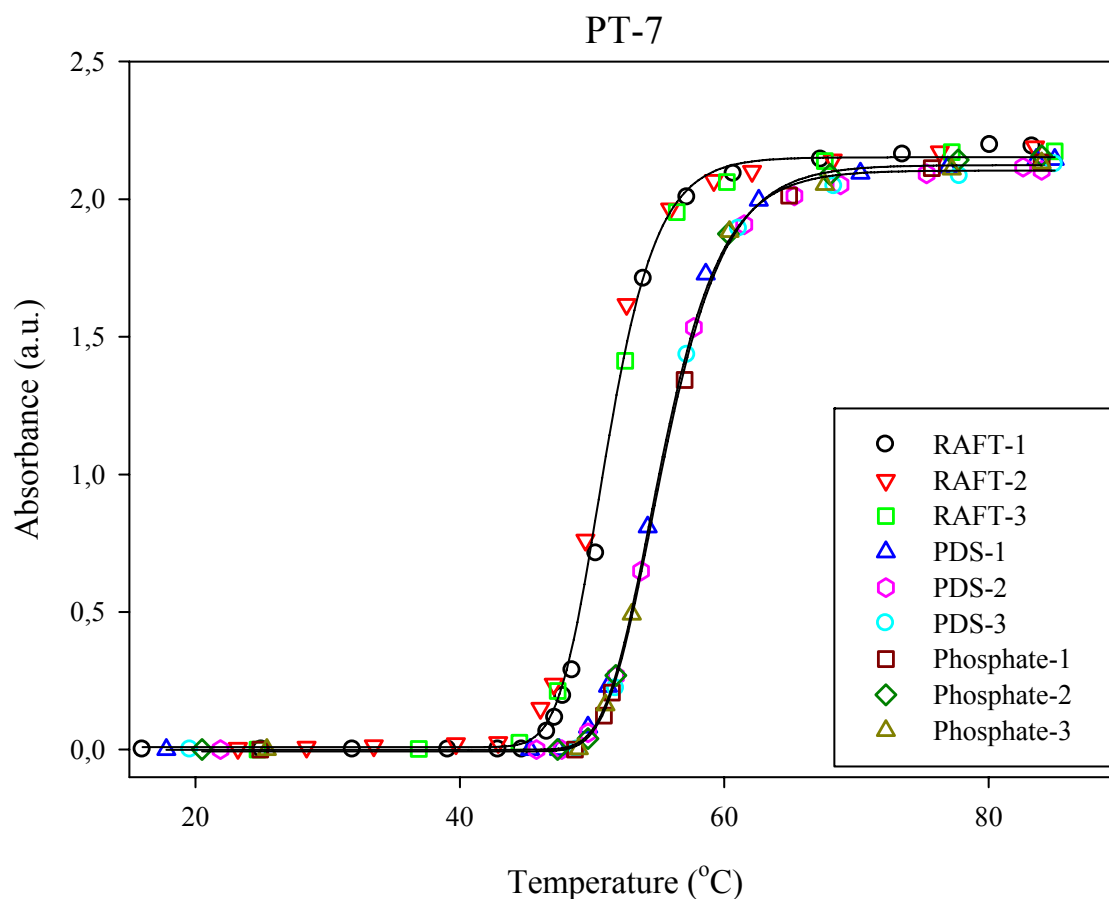
Figure A.2. Absorbance versus temperature graphs of poly(MEO$_2$MA) having Mn of 3.6 K, PDI of 1.14, $\overline{DP}$ of 18 (PT-2 coded polymer in Table 4.6) polymer with RAFT, PDS or phosphonate end-groups. Three different measurements of each sample are shown in the figure.
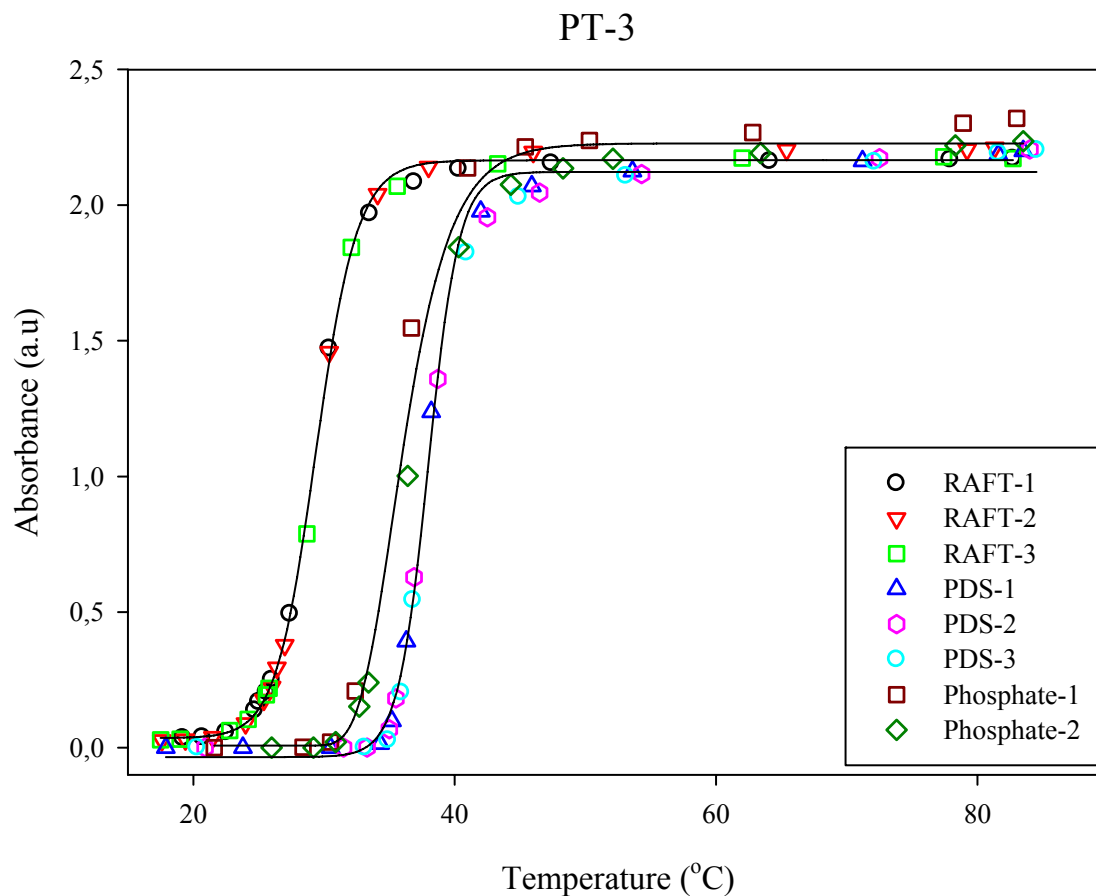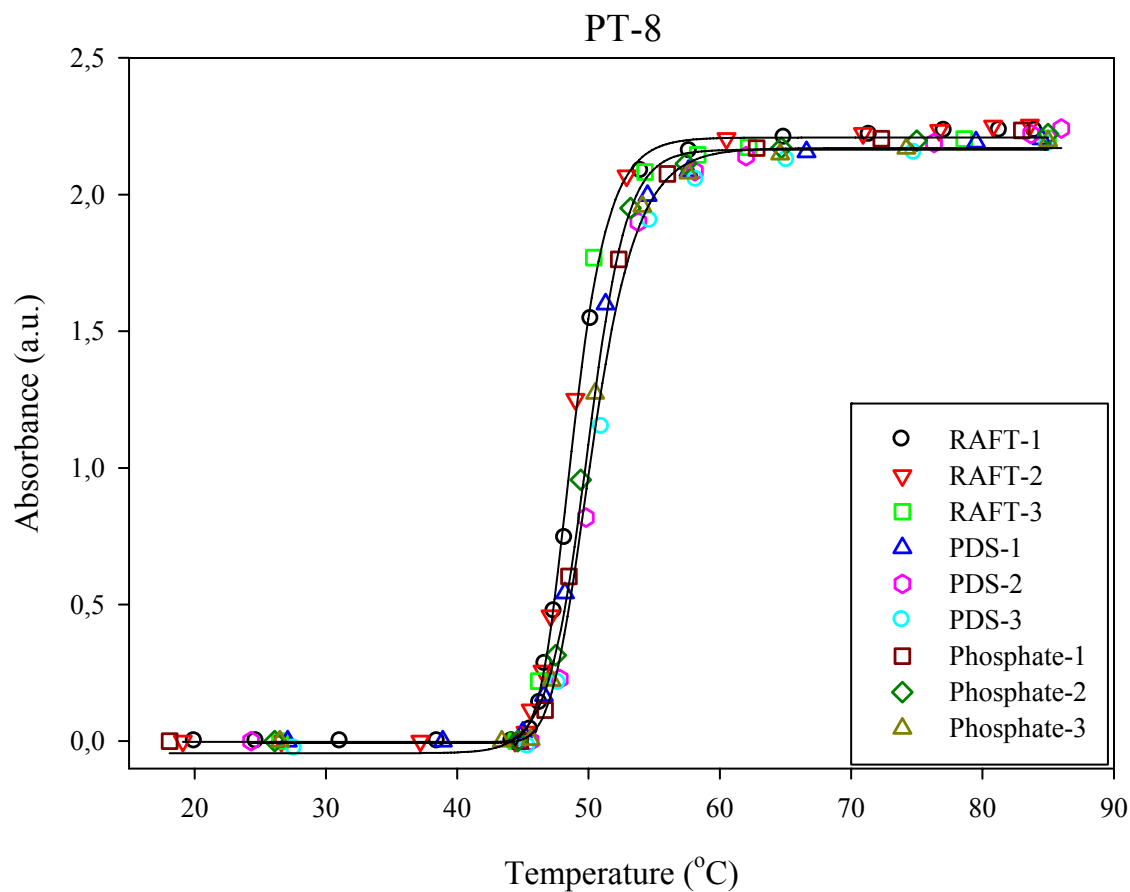
Figure A.3. Absorbance versus temperature graphs of poly(MEO₂MA) having Mn of
5.8 K, PDI of 1.22, $\overline{DP}$ of 29 (PT-3 coded polymer in Table 4.6) polymer
with RAFT, PDS or phosphonate end-groups. Three different measurements
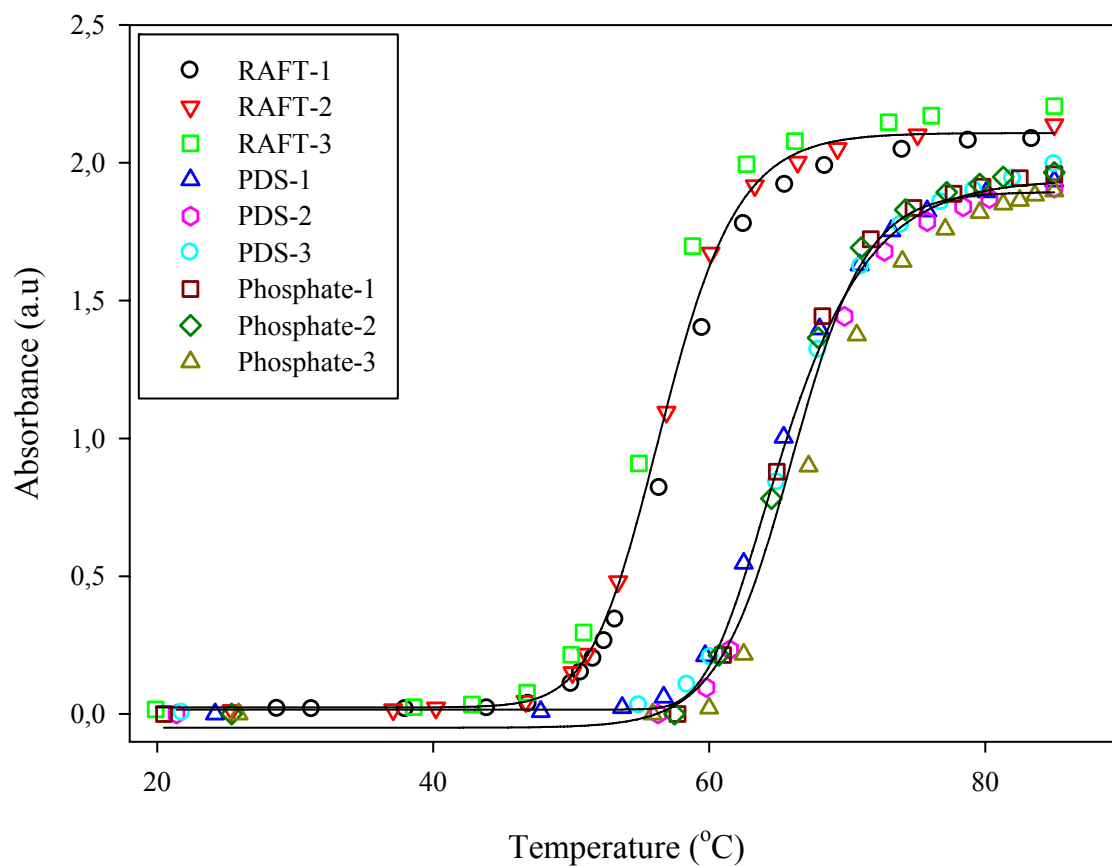of each sample are shown in the figure.
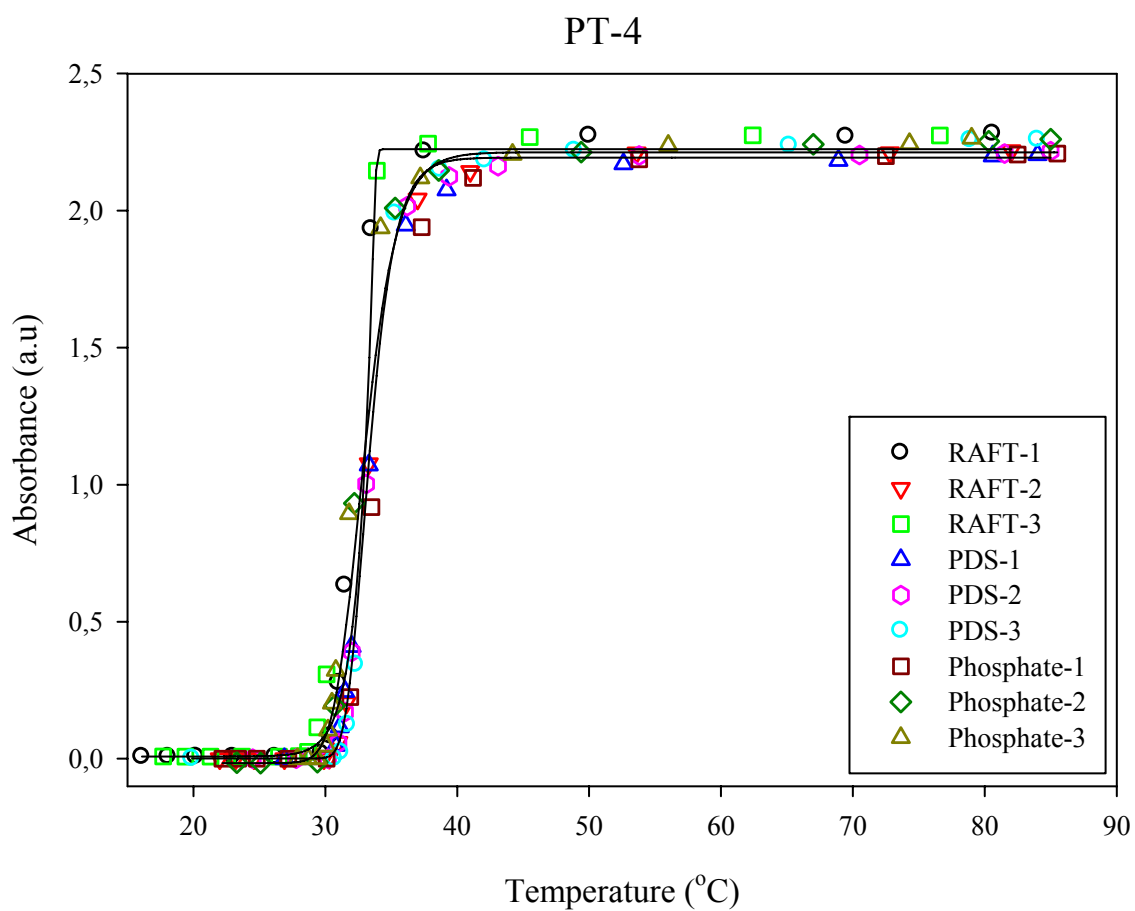
Figure A.4. Absorbance versus temperature graphs of poly(MEO$_2$MA) having Mn of 9.7 K, PDI of 1.18, $\overline{DP}$ of 53 (PT-4 coded polymer in Table 4.6) polymer with RAFT, PDS or phosphonate end-groups. Three different measurements of each sample are shown in the figure.

Figure A.5. Absorbance versus temperature graphs of poly(MEO$_2$MA$_{0.75}$-co-OEGMA$_{0.25}$) having Mn of 2.4 K, PDI of 1.20, $\overline{DP}$ of 10 (PT-5 coded polymer in Table 4.6) polymer with RAFT, PDS or phosphonate end-groups. Three different measurements of each sample are shown in the figure.
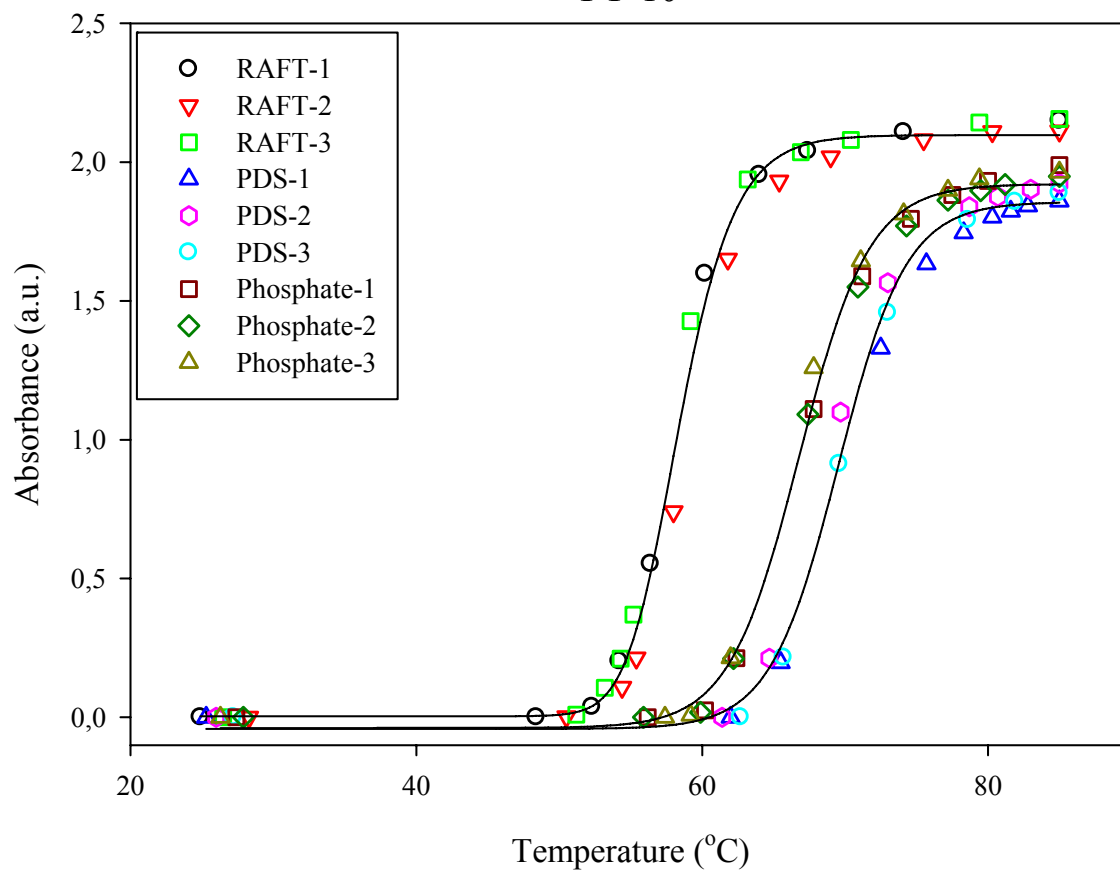
Figure A.6. Absorbance versus temperature graphs of poly(MEO$_2$MA$_{0.75}$-co-OEGMA$_{0.25}$) having Mn of 4.3 K, PDI of 1.08, $\overline{DP}$ of 19 (PT-6 coded polymer in Table 4.6) polymer with RAFT, PDS or phosphonate end-groups. Three different measurements of each sample are shown in the figure.
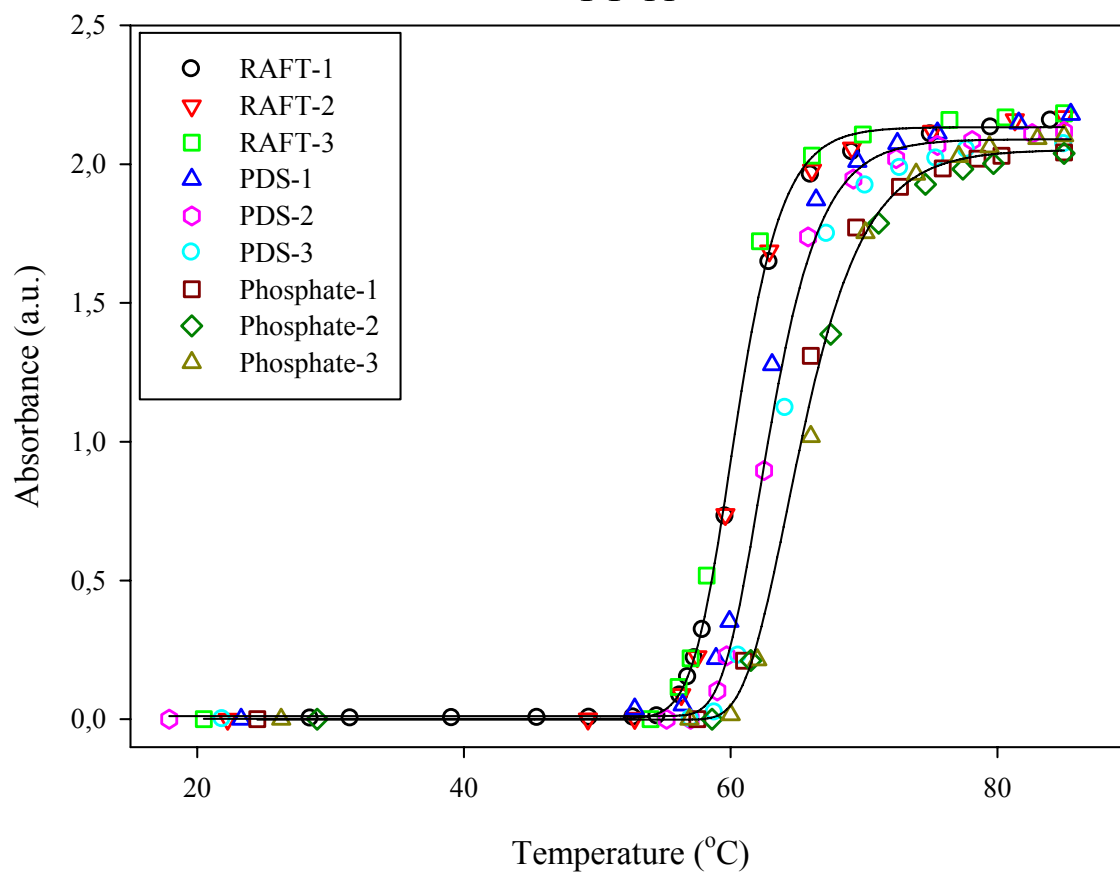
Figure A.7. Absorbance versus temperature graphs of poly(MEO$_2$MA$_{0.75}$-co-OEGMA$_{0.25}$) having Mn of 6.1 K, PDI of 1.08, $\overline{DP}$ of 27 (PT-7 coded polymer in Table 4.6) polymer with RAFT, PDS or phosphonate end-groups. Three different measurements of each sample are shown in the figure.

Figure A.8. Absorbance versus temperature graphs of poly(MEO$_2$MA$_{0.75}$-co-OEGMA$_{0.25}$) having Mn of 11.7 K, PDI of 1.21, $\overline{DP}$ of 53 (PT-8 coded polymer in Table 4.6) polymer with RAFT, PDS or phosphonate end-groups. Three different measurements of each sample are shown in the figure.
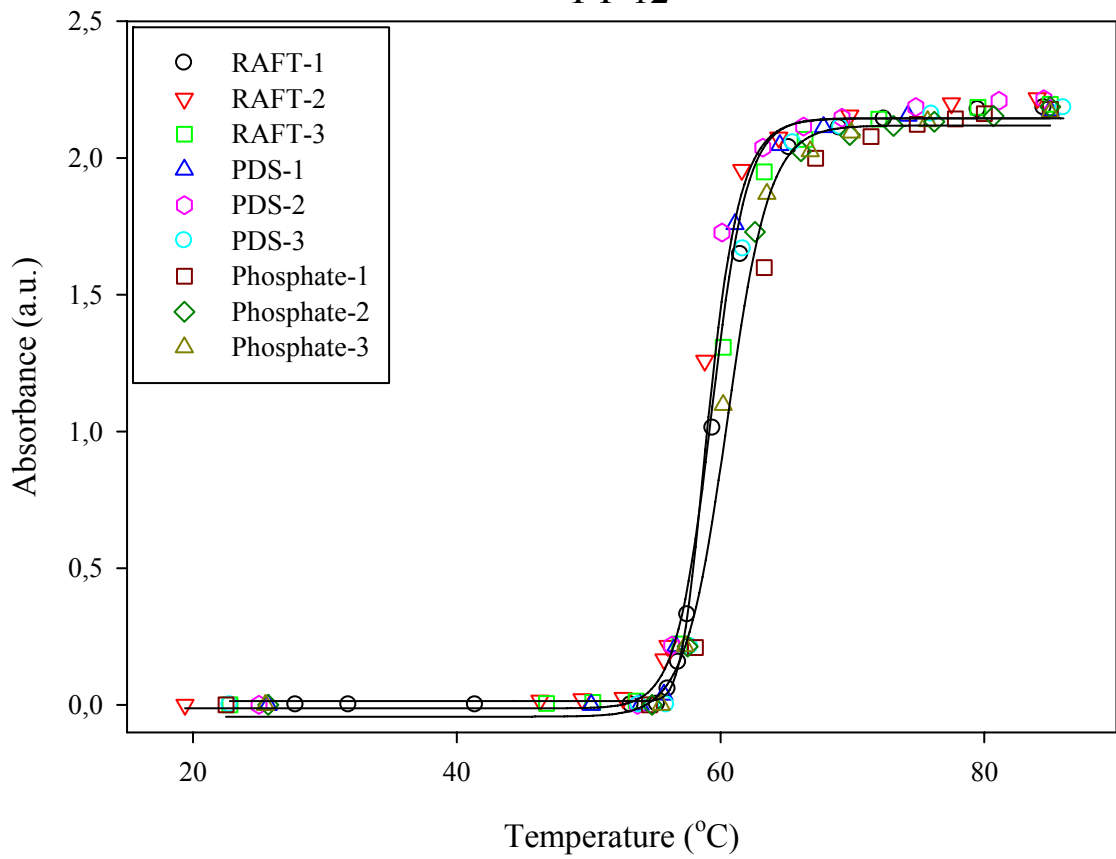
Figure A.9. Absorbance versus temperature graphs of poly(MEO$_2$MA$_{0.50}$-co-OEGMA$_{0.50}$) having Mn of 3.4 K, PDI of 1.08, $\overline{DP}$ of 12 (PT-9 coded polymer in Table 4.6) polymer with RAFT, PDS or phosphonate end-groups. Three different measurements of each sample are shown in the figure.
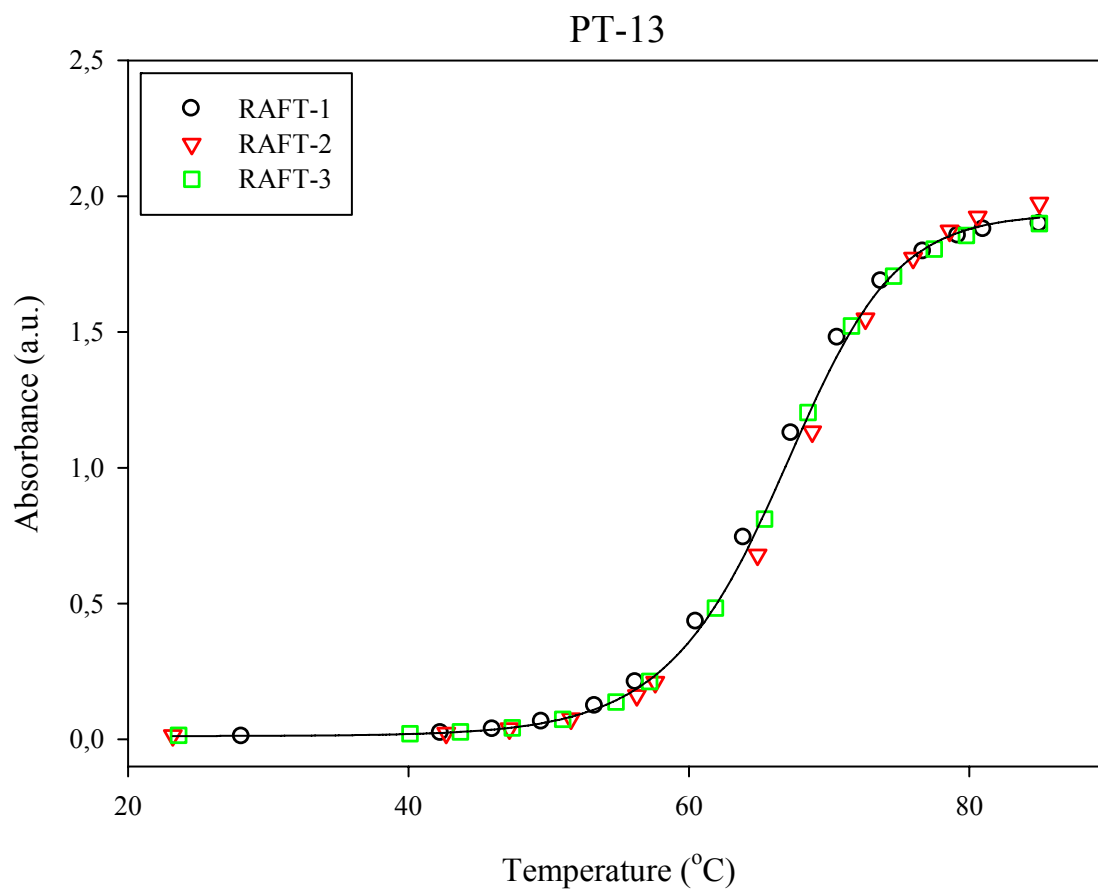
Figure A.10. Absorbance versus temperature graphs of poly(MEO$_2$MA$_{0.50}$-co-OEGMA$_{0.50}$) having Mn of 4.9 K, PDI of 1.14, $\overline{DP}$ of 19 (PT-10 coded polymer in Table 4.6) polymer with RAFT, PDS or phosphonate end-groups. Three different measurements of each sample are shown in the figure.
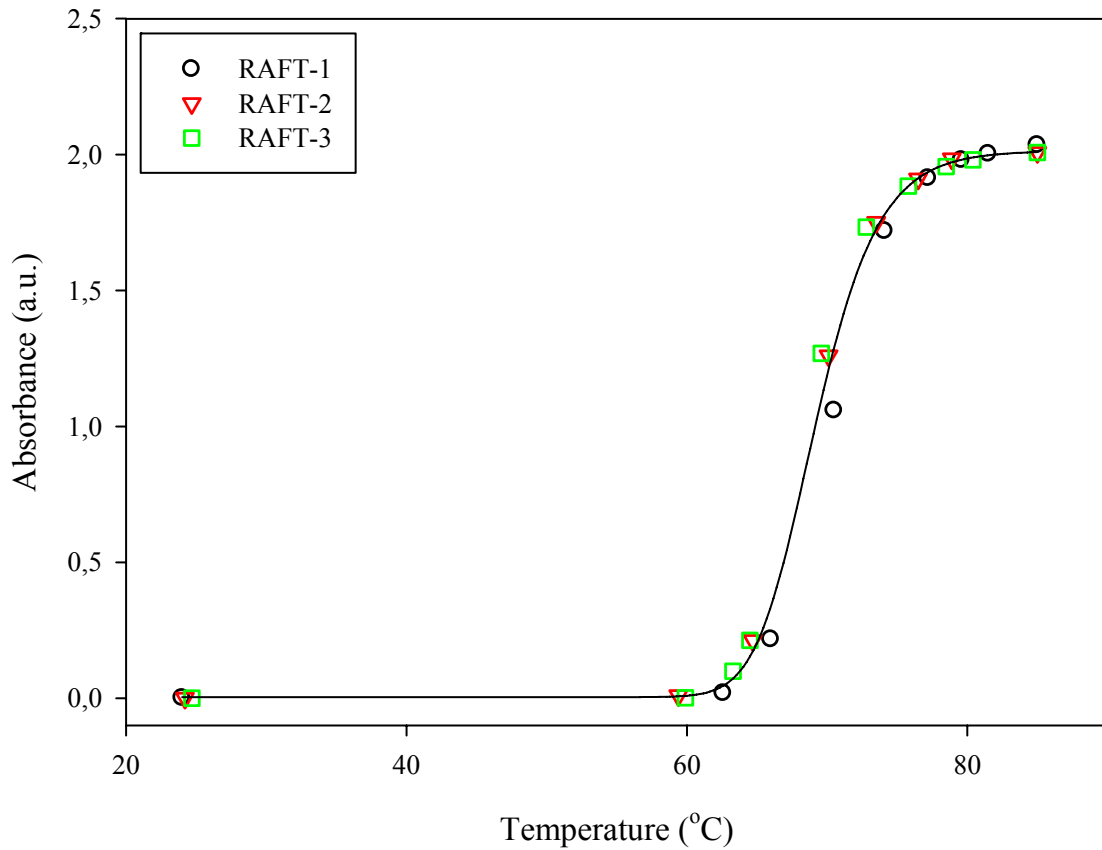
Figure A.11. Absorbance versus temperature graphs of poly(MEO$_2$MA$_{0.50}$-co-OEGMA$_{0.50}$) having Mn of 7.5 K, PDI of 1.18, $\overline{DP}$ of 29 (PT-11 coded polymer in Table 4.6) polymer with RAFT, PDS or phosphonate end-groups. Three different measurements of each sample are shown in the figure.

Figure A.12. Absorbance versus temperature graphs of poly(MEO$_2$MA$_{0.50}$-co-OEGMA$_{0.50}$) having Mn of 13.7 K, PDI of 1.29, $\overline{DP}$ of 55 (PT-12 coded polymer in Table 4.6) polymer with RAFT, PDS or phosphonate end-groups. Three different measurements of each sample are shown in the figure.

Figure A.13. Absorbance versus temperature graphs of poly($MEO_2MA_{0.25}$-co-$OEGMA_{0.75}$) having Mn of 3.2 K, PDI of 1.09, $\overline{DP}$ of 11 (PT-13 coded polymer in Table 4.6) polymer with RAFT end-group. Three different measurements of sample are shown in the figure.
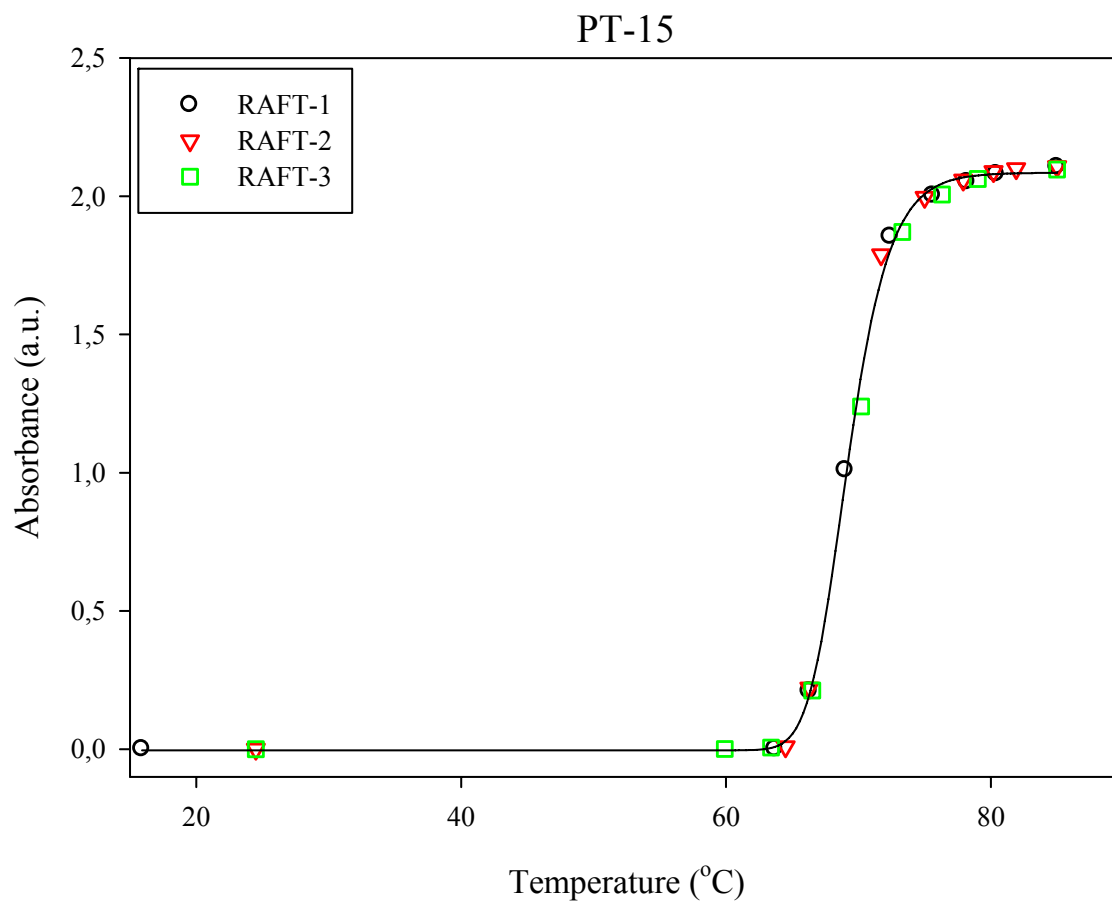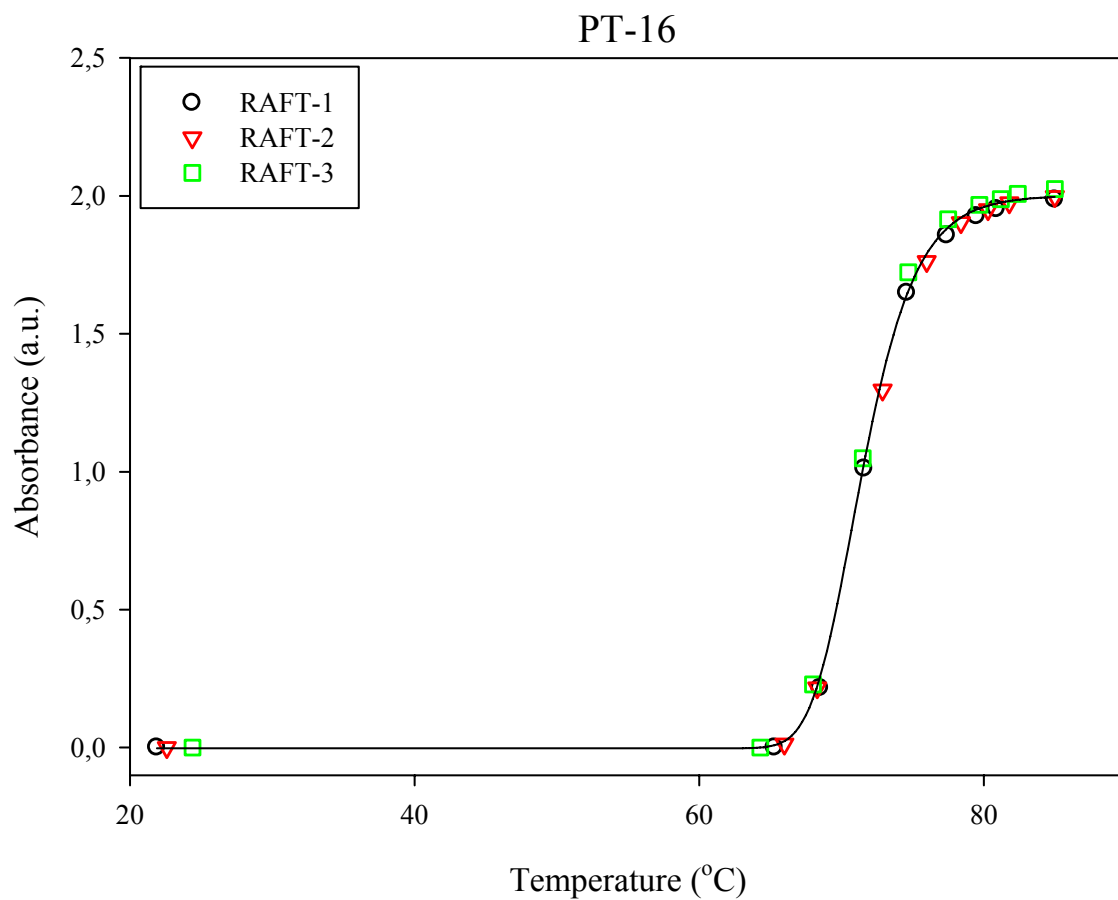
Figure A.14. Absorbance versus temperature graphs of poly(MEO$_2$MA$_{0.25}$-co-OEGMA$_{0.75}$) having Mn of 4.9 K, PDI of 1.15, $\overline{DP}$ of 17 (PT-14 coded polymer in Table 4.6) polymer with RAFT end-group. Three different measurements of sample are shown in the figure.

Figure A.15. Absorbance versus temperature graphs of poly(MEO$_2$MA$_{0.25}$-co-OEGMA$_{0.75}$) having Mn of 8.2 K, PDI of 1.23, $\overline{DP}$ of 29 (PT-15 coded polymer in Table 4.6) polymer with RAFT end-group. Three different measurements of sample are shown in the figure.

Figure A.16. Absorbance versus temperature graphs of poly(MEO$_2$MA$_{0.25}$-co-OEGMA$_{0.75}$) having Mn of 13.0 K, PDI of 1.21, $\overline{DP}$ of 47 (PT-16 coded polymer in Table 4.6) polymer with RAFT end-group. Three different measurements of sample are shown in the figure.
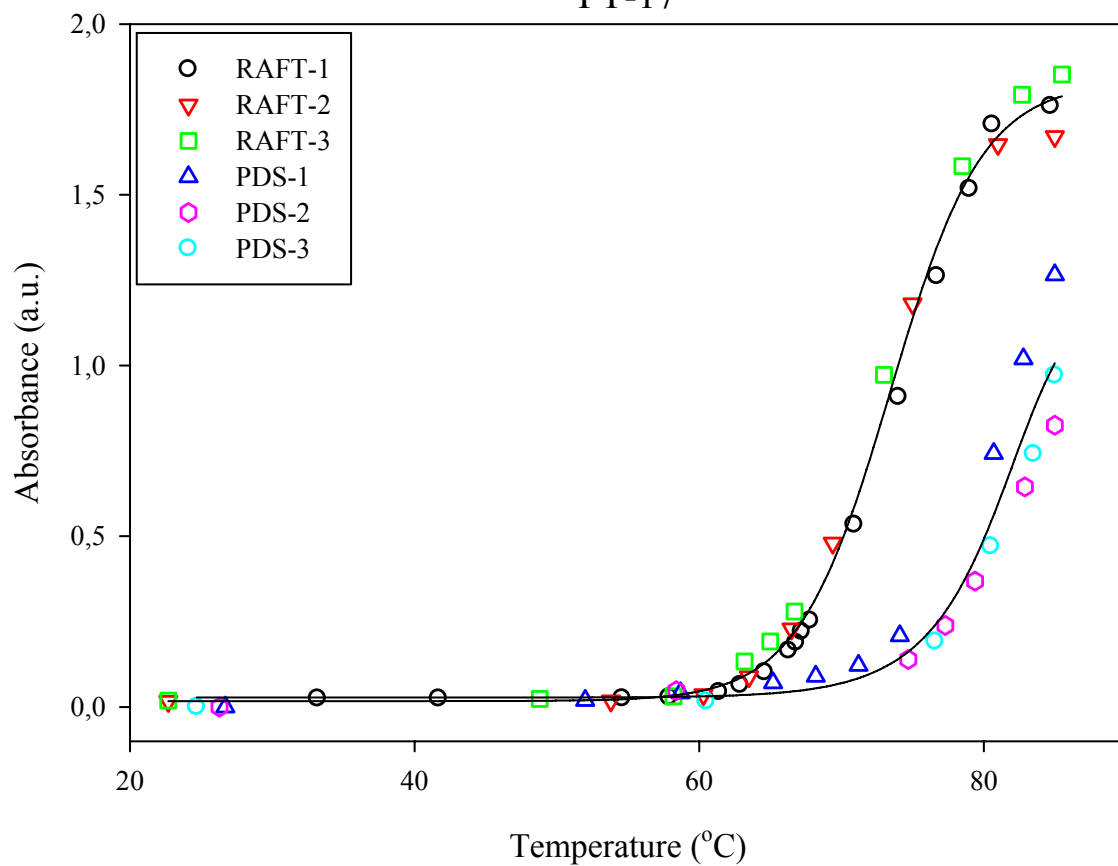
Figure A.17. Absorbance versus temperature graphs of poly(OEGMA) having Mn of 3.3 K, PDI of 1.20, $\overline{DP}$ of 10 (PT-17 coded polymer in Table 4.6) polymer with RAFT or PDS end-groups. Three different measurements of each sample are shown in the figure.
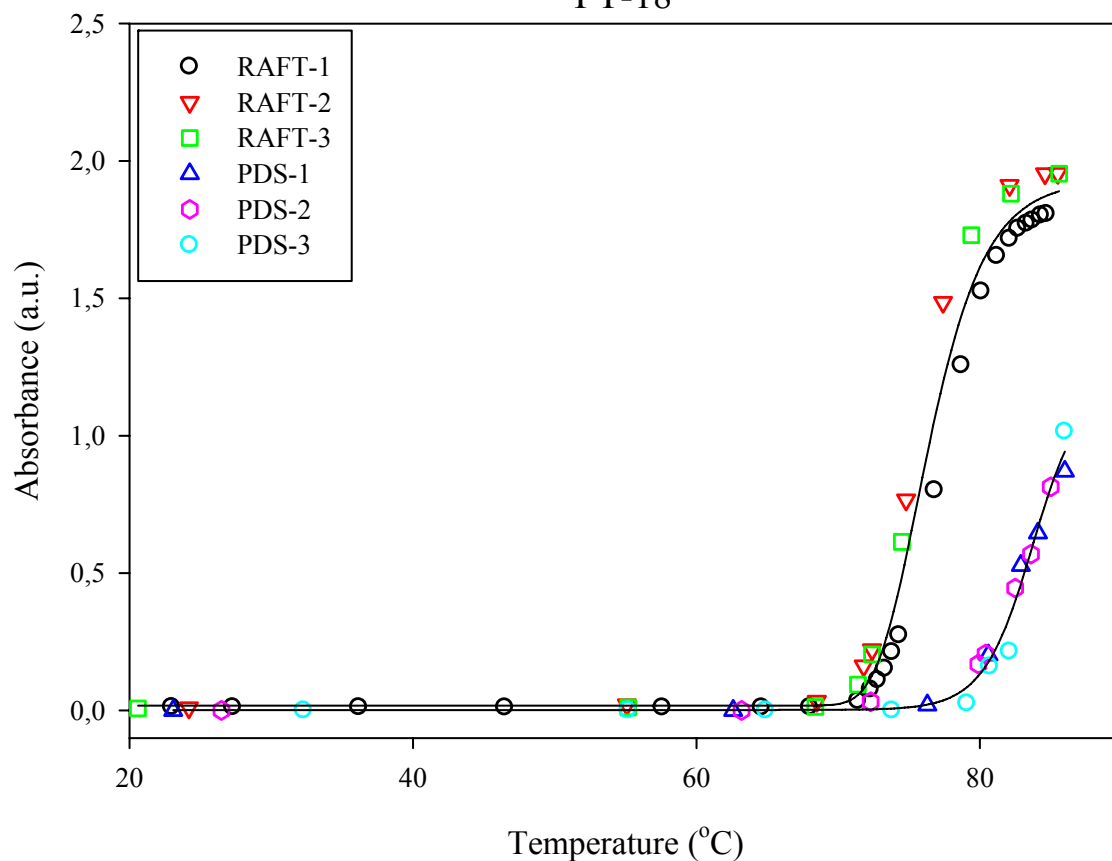
Figure A.18. Absorbance versus temperature graphs of poly(OEGMA) having Mn of 5.6 K, PDI of 1.15, $\overline{DP}$ of 18 (PT-18 coded polymer in Table 4.6) polymer with RAFT or PDS end-groups. Three different measurements of each sample are shown in the figure.

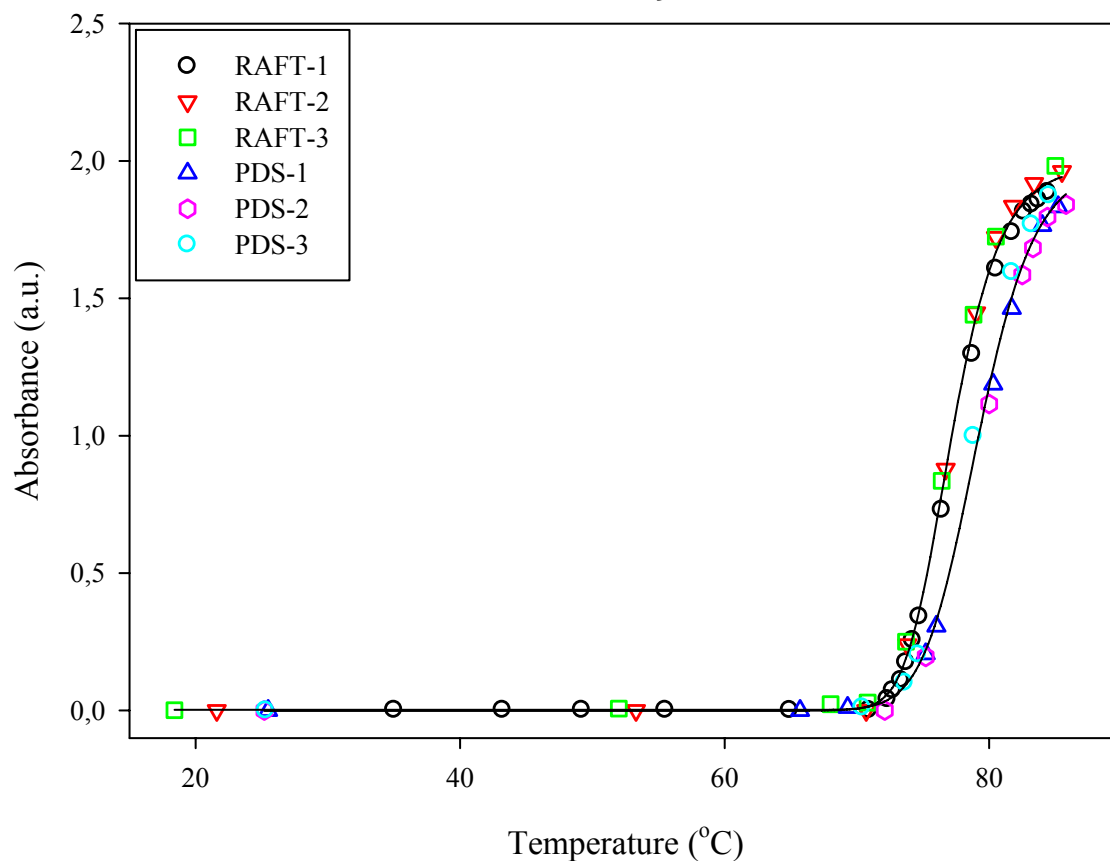Figure A.19. Absorbance versus temperature graphs of poly(OEGMA) having Mn of 8.7 K, PDI of 1.17, $\overline{DP}$ of 28 (PT-19 coded polymer in Table 4.6) polymer with RAFT or PDS end-groups. Three different measurements of each sample are shown in the figure.
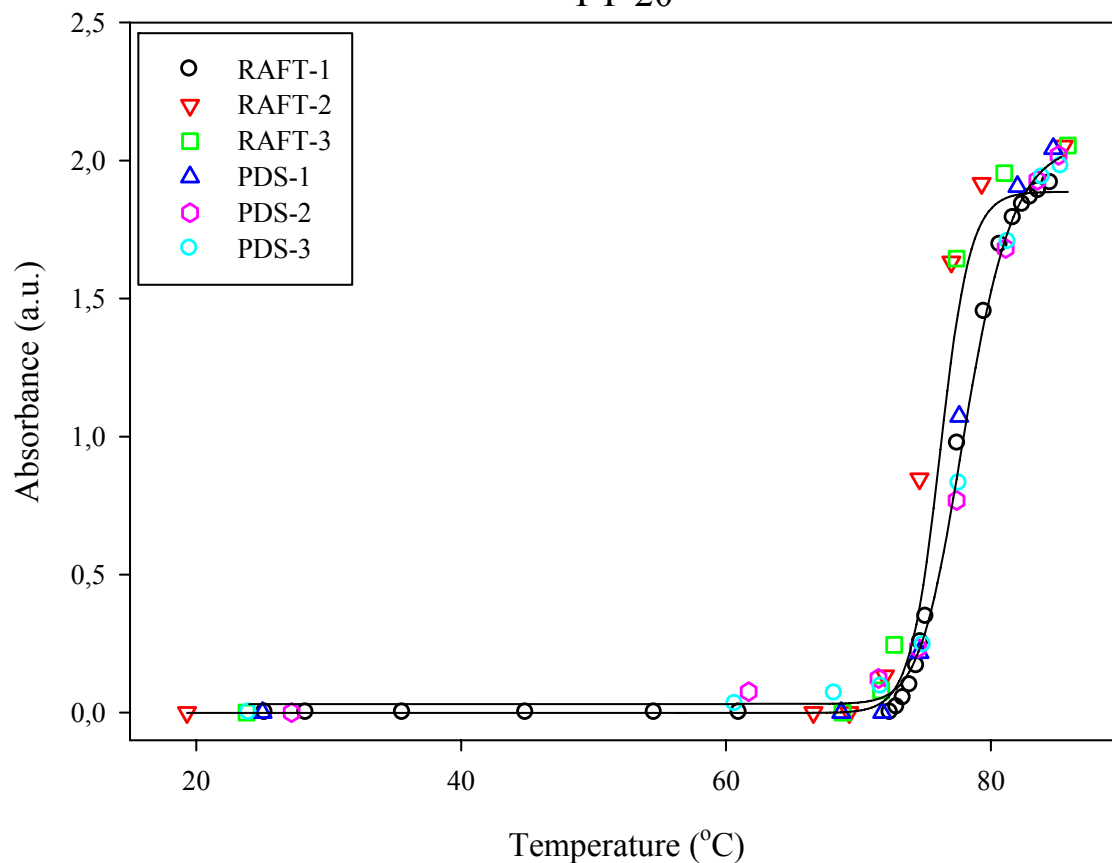
Figure A.20. Absorbance versus temperature graphs of poly(OEGMA) having Mn of 16.8 K, PDI of 1.22, $\overline{DP}$ of 55 (PT-20 coded polymer in Table 4.6) polymer with RAFT or PDS end-groups. Three different measurements of each sample are shown in the figure.